Energy dissipation, usually, mechanical damping and storage modulus of WC-Co coated A356.2 and their composites dispersed with silica rich rice husk ash (RHA) particulates have been studied . All the specimens are coated using HVOF technique with an optimum coating thickness of 100 mm as obtained by MATLAB. The damping and storage moduli have been measured using dynamic mechanical analyzer at three distinct frequencies (0.1, 1 and 10 Hz) over a temperature range of 35°C to 150°C. Introspection of these results reveals that the mechanical damping and storage modulus has been improved with the incorporation of RHA and further increases with the increase in the RHA content. Furthermore, coated WC-Co samples demonstrate higher mechanical damping than the base alloy and its composites, however, a loss in the storage modulus has been noticed which is due to the presence of W2C phase. Porosity, hardness and the residual stresses are the mechanisms responsible for the increase in mechanical damping of WC-Co coated Al/RHA composites.

Dr. N.Tulasi Radha, Associate Professor, MREC(A), 15 years of teaching experience and also worked as HOD 5 years and published papers in various journals. Member ships-ASME, IFERP, IAENG.
Dr. T Venkata Deepthi, Associate Professor, MREC(A), 14 years of teaching experience and published papers in various journals. Member ships-ASME, IFERP, IAENG.

9 786204 719399

Energy Dissipation in WC-Co Coated A/RHA

N TULASI RADHA
D SIVA PRASAD
T VENKATA DEEPTHI

Energy Dissipation in WC-Co Coated A356.2/RHA Composites

RADHA, PRASAD, DEEPTHI

LAP LAMBERT Academic Publishing

N TULASI RADHA
D SIVA PRASAD
T VENKATA DEEPTHI

Energy Dissipation in WC-Co Coated A356.2/RHA Composites

N TULASI RADHA
D SIVA PRASAD
T VENKATA DEEPTHI

Energy Dissipation in WC-Co Coated A356.2/RHA Composites

LAP LAMBERT Academic Publishing

Imprint

Cover image: www.ingimage.com

Publisher:
LAP LAMBERT Academic Publishing
is a trademark of
Dodo Books Indian Ocean Ltd., member of the OmniScriptum S.R.L Publishing group
str. A.Russo 15, of. 61, Chisinau-2068, Republic of Moldova Europe
Printed at: see last page
ISBN: 978-620-4-71939-9

ACKNOWLEDGEMENTS

Whatever value this study possesses is largely due to the example of **Dr. D. Siva Prasad,** my Research Director and his researches into the various fields of Mechanical Engineering. He first suggested that I undertake this topic and throughout, his encouragement and guidance have helped me to achieve this completed form. I am deeply indebted to my professor for his erudite comments on this work and I express my salutations for his tireless efforts, congenial and efficient guidance throughout my work.

I sincerely extend my heartfelt gratitude to **Prof**. **M.R.S. Satya Narayana**, Head of the Department, and other faculty members of the Department of Mechanical Engineering for their encouragement and also for extending all possible departmental facilities. I am also thankful to all the administrative staff of the department for their co-operation whenever I needed.

I express my sincere thanks to the former principal **Prof. K. Lakshmi Prasad** and Management of my present working institute, **GIT, GITAM University**, Visakhapatnam for their encouragement in continuing with my thesis work.

The greatest blessing, I enjoyed in all these years is the selfless, unwavering and unconditional love strength given to me by my **husband, daughter, parents, in-laws, brothers and sister-in law's.** I feel profuse gratitude to my entire family. They have always encouraged and supported me during my whole life. Their hearts and souls have enlightened my path all along the way to my righteousness and being an improved man.

P.Tulasi Radha

ABSTRACT

The functionality of the material systems depend on vibrational energy. The loss of vibrational energy (refer to as damping) and degradation pose a threat to the efficient functioning of material systems. Of late researchers have started different ways to reduce vibrational losses and corrosion deterioration. Now more thrust is on developing modern materials which would tremendously enhance the dissipation of effective energy and corrosion resistance. One such development is Metal Matrix Composites (MMC) which has got high retention of phenomenal trades when compared to monolithic materials such as like elevated specific strengths, stiffness, toughness, energy dissipation, corrosion and wear resistance.

With excellent mechanical properties like low density, machinability, durability, low weight-high strength ratio, exceptional corrosion abrasion and wear resistance, aluminium is predominantly used as metal matrix material for various applications. Researchers and industrialists stated that, among distinct reinforcements, rice husk ash (RHA) has gained lot of attraction compared to other discontinuous dispersoids because of its availability, low cost and low density. Among diverse fabrications techniques stir casting was considered as most preferable and least cost liquid fabrication technique. The present study utilizes stir casting technique to fabricate Al/RHA metal matrix composites with different compositions of RHA reinforcement i.e. 2, 4, and 6 wt. %. Properties like density, hardness, porosity, tensile strength of A356.2 base alloy and Al/RHA composites are investigated.

Plating's are extensively used for the enhancement of surface properties, but it has exhibited more adverse effect on environment and health issues because of emission of harmful gases in the plating technique. So, to overcome such situations modern techniques such as thermal spray process has been used extensively. Among the various

thermal spraying coating techniques, High velocity oxygen fuel (HVOF) spray process is the most feasible and most economical in nature. With the deposition of WC-Co using HVOF, the material life is enhanced with superior surface properties such as corrosion, wear and erosion resistant. However, from the literature, it is clear that there is a dearth of information on the damping behaviour of WC-Co coated Al/RHA composites. Hence the main objective of the work is to enhance the damping capacity by depositing WC-Co coating on the aluminium and its composites containing rice husk ash as reinforcement.

The HVOF coated surface morphology is characterized using SEM, FESEM and XRD techniques. The properties like hardness, adhesion and residual stresses acting on HVOF coated A356.2 base alloy and Al/RHA composites are investigated. The damping behaviour of A356.2 alloy, Al/RHA composites, WC-Co coated A356.2 alloy and Al/RHA metal matrix composites is thoroughly investigated using dynamic mechanical analyzer at different frequencies (0.1, 1 and 10 Hz) over a continual heating system from room temperature to 150 °C. All the specimens for damping measurements were machined using wire electric discharge machining (WEDM) process.

From the experiments, it is observed that with the escalation of particulate content, hardness and tensile strength increases while porosity and density decreases. It is observed that HVOF coated test specimens yielded better adhesion and hardness, with lower residual stresses. Al/RHA composites exhibited high damping capacity with increase in RHA particles. It is also observed that plastic zone, dislocation densities and porosity play a crucial role. Storage modulus is found to decrease with the deposition of WC-Co. Increased stiffness is achieved with the addition of reinforcement which might be the possible reason for the increase in storage modulus. Also, WC-Co coated alloy exhibits higher damping values and increases with the increase in the content of

RHA. The hardness of the composites induced residual stresses on the surface of the coating and the porosity play a vital role in the enhancement of the damping behaviour in WC-Co coated Al/RHA composites.

TABLE OF CONTENTS

LIST OF FIGURES

LIST OF TABLES

NOMENCLATURE

MMCs	Metal Matrix Composites
RHA	Rice Husk Ash
DMA	Dynamic Mechanical Analyzer
AMCs	Aluminium Matrix Composites
PRMMCs	Particulates Reinforced Metal Matrix Composites
CTE	Thermal expansion coefficient
ρ_{mmc}	Density of metal matrix composites
ρ_{Al}	Density of Aluminium alloy
ρ_{RHA}	Density of Rice husk ash
ρ	Dislocation Density
V_{RHA}	Volume fraction of rice husk ash particles
E'	Storage modulus
E"	Loss modulus
η	Loss factor
Q^{-1}	Inverse quality factor
C_s	Size of the plastic zone
W_r	Wear rate
b	Burgers vector
Ψ	Specific damping capacity
L	Sliding distance
T_{ON}	Pulse on Time
T_{OFF}	Pulse off time
IP	Peak Current

ABBREVIATIONS

MMC	Metal matrix composites
FAR	Federal aviation regulations
JAR	Joint aviation requirements
NVH	Noise vibration harshness
NACE	National Association of Corrosion Engineers
CMM	Ceramic matrix materials
AMC	Aluminium metal matrix composites
RHA	Rice husk ash
SEM	Scanning electron microscope
EDS	Energy dispersive X-ray spectroscopy
XRD	X-Ray Diffraction (XRD)

CHAPTER - I
INTRODUCTION

1.1 Composites

When two or more constituent materials which are physically and chemically contradictory to each other when combined, develops a new material which is of superior quality which is different from the individual materials are known as composites. Within the composites the constituent elements remain distinctive which makes them differentiate from solid solutions and mixtures. This system can be technically defined as multiphase material system (matrix phase, reinforcing phase) with peculiar phases, compositions, orientations bonded together to retain both the properties of individual materials without undergoing any chemical reaction. These individual components do not completely dissolve or diffuse, they simply form an interface with each other to facilitate the synergistic characteristics which are not attained by the sole original materials. The very nature of composites can be explained though this example, bone is natural composite consisting of organic components and inorganic components. Both these unique properties are best combined to give softness, flexibility, strength rigidity against breaking in normal conditions. Composites found their way since biblical period, where traditional bricks are combined with chopped straws in making building materials, straw-reinforced walls, bows and chariots made using layers of wood. With the invention of fibrous and particulate reinforcement materials in 1900's a new era of composites innovations has started. USA in 1937 has developed commercial glass fibre which further led to the development of glass fibre reinforced plastics in 1942. Day-by-day the demand for fibre and glass fibre reinforced plastics is increasing rapidly which is evident during the World War II when those materials were predominantly used in the aircraft and military industries. Boron, carbon fibres were qualified in making ropes from 1950. Polymer matrix composites are

initiated during the year 1960. The cold war in 1970 urged for the production of metal matrix composites in the field of military. Since 1984, worldwide over 11 million kilograms of composites have been manufactured out of which 60% of its consumption was done by USA for its utilization [1-2]. Innovations in the field of high temperature ceramic composites have started in the year 1990. There have been remarkable inventions in composites since many years which initiated from chopped straw bricks of ancient times to the present intellectual and smart materials [3].

1.2 Composites Classification

Basically the composites are categorized into two main type's i.e. natural and synthesized composites. As the name indicates natural composites are available in nature abundantly or developed by our ancients. Synthetic or artificial composites are invented by researches and industrialists by using various processing techniques and wide range of materials. These are further classified into various types based on reinforcement and matrix materials.

1.2.1Categorization of composites depending on reinforcements*:*

Classification of composites based on reinforcement is as follows:

1.2.1.1 Particulate reinforced composites

These materials consist of mixture of particles as its reinforcements in a pool of matrix materials. These particles are very short in size. Their aspect ratio is very low. These particles are of various shapes, sizes and made up of various materials such as glass, wood pieces etc. and these can be randomly oriented or preferred orientation. The perfect examples for this type are concrete and wooden particle boards. The gravel added to the cement matrix acts as binder and thus provides strength and stiffness to the concrete composite. Enhanced properties are obtained with these composites. [4].

1.2.1.2 Fibre reinforced composites

Fibres are short or discontinuous and long or continuous. These are layered as unidirectional or bidirectional in the matrix material. These composites are rich in tensile strengths. Buckling and bending loads are present in between the fibres of these composites [5].

1.2.1.3 Structural composites

In these composites the reinforcement materials are added in combination of layers in the matrix material such as laminates, sandwich panels etc. [6].

1.2.2 Categorization of composites depending on Matrix Material

In the production of composites different matrix materials used are titanium, magnesium, aluminium, cobalt and nickel alloys. Depending on the matrix material composites are broadly classified into various types such as polymer matrix composites, metal matrix composites, glass matrix composites and ceramic matrix composites and the same is shown in the Fig 1.1a and b. [7].

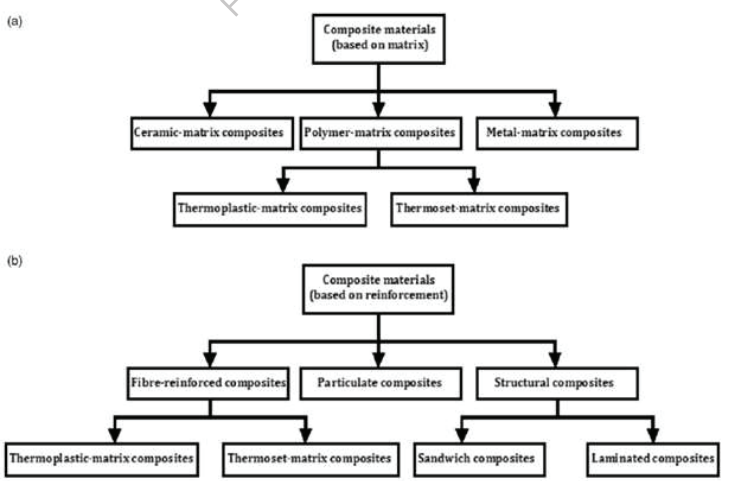

Fig 1.1: Classification of composites a) based on matrix b) based on reinforcement [7]

1.2.2.1 Polymer matrix composites (PMC)

These composites consist of organic and long chain matrices materials which are based on polymers and their operating temperature is less than 260 °C with anticipated light weight and required mechanical properties. The polymer matrix materials are largely classified into two types as thermoplastics and thermosets. During the curing process they become soft and ultimately they will melt when heated and if then cooled again they will solidify and become stiff again. In contradiction to this thermosets when heated there will not be much change in the overall structure but if certain threshold is crossed they will start developing cracks and decomposes itself and even after cooling they cannot regain their original structure [8].This very flexible nature of the thermosets is most suited as the matrix bases for fibre reinforced composites. Thermosets have an ample range of utilization in chopped fibre composites. They can hold off high temperatures easily, can be used in automobile parts, insulating materials, defense systems. The various applications of thermoplastic materials are automotive control panels, spoons, jugs, containers, electronic products encasement, bottles, toys etc.

1.2.2.2 Metal matrix composites (MMC)

Higher modulus, specify strength, damping capacity and exceptional corrosion and wear resistance are achieved with MMC's when compared to unreinforced alloys. Extensive research is being carried in developing low density, low cost metal matrix materials [10-11].

1.2.2.3 Glass matrix composites (GMC)

Composites fabricated with glass as base in the fabrication of the composites are glass matrix composites. The operating temperature of these composites is 750 – 1150 °C. High yield strengths and tensile ductility are high in bulk metallic glass matrix

composites. These are mainly used for only intended requirements. The main applications of such composites are found in electronics.

1.2.2.4 Ceramic matrix composites (CMC)

These composites are used when high ranges of operating temperatures are required such as 1150-1400 °C. The major applications of these composites are nose cones of missiles, aircraft engine turbine blades, and some re-entry vehicles. In these composites mainly two types of ceramic materials are used, lithium alumino silicate and calcium alumino silicate. Ceramic composites are mainly crystalline structure [9]. They have low fracture toughness which makes their applications less in structural engineering. Ceramics also have exceptional corrosive resistance.

1.3 Metal Matrix Composites

Composites fabricated with metal as base are said to be metal matrix composites. For these composites the operating temperature lies approximately in the range of 260 °C – 750 °C. Composites with more than one reinforcement are hybrid composites. There are always certain limitations in achieving good stiffness, strength, toughness, density of typical monolithic materials. In order to overthrow these imperfections as well as to meet forever raising demands of contemporary technology, metal matrix materials are the most promising materials.

With intensive research in the field of material science and engineering many new generation materials have come into vogue. One such development among new generation materials is metal matrix composites. To overcome the flaws in traditional metals like higher strength, toughness, stiffness and lower densities metal matrix composites have been developed. These new generation materials are in contrast with the conventional monolithic materials with regards to strength, toughness, stiffness and lower densities. The main distinction between metal matrix composites and

conventional alloys lies in the secondary phase. In alloys it occurs due to eutectic or eutectoid reactions while in metal matrix composites it is formed as a result of adding matrix material. The usage of the MMC's was restricted due to its complexity in manufacturing techniques and high cost reinforcements.

Due to the availability of extensive range of discontinuous reinforcements in the recent years, it has drawn attention in almost all fields which led to the easy fabricated and low cost effective techniques. Extensive research is carried out to develop light weight and meagre price matrix materials such as aluminium and magnesium in place of high cost matrix materials such as titanium, nickel steel zinc, lead, copper etc. Due to the various properties namely low density, machinability, durability, low weight/high strength ratio, exceptional corrosion abrasion and wear resistance, high thermal and electrical conductivity, when compared among the various matrix materials aluminium matrix system is mostly preferred.

Among several discontinuous reinforcements there has always been a large requirement for the development of low density and low cost reinforcements. To a large extent rice husk ash serves this purpose. This is present all over the world which is mostly available from rice industry. Rice husk ash is conventionally extracted from controlled burning of rice husk, thus the obtained rice husk ash contains almost 90-95% silica and minor traces of other oxides. Due to the presence of various accessible discontinuous dispersoids, the most cost effective and low density reinforcement is rice husk ash which is available for a meagre price. Thus with least fabrication expenses and with high mechanical properties metal matrix composites with RHA as reinforcement material is mostly considered. For the production of these composite materials various practices are currently in use such as squeeze casting, liquid metal infiltration, powder metallurgy etc. among such production techniques stir casting is

most preferably used. This has good dimensional accuracy and surface finish due to minimized presence of casting defects also it gained lot of attraction among researchers and manufacturers to obtain best quality products.

1.4 Aluminium and its Alloy A356.2

Next to oxygen and silicon the third most richly available metal is aluminium. Aluminium find its application in various sectors like aviation, automobile, marine, and electronics etc. due to its reasonable pricing, impressive thermal and electrical properties, less density and great ductility. It is highly preferable because of its light weight which is $1/3^{rd}$ in weight when compared to steel. Due to the presence of inherent oxide film aluminium has a natural tendency i.e. resistance to corrosion. The hard outer oxide layers with its self-renewing potential prevent the inner surface of aluminium from corrosion to a certain extent. Due to the existence of excellent qualities namely increased specific strength, high temperatures, excellent structural and dimensional steadiness and low co-efficient of thermal expansion in aluminium metal matrix composites is the main reason for its usage in various applications.

1.5 Damping

The energy dissipation process takes place in various elements and structural systems due to cyclic loading is defined as damping. Vibrations, noise and fatigue failure has to be reduced to a greater extent for the reduction of elastic waves in structures for many practical applications. There has been a progressive research that is being taken place for the attenuation of vibrations since the past five decades. To reduce both the internal and external vibrations during the world war a large variety of military equipment has been developed. The government has issued firm regulations on sound emissions due to noise from vibrations which are mostly considered has environmental hazards. The Federal Aviation Regulations (FAR) and Joint Aviation Requirements

(JAR) have issued serious laws on aircraft sound emissions. Automobiles with lower NVH (noise vibration harshness), levels and electronic appliance with lower noise emission attained popularity in day to day situations.

To supress the unwanted vibrations and noise researchers and industrialists explored various techniques such as encapsulation of vibrating source, addition of vibration absorption device to the material. The latest method is fabrication of modern materials which inherit the property of absorbing vibrations. Out of all these methods designing materials that dissipate vibrations to much great extent is the best method in comparison to the other methods as it reduces price, complexity, weight, and enhance functionality. In extension to it an alternative and an innovative approach is coating of components which is evidenced more efficient in vibrations reduction. Thus along with the other characteristics of the materials namely toughness, stiffness, tensile strength, thermal conductivity etc. damping capacity has also gained the equal importance. Most monolithic metals render high strength and stiffness but they often tend to produce unwanted vibrations that lead to the mechanical failure of the system. Thus, higher damping metal matrix materials are being developed to improve the reflexive damping characteristics, strength and stiffness and to overwhelm the unwanted phenomena.

Properties such as low weight and high strength stability of aluminium metal matrix composites has led to various applications in various fields such as automobile, aerospace and marine. These aluminium metals are prone to vibration losses. To maintain higher stability of the core system, the components which are used in aerospace and automobile sectors requires materials with desirable properties such as high stiffness, higher strengths and higher damping capacities. It is also a known fact that surface coatings on reinforced substrates have higher damping capacities to a great extent when compared to uncoated specimens. To enhance the energy dissipation,

coating contents, coating thickness and the intermetallic phases of the coated area plays a very vital role. Therefore, exploring and developing modern surface coated composite material system with remarkable damping characteristics and excellent mechanical properties is the need of the hour.

1.6 Coatings

Due to adverse environmental effects various monolithic metals, non-metals, composites etc. are vulnerable to various external affects. A material life will have great threats due to those effects.The materials surface is exposed to the chemical, thermal, electrical and mechanical actions. To safeguard and protect the materials, superficial surface treatments are employed. To achieve the desired characteristics, surface modification plays a vital role. This can be done in many ways among which mostly used is coatings.

Tiny coating layers are applied to improve the perilous characteristics of the surface of base material known as substrate and to act as intermediate obstacle against environmental deteriorations. To increase the life and for aesthetic enhancement and other functions, coatings are used as a post process technique. Coatings may be applied to few parts of the substrate or the entire substrate. For effective usage and extension of the materials life different ways like chemical vapour deposition, conversion coating, thermal spraying, and electro chemical are effectually employed. HVOF coating of a spray process is more widely used among these different coating methods because of its availability of a variety of materials. The coated layers can be stripped off from the surface of the materials without any changes to the component. The materials available for HVOF coating process are metals, alloys, ceramics, plastics and composites. . Based on the heat source, the thermal spray coating process can be classified as shown in following flow chart Fig 1.2.

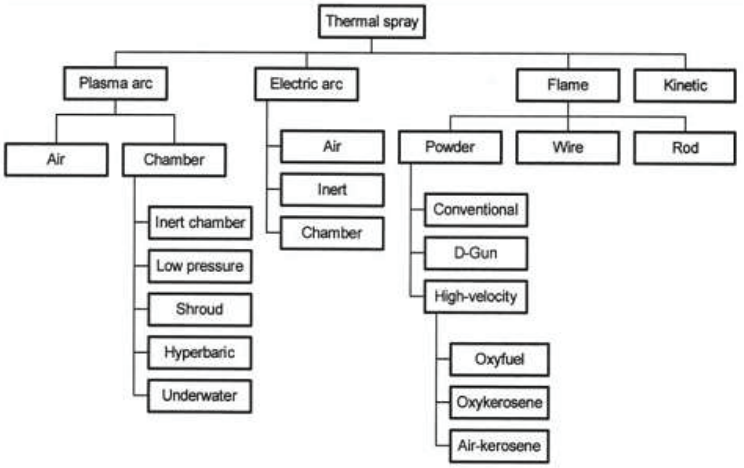

Fig 1.2: Classification of thermal spray process

1.7 Motivation of the Work

In most of the metals vibrational energy losses are pervasive. These will have various opposing effects on the materials life as well as on the effective functioning. Substrates with various coating applications is the feasible way to reduce the unwanted vibrations. Metal matrix composites and coating techniques often involve higher fabricating costs. The base metal and reinforcement systems employed for composite fabrication are narrowly available and pose a serious threat of extermination of the natural resources. The present researcher is predominantly enthusiastic about developing a low cost, abundantly available and highly efficient surface coated metal matrix system with high damping capacity and enhanced energy dissipation. Although many research enthusiasts have investigated the damping behaviour of aluminium alloys and conventional aluminium alloy-based composites, there is dearth of investigation regarding the damping of WC-Co coated A356.2 alloy reinforced rice husk ash particulates and hence, the present dissertation mainly aspires in developing a low cost WC-Co coated metal matrix system with improved damping capacity.

1.8 Objective of the Work

The objectives of the present work are:

- To fabricate Al/RHA composites via liquid state processing technique.
- To study the mechanical properties like tensile strength, hardness and density of the base alloy and Al/RHA composites.
- To deposit WC-Co coating on the base alloy and Al/RHA composites through HVOF technique.
- To obtain an optimal coating thickness numerically using MATLAB for maximum *E*tanδ.
- To optimize the parameters for Wire Electrical Discharge machining to obtain maximum damping capacity.
- To investigate the damping behavior of base alloy and its composites.
- To investigate damping behavior of WC-Co coated base alloy and WC-Co coated Al/RHA metal matrix composites.

1.9 Thesis Organization

Chapter 2 includes a detailed discussion of the literature relating to the matrix material selection, strengthening mechanisms, different fabrication techniques involved in MMC's, coatings and damping behaviour of the composites is presented.

Chapter 3 describes the detail description about the usage of various materials and methods used for the present study.

Chapter 4 illustrates the optimization of Wire EDM parameters for maximum damping capacity.

Chapter 5 depicts the microstructural characterization, mechanical and damping behaviour of base alloy and Al/RHA composites.

Chapter 6 presents the characterization and damping behaviour of WC-Co coated A356.2 alloy and Al/RHA reinforced composites.

Chapter 7 depicts overall conclusions and future scope.

CHAPTER - II
LITERATURE REVIEW

This chapter mainly focuses on the techniques and procedures that are used in several ways and their background information that is to be enlightened and correlated to the present work. Different alloys and metal matrix composite materials, types of coatings applied to those alloys and metal matrix composites, their mechanical and damping properties and their machining capabilities are also emphasized in this literature review.

2.1 Choice of Matrix Alloy System

The overall performance of the composite does not only depend on the fibres used but also depends on the matrix materials used during the fabrication process. Essentially main functions of the matrix material are:

- To give physical shape of the composite by binding all the fibres.
- For uniform transmission of load and stress between all the fibres to develop an efficient composite.
- Supports the overall structure.
- Protects composites from external agents such as chemicals and moisture.
- Protects fibres from damage due to loading.

The matrix is a sea of material in which the reinforcements are embedded in it. During the selection of matrix material the various considerations required are specific gravity, mechanical properties of the materials i.e. thermal conductivity, young's modulus of the material, coefficient of thermal expansion between the matrix and reinforcement, ultimate tensile strength, melting temperature, curing temperature of matrix, viscosity, reactivity with fibres, reactivity with ambient environment and cost. MMC's contains more appealing properties than organic matrix systems. Particulates

are entrenched with the matrix material so that now they are feasible to exhibit good strength and profound properties [12-14]. Uniform distributions of loads and stress is the significant property of matrix system. Composites may contain reinforcements as continuous or discontinuous. When compared to discontinuous reinforcements, continuous reinforcements offer more strengths to composites since the loading transformations between the fibres are uniform and these also render more toughness than compared to strength. Another criterion of matrix material is to absorb cracks. Under axial loading to have high strengths continuous reinforced matrix materials are selected [15-16]. They also possess properties such as high toughness, lower strength in multiple directions and are more ductile.

For isotropic materials, due to discontinuous fibres mechanical properties are independent to the direction of the applied force. These are more prone to stress cracking and have enhanced resistance against tensile loading. Although discontinuous reinforcement offers lower strengths in particular direction when compared to the continuous reinforcement these fibres can withstand higher loads in almost any direction which is not applicable with the continuous reinforced systems [17-18]. Continuous fibres render phenomenal properties under axial loading but are not best suited for transverse loading.

Composites performance mainly depends on the reinforcement and matrix materials to a great extent. So, during the fabrication of the composites the selection of reinforcement and matrix are to be considered accurately which is directly related to the service life of the composites. During the cyclic loading the matrix system behaviour changes rapidly. The selection of the matrix and reinforcements materials should be done carefully for high operating temperatures if not so, the difference in coefficient of thermal expansions leads to the failure of the composites. Whenever there

are differences in temperature between matrix and reinforcement, it is always important to consider creep and internal stresses affecting the metallic interfaces. Thermodynamically stable dispersoids are incorporated into the matrix system for composites operating in elevated temperatures. Low density and high thermal conductivity of aluminium and magnesium matrix materials have made their wide usage in almost all fields like marine, automobile, aerospace etc. The addition of minor alloying elements such as grain refiners should be avoided as they result in coarse inter-metallic compounds which reduce the tensile strength. Based on the matrix material, metal matrix composites are classified into the following types.

2.1.1 Magnesium MMC

Due to alluring properties of magnesium such as light weight and excellent performance behaviour, it has gained lot of importance during manufacturing. Magnesium Aluminium (Mg-Al) matrix material is most commonly used in engineering light weight structures, aerospace and military industries. Another, major applications of magnesium metal matrix materials are found in automobile sector that include piston rings, gears, bearings, connecting rods and disk shafts [19].

2.1.2 Titanium MMC

Titanium composites are known for their excellent qualities of maximum strength to weight ratio in comparison to typical monolithic materials. Most often used fabrication techniques of titanium metal matrix composite are matrix-coated fibre, foil-fibre-foil [20].

2.1.3 Copper MMC

Copper metal matrix composites endure high temperature resistant properties, elevated thermal conductivity and enhanced machinability. High electrical, thermal

conductivities, resistance to annealing, higher strength are obtained when the copper matrix is embedded with Al_2O_3 [21].

2.1.5 Super Alloy MMC

Super alloys are namely cobalt and nickel. Gas turbine blades uses super alloy based matrix materials. These matrix materials are predetermined for elevated operating temperatures. Reduction in overall stresses, higher tensile strengths and higher corrosive resistance can be easily achieved through these composite systems [22]. Liquid phase infiltration and solid state diffusion bonding are some of the processing techniques involved in fabricating these super alloy composites. All these commercially available class of composites endure greater strengths and modulus in comparison to the typical monolithic materials as shown in Fig. 2.1 [23].

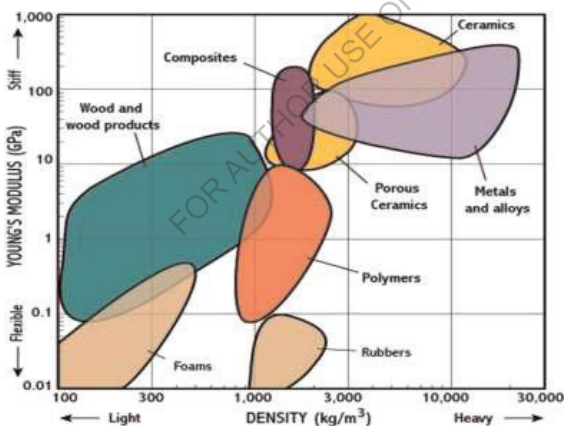

Fig 2.1: Strength versus density for different classes of materials [23].

2.1.6 Aluminium MMC (AMMC)

Weight is the main criteria of the material which plays vital role in various applications and fabrication techniques. Magnesium is of very low density i.e. 1.74 whereas the density of aluminium is 2.7 but the main drawback of magnesium is that it reacts with oxygen. Due to this, aluminium and its alloys are mostly used lightweight

materials. Automobile, aerospace industries profoundly uses aluminium based metal matrix composites mainly due to its exclusive properties of low density, higher strength, enhanced stiffness, controlled thermal expansion, higher wear resistance. Among the various types of cast aluminium, A356.2 aluminium alloy serves with some outstanding properties which enable its utilization in automobile transmission cases, aircraft fuel pump components, aircraft fittings and engine control units, flywheel castings, nuclear energy installations. A356.2 aluminium alloy fits under the group of hypoeutectic Al-Si alloys. This A356.2 alloy is most commonly used in complex casting shapes. These castings display enhanced properties like acceptable high strength to low weight ratio, outstanding wear, and fine weldability [24-26]. The mechanical properties of this alloy system depend on the microstructure of casting and the fabrication techniques employed. The key reasons for selecting A356.2 alloy are due to various factors such as abundant availability, higher strength, ductility, greater elongation, refined mechanical properties due to the lower Fe content and exceptional corrosion resistance.

The matrix material is either aluminium or aluminium alloy in aluminium metal matrix composites. The other constituents like zirconium can be embedded into the aluminium or aluminium alloy matrix which serves as reinforcements. The reinforcements embedded to matrix material system should be non-reactive and behave stable under elevated operating temperatures. With silicon carbide as reinforcement various characteristics like tensile strength, hardness, density and wear resistance of aluminium alloy are elevated [27-28].

Though magnesium possesses similar properties that of aluminium they are used less when compared to aluminium due to complicated fabrication techniques of magnesium, low thermal conductivity and highly reactive nature. Particle distribution which can be enhanced through intensive stirring performs a key role in boosting

properties of aluminium MMC. Al_2O_3 reinforcement yields greater wear resistance and compressive strengths [29].

Boron carbide material was very hard due to the presence of various characteristics like high modulus of elasticity and high fracture toughness. When boron carbide (B_4C) was reinforced with aluminium matrix the hardness was elevated to higher level, but change in wear resistance was not identified [30].The strength needed by the matrix and other properties are improved by the addition of fibres which categorize under vital class of reinforcements. Also, wear and corrosion resistance is elevated significantly by incorporating zircon hybrid reinforcement into aluminium core system [31].

Most frequently used aluminium metal matrix composites (AMC) are:

- Fly ash reinforced AMC
- Rice husk ash reinforced AMC

2.1.6.1 Advantages of aluminium metal matrix composites

Aluminium metal matrix composites has a prominent role in all sectors of manufacturing applications mainly due to its light weight. They have lot of applications in automobile industry. During the fabrication of aluminium metal matrix composite materials with low density reinforcements such as fibres, high strengths and stiffness is achieved. Due to this combination, high strength and stiffness to weight ratios composites are produced which are ideal for increasing demands for new materials. These composite materials are mainly utilized in lightweight objects such as, cars, trains and aircrafts which make them more efficient. The main objectives for the improvement of lightweight metal composite materials are due to improved damping properties and many other like higher yield strength, increased creep resistance, elevated thermal

shock resistance, improved corrosion resistance, higher young's modulus and low thermal elongation.

Aluminium matrix composites are used in almost all structural, non-structural, engineering fields due to their obvious benefits regarding environmental, performance and economical. Automobile, aerospace and marine sectors primarily use aluminium matrix composites due to cheaper and faster processing techniques, lower fuel consumptions and less noise emissions. The usage of various metals in the above sectors is shown in bar Fig 2.2.

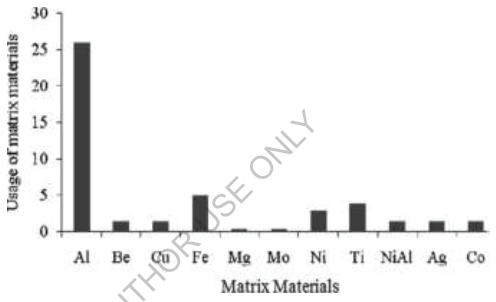

Fig 2.2: Usage of various matrix materials in MMCs [23]

2.2 Variety of Reinforcement Systems

Reinforcement is the main fundamental material that affects the mechanical properties of the entire composite system. There are different types of fibres used as reinforcements with each of their unique properties. The characteristics of the composite system depend on the kind of reinforcement used and its property. Reinforcements are responsible for the elevated strengths, stiffness, and high temperature resistance at much lower densities in metal matrix composites. Selection of reinforcement has crucial impact in determining the composites mechanical properties. A superior reinforcing material system should retain the following characteristics.

- ❖ Lower densities
- ❖ Exceptional chemical and mechanical properties
- ❖ Higher tensile and compression strengths
- ❖ Higher young's modulus
- ❖ Higher Thermal stabilities
- ❖ Ease of fabrication
- ❖ Economical in nature

While selecting the reinforcements various characteristics are to be considered such as size, shape, surface morphology, fabrication compatibility, micro structural defects. Among the various classes of reinforcements, particulate reinforcements attained popularity both by industrialists and research enthusiastic due to their low costs and wide range of availability. Depending on the strengthening mechanisms particle-reinforced composites are classified into the following two types:

2.2.1 Particulate composites

The matrix material is embedded with large granular size reinforcement during fabrication. These reinforcement materials are of high strength and stiffer than the matrix material. In larger size particulate reinforcements inter molecular reactions do not exist between the matrix and reinforcement and even restricts the free movement of the matrix phase. Therefore, under the application of various loads the matrix bears a small portion of load [32]. Mechanical characteristics of these composites depend on the nature of the bond that is formed between the matrix and reinforcements.

2.2.2 Dispersion-strengthened

In contrast to particulate composites, these consist of very small and tiny particles ranging from 0.01 – 0.1nm. Composites with these reinforcements possess property such as precipitation hardening. Inter metallic interactions nucleating between

the matrix and reinforcement is usually of molecular or atomic level [33]. The matrix materials hold maximum amount of stress exerted upon, whereas randomly dispersed particulates hinder the dislocations.

2.2.3 Cost effective reinforcements

Most often used reinforcements used by the industrialists such as graphite, alumina, boron carbide, silicon carbide are of more expensive. Among the various discontinuous dispersoids, one such reinforcing material which is abundantly available agricultural by-product, low density and of low cost is rice husk ash (RHA). When this is utilized as reinforcing material for aluminium metal matrix composites, it has elevated the mechanical characteristics of the resultant composite as in Fig 2.3 but reduced the fabrication cost incurred during the process [34-36]. Till date fly ash is used as reinforcements as it is easily available from thermal plants as a by-product and which is of low cost. The electromagnetic shielding of aluminium metal matrix composites is increased greatly when fly ash and rice husk ash particles are utilized as reinforcements.

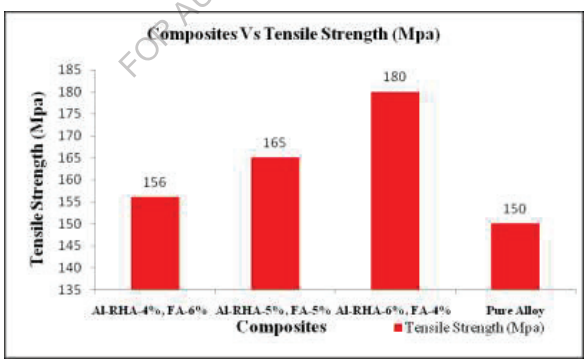

Fig 2.3: Variation of Tensile Strength vs Weight fractions of RHA&FA [34]

Aluminium matrix embedded with rice husk ash particles are more widely used due to elevated properties and of low cost [37-39]. When rice husk particles are reinforced with aluminium matrix, thus obtained composites possess various

characteristics such as low density, low thermal conductivity, light weight, and high electrical resistivity.

2.3 Selection of Composite Fabrication Process

During the fabrication of composites there are different scenarios such as:

- Material and the final product will be produced at the same stage.
- Material will be produced earlier and in later stages final product will be produced from the material.
- Development of intermediate materials and final product is produced at a different stage.

There are two main factors on which selection of fabrication process depends are:

- Chemical nature of the matrix material
- Temperature required to melt, form and cure the matrix material

After selecting a particular process it is to be confirmed whether it is a correct path or not. To identify the apt fabrication process the various factors that are to be verified after the fabrication process are:

- Uniform curing of matrix material
- Fibres shape and orientation
- Good adhesion between fibres and matrix material
- Voids and porosity should as less as possible
- Residual stress should be minimum.
- Surface finish of the composite must be very 2.4 Production of Metal Matrix Composites

2.4 Production of Metal Matrix Composites

In these, metals melt at high temperatures. So, for the fabrication of these composites, high temperatures are required. Materials properties and overall production

cost has a significant part in choosing the fabrication procedure. By altering processing time and fabrication methods the composite properties can be altered significantly even the same amounts and compositions of materials are used. Two major challenges to overcome during the processing of composites are:

- Finding a low cost technique for homogeneous distribution of the reinforced phase into the core matrix system in a desired volume fraction.
- To attain strong bonding between the reinforcement and the matrix body without any load failure.

Most often metal matrix composites are fabricated using two approaches i.e. solid and liquid- state processing.

2.4.1Solid-state processing

During the composites fabrication the metal matrix materials are processed in solid shape i.e. in the form of powders. Many techniques are available to process these metals in powder forms. Two methods which are more often utilised to produce composites are powder metallurgy and diffusion bonding.

2.4.1.1 Powder metallurgy

Since 1200 B.C ancient years this powder metallurgy fabrication is in vogue in some parts of the countries like Central Africa and India. From early 20^{th} centuries the usage of this fabrication process in the industrial sector was increased tremendously with the manufacturing of self-lubricating bearings. This technique is mainly used with the metal powders which have high melting points so that they will not be brittle when they are processed in liquid state. During the fabrication process of composites, the metal powders are heated to just below their melting points, so that they stick to each other at these temperatures. For the fabrication of composites when powder metallurgy is used, the blending of metals and reinforcements powders is excellent and they tend

to possess high particulate strengths to composites. The various stages of this technique are illustrated in Fig 2.4. This has extensive choice of operating temperatures in comparison with other processes, so minimizes the chance of inter molecular reactions between matrix and reinforcement materials. Powder metallurgy technique provides even distribution of reinforcement phases into matrix material and thus elevates stiffness and toughness and reduces porosity of the finished composites. Powder metallurgy overcomes the challenges by using materials with high operating temperatures, inequalities in melting points and densities between reinforcements and matrix materials and which cannot be processed using conventional casting techniques [40-41]. Even though powder metallurgy has many applications it also has various limitations like they process is more expensive among the available with fabrication, maintenance and equipment costs.

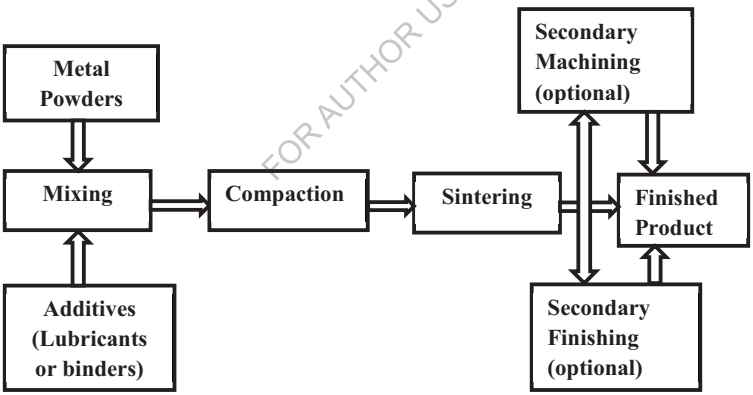

Fig 2.4: Schematic representation of powder metallurgy [42]

2.4.1.2 Diffusion bonding

This solid state fabrication technique mainly used for fibre reinforced composites. Here matrix and reinforcement materials are arranged in some pre-order fashion and by applying temperature and pressure the composite is thus obtained. This method uses long fibres as reinforcement material and matrix material used are

traditional metals and alloys in sheets form. Due to embossing or due to hot pressing bonding takes place between matrix and reinforcement material. In some situations reinforcing fibres are plasma sprayed to have better bonding between the intermetallic phases of matrix and reinforcement materials [43].

2.4.2 Liquid-state processing

As the name implies, the matrix material is melted and taken into molten form in which the reinforcement fibres are added later to it and are allowed to be cooled and solidified in this processing system. Due to the molten state of the matrix material, inter metallic gelling of the matrix material and fibres is accomplished and the desired characters of metal matrix composites are achieved. To achieve better addition and to minimize the chemical bonding the coatings are also applied to the fibres. It involves main techniques such as squeeze casting, stir casting and situ process.

2.4.2.1 Squeeze casting

Since 1960, squeeze casting technique is being used as fabrication process. There is no gating system in this technique and the compaction of the molten metal is done with the help of dies thus avoiding air gaps, porosity and shrinkages due to application of large pressures. Before the starting of the fabrication process the dies are pre heated to the 300-400 °C. Liquid material is poured in the die and pushed into the die cavity at a speed of 10 m/s for compression. The molten metal is squeezed into the fibres which are pre-arranged in the mould at a pressure of 20-30 MPa to obtain a mixture of fibre and molten metal composite [44]. This technique requires high pressures in the range of 50-100 MPa to solidify molten metal and to improve properties such as high tolerances and appealing finished composites as shown in Fig 2.5 [45]. The resultant composites is allowed to cooled and solidify for 5 to 10 min and with constant application of ramming pressure the required composite casting is obtained.

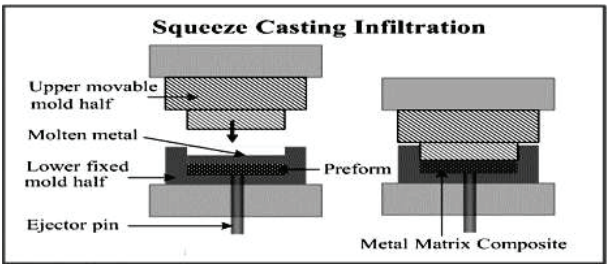

Fig 2.5: Schematic representation of squeeze casting [45]

2.4.2.2 Stir casting

The most frequently used production method that is the least cost and that can be done with more ease is stir casting. Stir casting process attains better adhesion among particles due to the stirring action. In this technique the reinforcing phase which is usually in powder form is embedded into the molten matrix material. Mechanical stirring plays a vital role in this procedure depicted in Fig 2.6. For this process categorizations of reinforcement particles needs lot of attention. The final fabricated composite depends on various criteria like particles wetting condition, solidification rate, relative density, geometry and placement of stirrer in the molten metal, melting temperatures, characteristics of reinforcement particles and strength of mixing. This method have paved a new path for the metal matrix composites fabrication [46-48].

In this process, the matrix material is taken inside the crucible and heated above the material's melting temperature until the entire material is melted and changed to the molten form. Then the powder form reinforcements are added to the crucible which contains the molten metal with constant stirring of mechanical stirrer for uniform blending of the mixture. This is carried out in inert ambient conditions to avoid oxidation. Vortex method is employed for uniform blending of reinforcements and matrix material until cooled slurry is formed and then casting is processed.

Two step mixing process in stir casting is developed through recent investigations. In this process the matrix material is heated above the temperature of its liquid state, causing this molten metal to cool down at room temperature between the level of liquid and solidus and to be held in semi-solid state. At this stage, preheated particles are added and then mixed. The slurry is then heated again to a complete liquid state and mixed vigorously afterwards.

The uniform blending and the mixing of the matrix material and reinforcement particles is due to elevated stirring speeds and time. The wettability characteristics of these materials can be increased by heat treatment prior to adding of matrix material and matrix materials are coated with wettable metals or alloys before the process [49-50]. By employing vacuum ambient conditions, extruding and rolling operations the porosity of the fabricated product can be reduced.

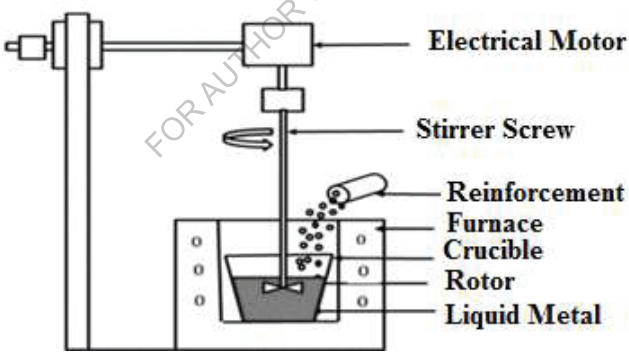

Fig 2.6: Schematic representation of stir casting [51]

2.5 Strengthening Methods in MMC's

The various methods that are available for strengthening of metal matrix composites are:

2.5.1 Dislocation strengthening

Density dislocations will appear in reinforced composites when compared to that of unreinforced materials. When there exists a thermal mismatch between a matrix and a composite material, and when external load is applied, due to the straining effect then these dislocations will occur [23]. The number of dislocations in a material is expressed as the dislocation density. The number of dislocations increases with plastic deformation.

2.5.2 Orowan mechanism

This mechanism is more often present in composites with fine discontinuous reinforced particles which are bonded firmly. By this mechanism the numbers of dislocations are reduced there by increasing the strength of the core system. This mechanism is not applicable to the strengthen composites which contain reinforcements of large coarse size [23].

2.5.3 Hall–Petch strengthening

This is also known as grain refinement strengthening, which strengthens the material core system by altering the grain size. This mechanism strengthens the composite by refining the grain structure and size there by reducing the dislocations. This method mainly depends upon the particulate grain size [23].

2.6 Coatings

To improve the perilous characteristics of the surface of base material known as substrate and to acts as intermediate obstacle against environmental deteriorations tiny coating layers are applied. To increase substrate life, for enhancing the look and functioning coatings is used as a post process technique. Coatings may be applied to few parts of the substrate or the entire substrate. For effective usage and extension of the materials life different kinds ways like conversion coating, thermal spraying, and

electro chemical are effectually employed. Among these various coating techniques High velocity oxy fuel (HVOF) coating of thermal spray process is more prevalently used due to large availability of various materials. These layers can be stripped and again recoated without any harm or changing the component. The materials available for HVOF coating process are metals, alloys, ceramics, plastics and composites.

Before applying the coating, the substrate material has to be grit or sand blasted for better adhesion of the coating.

2.6.1 Sand blasting

Sandblasting technique is an abrasive machining procedure and it more prevalently for strengthening of surface [52]. This surface treatment is also prevalently used for other conditions such as Surface alteration [53], cleaning and removal of rust [54-55]. This can be used for many types of materials. This process is appropriate for all types of specimens for a best surface treatment [56].

Abrasive blasting also called as sand blasting, is a process of powerfully bombarding of abrasive grits on to the targeted workpieces under high pressure of compressed air to obtain smoother surface or to remove any impurities present on the workpiece [57]. Many materials are used for sand blasting process such as sand, glass beads, walnut shells, bits of coconut shell etc. Most widely used material as sand blasting grit is Quartz, which is also known as silica. Sand blasted samples have shown improved properties in terms of grain elongation, hardness of material and ultimate tensile strength. The materials used in the test are parent material (PM), mechanically formed materials (MF), and laser formed materials (LF), parent material sand blasted (PM_SB), mechanically formed sand blasted (MF_SB) and laser formed sand blasted (LF_SB). The patterns formed are as shown in Fig's 2.7, 2.8and 2.9 [58]. Kosmac et al [59] stated that sand blasting is a powerful procedure than compared to grinding since

grinded zirconia elements has strength degradation and hence sand blasted is more preferred.

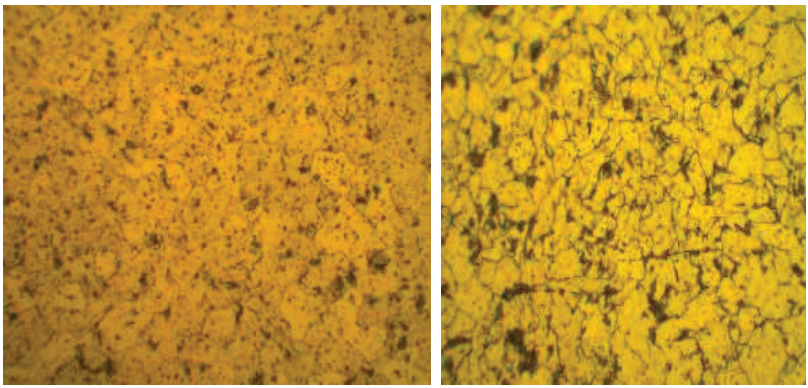

Fig 2.7: Microstructural changes before and after sand blasting PM [58]

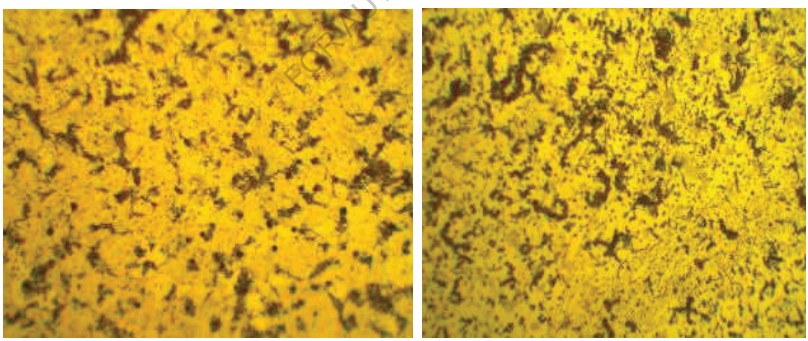

Fig 2.8: Microstructural changes before and after sand blasting MF [58]

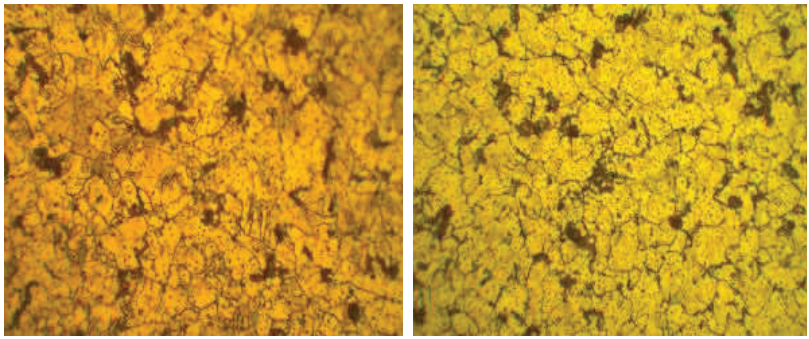

Fig 2.9: Microstructural changes before and after sand blasting LF [58]

As compared to sand blasting shot peening involves blasting surface of specimen by impacting with high velocity particles to produce plastic distortion and to yield a compressive residual stress which is considered an effective life enhancement process [60-61] and smoother surface is obtained during sand blasting then compared to shot peening. Xiaojun et al [62] have reported that due to the decreased residual stress and low carburization of the interlayer, sand blasted stainless steel exhibits better adhesion strength then compared to the mirror polished stainless steel and due to sand blasting stainless steel has phase transformation and surface roughening as shown in fig 2.10. in 1870 [63]. This surface treatment process is often preferred to be applied to the various specimens of structural materials prior to adhesive bonding such as steel [64], titanium or titanium alloys [65-66], aluminium alloys [67], and polymers or composites [68].

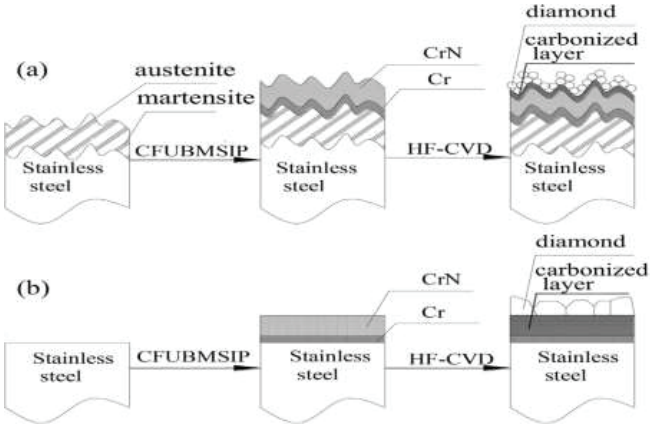

Fig 2.10: Schematic diagram of diamond film preparation on (a) stainless steel with Sandblasting and (b) mirror-polished stainless steel. [62]

The first abrasive blasting process was patented by Benjamin Chew Tilghnam

Bressson.et al [69] have reported that sand blasting relies on different parameters like compressed air pressure and grit particles type and size used for the process. Anna Rudawska.et al[70] have reported that both the surface roughness parameters and properties required for adhesion due to sand blasting relies upon on the grit particles viz. the size and shape rather than on the pressure applied during the processes and as the surface roughness increases, the dispersive component i.e. surface – free energy also increases proportionally. Formation of local plastic deformation and removal of oxide layer happens on the specimen's surface in the sand blasting process since the specimens are repeatedly bombarded by the grit particles with high pressure. Sun et al [71] have investigated that even other processes such as acid pickling and passivation used for corrosion resistance, sand blasted specimens have exhibited high corrosion resistance than above due to the phase change and dislocation density.

Micro - arc oxidation is a recently developed technique which is used along with sand blasting as pre-treatment on the titanium material that has an important part in

medical applications towards the improvement of bioactive properties and to have optimum performance [72].Tang et al [73] indicated that this was a powerful technique to enhance the composites surface bio-performances which is used as an implant material for orthopedic applications when compared with the surface produced using abrasive papers. Even titanium is most extensively used material for dental implants due to its properties and behaviour. Sand blasted zirconia implants was observed to have better osteogenesis and in bone growth [74]. Gil et al [75] have reported that shot blasted titanium dental implants improves fatigue life. The shot blasting process when combined with boronizing process increases the hardness of the material such as 316 stainless steel as depicted in Fig 2.11, but the roughness of the surface does not affect the hardness of the material [76].

Ji.et.al [77] have stated that the shot peening process have considerable effect on the fatigue performance of the ductile iron which can extend their fatigue life due to the existence of the residual stresses and work hardening which leads to density reduction and retardation of crack nucleation and growth.

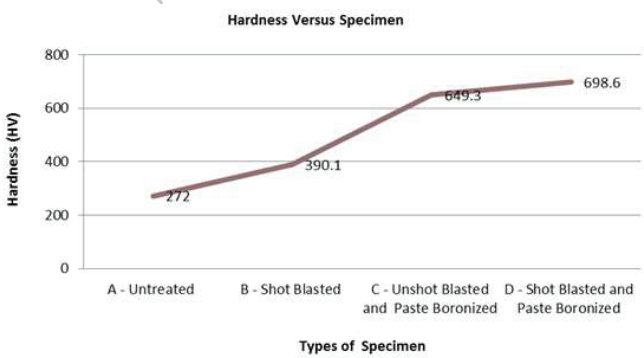

Fig 2.11: Hardness versus different types of specimen [76].

. He et al [78] have investigated that various shot peening techniques were used and the results have proven that all these techniques had similar investigations in the

deformation. During the comparison between metallic shot peening and laser shock peening, the later has almost complete absence of deforming twinning where this was frequently observed during the metallic shot peening due to localized work hardening, but the combination of the two processes LSP followed by MSP will produce a beneficial result than possible with either technique alone. [79].

2.6.2 HVOF coating process

This is a method where by powder material is melted and accelerated at extreme velocity, using oxygen and gas fuel mixture. This comprises various units. In this technique oxygen and fuel are mixed and ignited in a combustion chamber by allowing and accelerating the high pressure gas through a nozzle to produce gas stream. The powder is then added to this stream to be heated and accelerated towards the surface of the components as shown in Fig 2.12 [80-81].

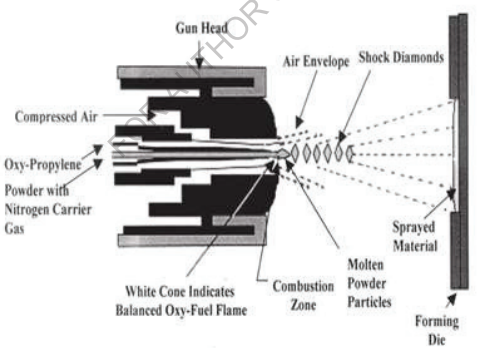

Fig 2.12: Schematic representation of HVOF process [81]

Plating's has shown more adverse effect on environment and health issues of the emission of Cr^{+6} ion known as Carcinogen as shown in Fig 2.13 [83-87]. The use of suitable coatings provides higher melting temperature, maintain high hardness and strength at higher temperatures, better emission, higher resistance towards corrosion

and oxidation. Thermal spray method has been popularly used as a beneficiary replacement for EHC plating technique. [83, 85-87].

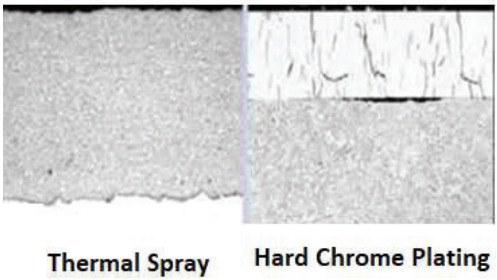

Fig 2.13: Comparison of HVOF and EHC Coating [83]

This method is more popularly utilized in various industrial sectors like cements and many other materials and metals [82]. The incorporation of several materials is done simultaneously to have effect on the continuous increase in the cost of materials and requirements, coating techniques has more wide applications in the present days. [88].To enhance the look and functions of the materials and to smoothen them coatings are chosen as substitutes.

Rao [89] had stated that, in comparison with other methods, coatings produced through HVOF technique displayed less porosity and incremental bond strength. Sobolev et al [90] have reported that various factors that affects coating are the temperature of flame and speed of the particle and these which differentiates them form the other methods as shown in Fig 2.14.

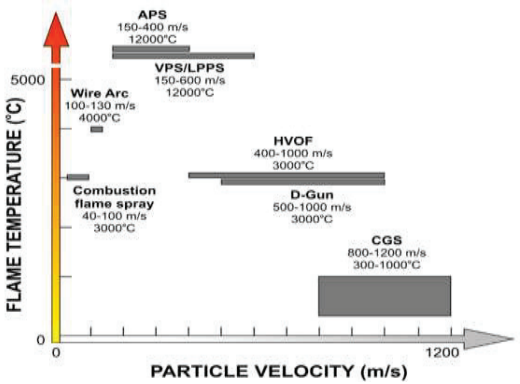

Fig 2.14: Flame Temperature *vs* Particle velocity of various processes [90]

Quality of the coatings depends significantly on the velocity and temperature of the powder particles impinging onto the substrate surface, which in turn is associated with the gas pressure developed in the combustion chamber. The 3rd generation HVOF systems work at elevated pressure ranging from 6-10 bar. In this process, some in-flight powder particles gets oxidized. This can be minimized by shielding the in-flight particles from the atmosphere by inert gas. Coatings used in the marine structure must be strong, hard and adherent. The formation of hard coatings are as a result of particles deformation not in the liquid state but in aplastic state. This is caused by the particles elevated kinetic energy in the HVOF process. The particles high kinetic energy leads levelling due to deformation, resulting in thick coats with less porosity and less oxygen which is a main feature of HVOF process [91-92].

Murugan et al [115] has developed an empirical relation to predict the hardness of the coating by selecting the substrate as naval brass and coating powder used is WC-10Co-4Cr. They have predicted that coating with optimal oxygen gas flow shows high hardness when compared with low or high optimal gas flow rates. Porosity and hardness are highly affected by the rate of powder feed rate. Higher feed rate has increasing effect

of porosity. The excessive melting of particles, vaporization and lower feed rates results leads to cracks and elevated porosity levels. At optimum condition low porosity and high hardness coating is achieved. When spray distance is short, substrate gets overheated, coatings will be dense but large cracks will be formed due to the internal stresses. When the spray distance is high, coatings obtained are of lower density as shown in Fig 2.15. Porosity decreases with high fuel rate, but at very high rate there will be gas entrapment and poor quality is obtained. As porosity increases, coating stiffness decreases and hardness value decreases. It is of utmost importance to choose and fabricate the optimum coating material. This is to maintain nice balance across all performances. The components such as spraying gun, its flow rates and distances, and powder structure i.e. powder size primarily and secondary and its method of formation etc. [116-117].

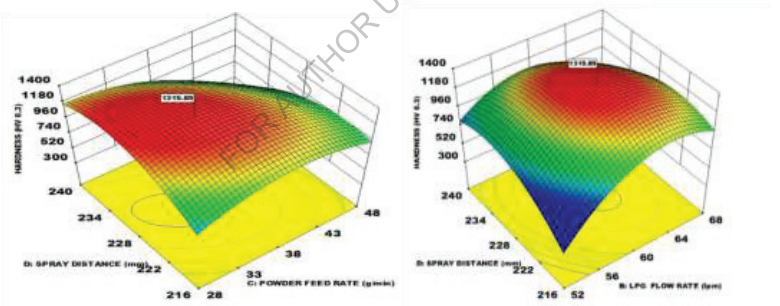

Fig 2.15: Effect of process parameters on coating hardness [115]

2.6.3 Effect of HVOF coating process on MMC's

The oxides such as Al_2O_3 and $CeAlO_3$ prevents formation of the carbides in the substrates [93].Cho et al[82] has investigated that metal carbides when combined with oxygen form coatings with high porosity and this can be reduced by laser heating. Also, porosity is decreased by 500% i.e. from 2.2 to $\pm$0.3% to 0.4 $\pm$ 0.1% and hardness of

IN718 (Inconel 718) coating was elevated by 320% which there by increases the durability of the machine components.

Nygards et al [94] while investigating the application of cermet coating on steel substrate by HVOF process, a sphere-shaped indentation of WC intender was applied and this stress was done on many specimens with and without coatings and the observed value for delamination is 7MPa. As per the observations of Maiti et al [95] while coating WC-9Co-5Cr powder on the stainless steel AISI 410 substrate, the samples with 200 μm grinded surface have shown increase in abrasive wear resistance by 64.3% and erosive wear resistance by 83.4%. This was due to the incorporation of residual stresses during surface grinding. SEM studies of worn out surfaces shows that carbide grain pull out due to plastic deformation of softer particles i.e. cobalt and chromium during abrasive wear cracking of tungsten carbide(WC)followed by carbide pull is due to erosive wear behaviour.

Picas et al [96] stated that two important materials of carbide namely CrC-NiCr and WC-Co systems are being utilized in thermal spray process. An increase in the resistance to wear and tear has been observed while using such coatings in automobiles. As compared to CrC-NiCr coatings, WC-Co system tend to be harder and give more wear resistance and the decarburization of WC into W_2C, W_3C and metallic phase results in deterioration of coating features and reduces the usage of these in a temperature range of 450-530°C [97]. Hence, WC-Co system is mostly preferred due to its firmness. This system is found to be harder than CrC-NiCr [98]. Various studies and researches indicated that corrosion and its related problems can be resolved by selecting the appropriate coating for different conditions. By improving HVOF technique, grain structure and surface properties have improved a lot. The

microstructure of the sprayed coatings and their properties plays a vital role on the particles during flight [99].

Cermet carbide composite coatings such as WC and $Cr_3 C_2$ are refractory compounds that have many advantages such as high hardness, certain plasticity and good wettability with the substrate [99]. Chen et al [100] had stated that the favorable combination of these properties can make these materials more popularly used for protective coating with enhanced resistance against erosion, corrosion and mechanical wear. Zhao et al [101] explained that, when WC-Co-Cr (WOKA 9010 Cr) was coated on the substrate mild steel –ST 37, it is identified that the particle and its coating properties are influenced by HVOF process parameters. Generally, in coatings wear resistance, total gas flow rate exerted have a great influence. To obtain a higher wear resistance gas flow rate is significant parameter to control than powder feed rate. As per elevated compression residual stresses observed in shot peening are found to be very useful to enhance the material strength. Increase in compressive residual stress is observed with intensity of shot peening [103].

Chun et al [104] researched that optimum method of coating and laser heating (LH) would influence the interface between the matrix and the substrate. LH process also, affects surface morphologies, porosity, hardness, friction and surface and wear characteristics. With HVOF process when Inconel 718 substrate is coated by WC-CrCNi powder and then followed by the heat treatment process, the researchers have identified that porosity was reduced by 7 times i.e. from 2.6 $\pm$ 0.4% to 0.35 $\pm$ 0.06%. It was also noticed that the substrate surface hardness was increased from 400$\pm$ 10 HV to 983 $\pm$ 100 HV due to optimal coating process and then increased to 1426 $\pm$ 94 HV by laser heat –treatment process. The friction co-efficient of the substrate surface is reduced from 0.45$\pm$ 0.08 to 0.35 $\pm$ 0.05 due to optimal coating process, later it was

further decreased to 0.23± 0.05 due to laser heat treatment. The substrate surface hardness was increased due to optimal process and further incremented due to the process of laser treatment as shown in Fig 2.16 and 2.17.

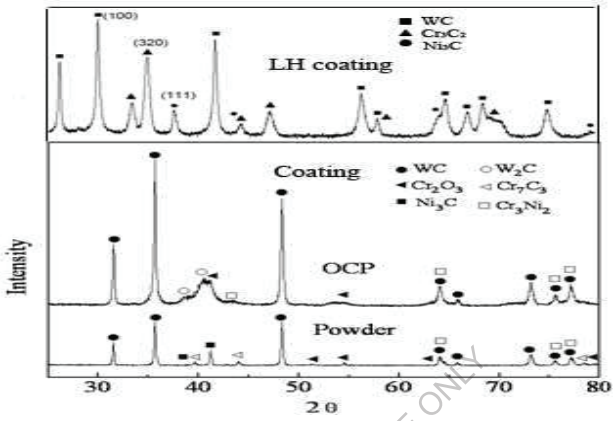

Fig 2.16: Crystalline phases in powder, coating and LH coating [104]

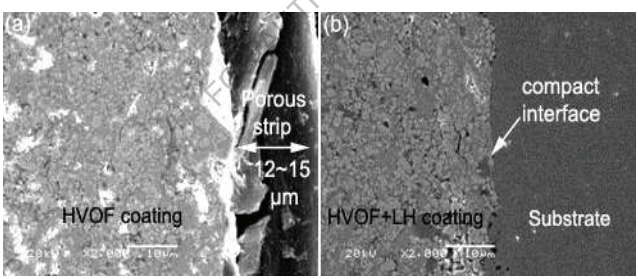

Fig 2.17: Cross section of the coating and LH coating near interface [104]

If the cold spray technique be operated at the spray materials temperature being less than its melting point then, trouble of decarburization can be cleared [97, 105]. To enhance the corrosion and wear resistance binders like cobalt and nickel were used to strengthen WC [106].

2.6.4 Effect of HVOF coating process on fatigue strength

In assessing a materials fatigue strength the importance of Substrate type and sprayed coating cannot be undermined [107].To overcome interfacial delamination, the thickness of the coating should be correctly balanced [108]. In fatigue behaviour consideration thinner coatings are better than thicker coatings (450μm) since the thicker coating has chance to increase the cracks [109]. Though the coating substrate bond is improved by surface preparation, due to grit blasting, the fatigue strength of the substrate decreases [110]. During grit blasting, particles that are retrained in the substrate increases fatigue cracks due to stress concentration hence decrease the fatigue strength [108-112].

Al-Fadhli et al [113] have identified that, coating failures are minimized when AISI stainless steel was coated by nickel based powder (NiCrMoNb) that is equivalent to Inconel 625. The coating was applied over the plain and welded substrates.There are fatigue cracks formed at the interface between coating and substrate, and in the coating itself. Coating micro structure and grit embedment dominated the fatigue behaviour of the coated surface. Presence of non-melted alumina particles of coating lead to the development of cracks at the interface that can be observed from the Fig's 2.18 and 2.19 which were examined before and after corrosion fatigue test.

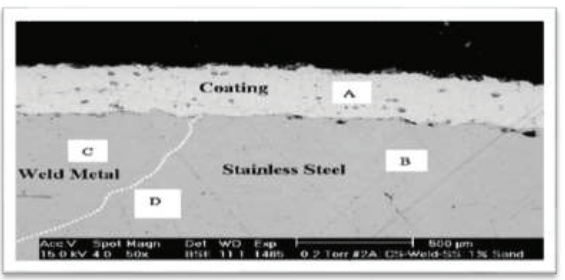

Fig 2.18: Sample before corrosion–fatigue test: (a) inconel-625 coating over stainless steel and weld, (b) stainless steel substrate, (c) weld and (d) heat affected zone [113]

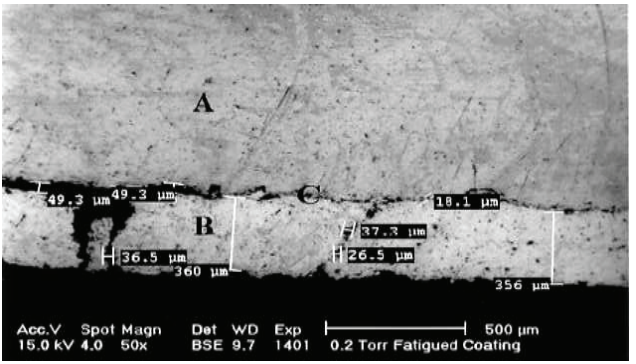

Fig 2.19: Sample after the corrosion–fatigue test: (a) stainless steel substrate, (b) inconel-625coating and (c) interface between coating and substrate. [113]

According to Voorwald et al [114] the shot peening procedure was useful in enhancing the fatigue strength of the base metal. Strength of the coated substituted was decreased by 17.6% as compared with the uncoated base metal due to the pressure of oxides and poses in the coating but this method enhanced strength of the coated surface by 13.3%.

2.6.5 Effect of HVOF Coating Process on Residual Stress

During the process of coating metallurgical changes may occur due to heating and cooling rates and this modifies the residual stress levels in it. High temperature gradients are developed in the HVOF coating, which result in the formation of high residual stress levels. Stokes et al [118] had analyzed that, as the thickness of coating is reduced, the residual stress level changes from tensile to compressive that were formed due to HVOF coating technique. Santana et al [119] identified that based on the properties of the base material and its coatings residual stresses are found to be tensile. Azar et al [120] examined that with an increase in the coating layers thickness the residual stresses levels also tend to increase.

Coated materials fatigue life depends on the residual stresses that are developed in that coating. This feature is also found to depend on the quantity of the tungsten carbide (WC) that is present in the coating [121]. Zhao et al [122] have observed the effect of the spray criteria on HVOF coating of WC-Co-Cr properties and revealed that resistance of the coating significantly lies on the flow rate of the gas. Taha et al [123] identified that during coating steel 304 with a mixture of diamalloy 1005 (Inconel 625) powder with WC particles, the percentage of WC increases while its temperature gradient has been decreased and that can be identified from the XRD Fig 2.20.

From the figure it was observed that small cells have been formed due to the presence of WC. Fatigue toughness and elastic modulus of the coating has been increased due to increase in WC contents. Further, this may lead to the increase in the residual stresses in the coatings.

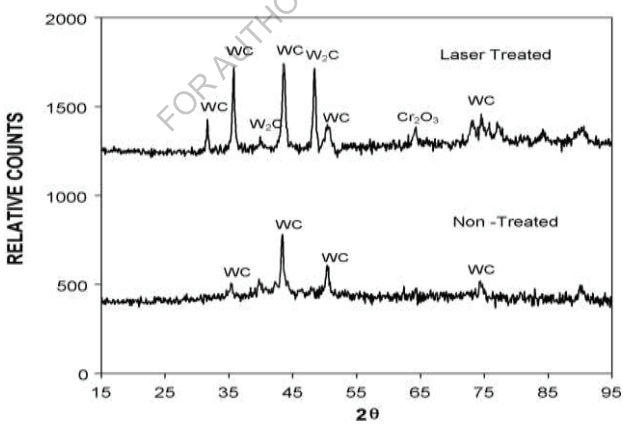

Fig2.20: XRD results for laser treated and un-treated coating [123]

2.6.6 Selection of HVOF Coating as an alternate to plating's

Compared to hard chrome plating which has negative effects [83-87], CrN based composites are found as one of the green manufacturing technologies. Such

coatings seem to be more thermal and firmer with high temperature and wear resistance [124-125]. Hai et al [126] reported that the coatings hardness were in the order as CrTiAlN>CrAlN>CrN. The phase structure of the composite film include Cr, CrN, Cr_2 N and TiN phases and CrTiAlN appear column crystal structure and CrTiAlN composite coated piston rings had high temperature wear resistance when compared to the others and chrome electro plating.

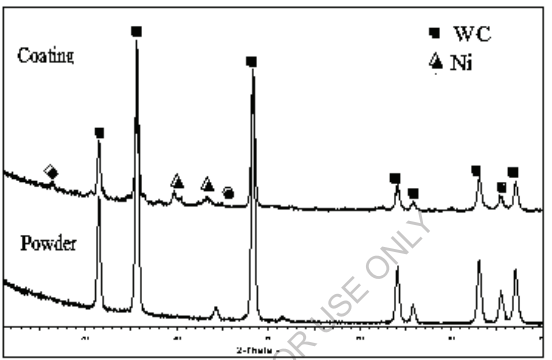

Fig 2.21: XRD patterns for as-sprayed HVOF coatings [127]

As per the suggestions of Ahmad et al [127] when a carbon steel blade is coated with WC-10 Ni, it recognized that WC particles get melted into Ni phases hence it has higher number of carbide particles as shown in Fig 2.21. The hardness of the coating also has been increased while porosity reduced.

Even though chromium carbide has excellent wear and corrosion resistance it is not mostly used in industrial applications due to its lower hardness and normal temperature (550 °C) when compared with Tungsten Carbide (WC) [128]. Chromium Carbide is used with the combination of Ni-Cr which improves the toughness of the coatings and also the ductility. These types of coatings are named as "$Cr_3 C_2$ – NiCr" coatings. Manjunatha et al [129] have reported that, when $Cr_3 C_2$ – NiCr was coated on

AISI 316 austenitic steel plates by HVOF process, it has been noticed that the erosion rate was decreased with increased NiCr content as it acts as metallic binder thus decreases the porosity of the coating as seen in Fig 2.22. Also, it is noticed that prior heat treatment of Cr_3C_2 – NiCr (85/15 %) at 650 °C has enhanced the erosion resistance.

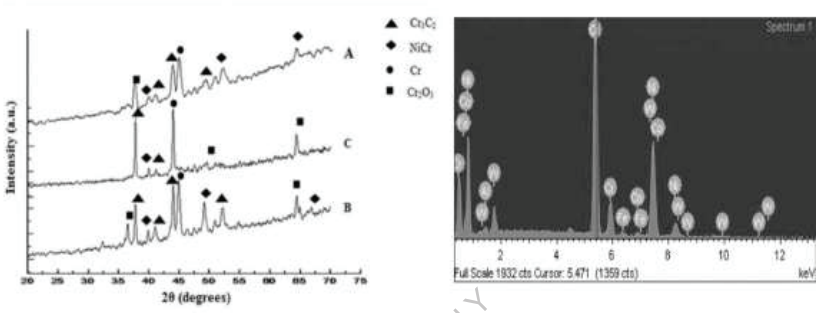

Fig 2.22: XRD patterns and profile mapping for Cr_3C_2/Ni Cr [129]

Hamatani et al [130] observed that coating with a carbon content of 0.58% mass has the most preferable properties with a good balance of hardness, strength and thermal shock resistance when carbide is sprayed by HVOF process on copper Ni electroplated substrate. This thermal shock resistance depended not only on the strength of the coating but also on the volume of contraction. Under the optimum spray distance hardness of 300 HV and adhesion strength of 200Mpa is achieved. Also 20% increase in adhesion strength, corrosion resistance and thermal shock resistance is obtained for NiCr-Cr_3C_2 coatings. Nickel Silicide (Ni_2Si) is an intermetallic compound that has multifunctional characters like low electrical resistivity, good corrosion and ear resistance [131-132].

Among different thermal spray processes, HVOF is most preferable due to its excellent properties [133-134]. Verdian et al [135] reported that when Ni_2Si intermetallic powders were used as coatings on the steel substrate, hardness, anodic

polarization behavior and composition of the coated powder was found to have same as that of the sintered material. Finally, they concluded that this behavior may be obtained due to the fine quality and dense coating structure of the coated material.

2.7 Damping

The energy dissipation process that takes place in various elements and structural systems due to the mechanical vibrations is defined as damping. Vibrations, noise and fatigue failure has to be reduced to a greater extent for the reduction of elastic waves in structures for many practical applications. Materials with higher damping ability lessen the vibration and noise arising in a system. Damping is of peculiar interest for designers and dynamists who are anxious with development and analysis of equipment which is intended to sustain in the mechanical environment. Materials with satisfying damping and mechanical properties are utilized in marine, aerospace and automotive industries.

2.7.1 Damping of Metals and Alloys

Characterization of the damping capacity of commercial metals and alloys is immensely sensitive to the testing's conditions like frequency, temperature, and strain amplitude, stress field state, humidity, specimen geometry and specimen grip system. Damping index which is also termed as specific damping capacity is determined as a shear stress equal to one-tenth of the tensile yield stress at 0.2% strain offset. Damping capacities of different materials can be compared using the damping index. However damping index does not give accurate values. So, it can be used as a scale due to variations in damping which is based on strain amplitude. Typical monolithic metals have lesser damping capacities. Much stiffer and stronger metals tend to possess lower damping capacities as shown in Fig 2.23. For instance modulus and damping loss factor

for aluminium is 72 GPa and 0.0001 whereas for magnesium the damping and modulus values are 40 GPa and 0.005 [136-137].

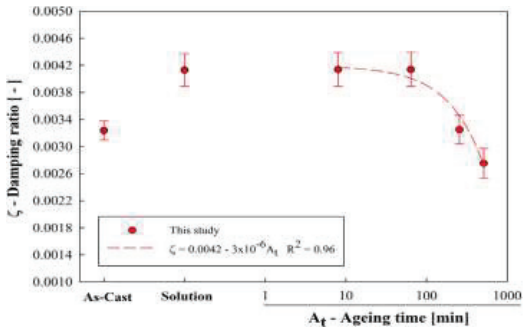

Fig 2.23: Damping ratios for different heat treatments. [136]

Damping behaviour was first studied by Coulomb in the year 1784 under torsional vibration conditions. This marked up for the beginning of various research works on higher damping materials. Damping related mechanics were first demonstrated by Lazan in the year 1968 [138-139]. Traditional magnesium serves as excellent damping material but has substandard mechanical properties. In order to overcome this flaw soluble alloying elements like aluminium may be added to it. Tian et al [140] showed that the alloying particles of Mg-Si alloy system displayed better damping and mechanical properties in comparison to typical mono metal systems due to the presence of Mg_2Si brittle phase [141]. From, the previous literature it is concluded that various characteristics attributed for elevated damping capacities [142-143].Well damped materials should be efficient enough to dissipate energy even at higher frequencies and temperatures.

2.7.2 Damping Behaviour of Metal Matrix Composites

The interest to explore materials with good attributes has gained attention in recent years. MMCs are considered as best option. Materials with good damping and

mechanical properties are desirable in several applications such as aerospace, marine, automotive, etc. The introduction of reinforcing particulates with high intrinsic damping properties improves the damping behaviour of MMCs by changing the grain structure [144]. Discontinuously reinforced composites have gained considerable attention because of their improved mechanical properties and prominent damping properties. Aluminium reinforced metal matrixes are the most frequently used MMC in various sectors because of due to less density also their ability to dampen unnecessary vibrations as shown in Fig's 2.24 and 2.25[145].

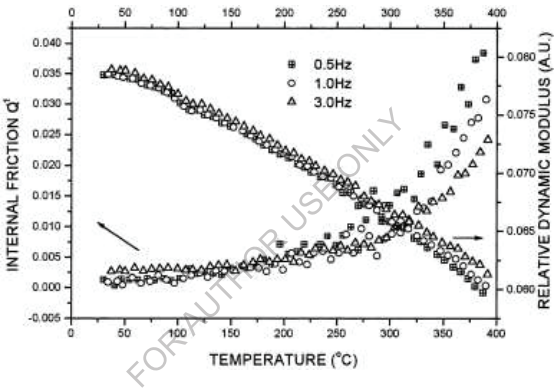

Fig 2.24: Internal friction spectrum as a function of the temperature for the commercially pure aluminum, cycled between 25 and 400 °C. [145]

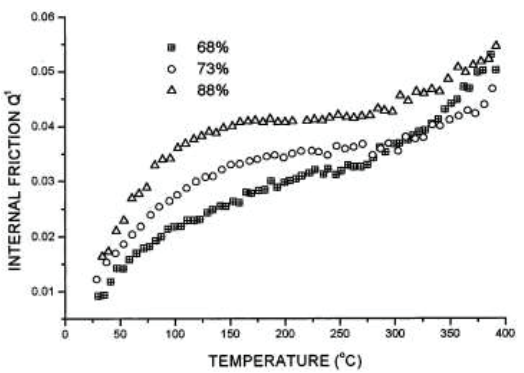

Fig 2.25: A total of 1.0 Hz comparison of internal friction of Al/Gr MMCs [145]

In addition of reinforcements like SiC [146-151], graphite [152-154], Al_2O_3 [155-156], oxides, nitrides, ceramics have been researched extensively. Traditional aluminium displays relatively lower damping capacities, incorporating stronger reinforcing materials that enhance the matrix microstructure thereby increasing the damping behaviour. Zhang et al [157-159] reinforced aluminium matrix with SiC, graphite and Al_2O_3, and observed that both SiC and Al_2O_3 reinforced composites showed similar damping capacities as the unreinforced aluminium alloy at 50 $^{\circ}$C. When the working temperature is elevated to 250 $^{\circ}$C the SiC and Al_2O_3 reinforced composites showed similar damping values than the unreinforced alloy. This exceptional damping phenomenon can be attributed due to thermally induced grain boundary damping, higher dislocation densities and interfacial damping. Lavernia et al [160] stated that inclusion of tiny fibre particulates in the aluminium alloy enhances its damping capacity when compared to the unreinforced alloy. The damping behaviour of Al-Li-SiCp composites was researched by Ranjit and Surappa [161]. Wei et al [162] noted that with a larger volume fraction of the reinforcements, the damping capacity of pure aluminium reinforced with graphite particles has increased. Zhonghua et al [163] concluded that, number of microscopic pores occurring at graphite aluminium interphase has altered the damping properties exceptionally.

Rohatgi et al [164] reviewed about the damping behaviour of Al based composites reinforced with silicon carbide and graphite particles. In comparison, Srikanth et al [165] stated that the damping capacity increased with the incorporation of SiC particulates in magnesium. Addition of CaO reinforcement on to the magnesium matrix system has altered the ultimate tensile strength and damping behaviour and was reported by Dong et al [166]. Damping behaviour of 8090 Al alloy strengthened with

SiC particles was inspected by RanjitBauri et al [167] by employing GABO Eplexor dynamic mechanical analyser. Observations were conducted under the application of a dynamic load of 10 N at four different frequencies i.e. 0.1, 1, 10, 20 Hz, and shown in the Fig 2.26. With the addition of the reinforcement the materials damping capacity tends to increase and this can associated to higher interface, grain boundary and dislocation damping.

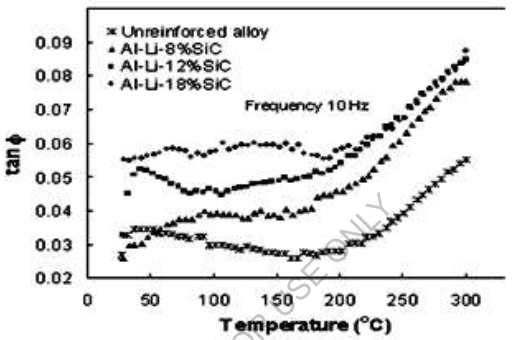

Fig 2.26: Damping capacity of the unreinforced alloy and the composites as a function of temperature at 10 Hz [167]

Deng et .al [168] studied the damping characteristics damping characteristics of the composite specimens were examined at frequency of 0.5, 1, 5, 10 and 30 Hz, from temperatures 25 – 400 $^{\circ}$C using dynamic mechanical analyser. It was concluded that at 0.5 Hz and at 400 $^{\circ}$C the CNT/2024Al reinforced composite showed the highest damping capacity even at elevated temperatures without affecting the mechanical properties. Dunnad and Mortensen [169] reviewed that the elevated damping capacities in MMC's are accounted for the initiation of plastic stretch around the metallic interface that is because of thermal mismatch in matrix and reinforcement systems. Taya and Arsenault [170] reported that the damping behaviour is usually altered because of high density dislocations occurring in intermetallic phases between materials. Bishop and

Kinra et al [171] concluded that incorporation of ceramic phases leads to increased energy dissipation due to the thermoelastic damping. Srikanth et al [172] reported that the incorporation of titanium particulates into aluminium core system has elevated the damping behaviour and the total stiffness of composite material. This may be due to the existence of brittle intermetallic phases. In a case study by Thirumalai and Gibson [173] it is concluded that the iron fibres fused with aluminium matrix has reduced the overall damping capacity, conversely it was noted by Liu et al [174] that the energy dissipation has enhanced with the enhancement the volume % of iron wire of aluminium matrix.

2.7.3 Damping behaviour of cost effective reinforced MMC's

Ceramic hollow sphere fly ash particulates are a kind of reinforcement, which is inexpensive, low density and available abundantly in large quantities and which is being used by researchers in enhancing the damping capacity of MMC.

Sudarshan and Surappa [175] identified that fly ash/A356 MMCs, exhibited increased damping capacity at medium temperature. One more type of reinforcement with lesser density is RHA which is found abundantly across the globe. With the inclusion of RHA particles damping improved significantly [176-177].

A detailed review on the damping behaviour of metal matrix composites has been presented by Prasad et al [178] and the scanning electron micrograph is shown in the in Fig 2.27. Wu et al [179] stated, with inclusion of fly ash in aluminium has elevated damping capacities in comparison to the unreinforced alloy. Yadollahpour et al [180] inspected that, reinforcing the metal matrix improves the damping behavior in comparison with the conventional alloys.

The influence of the grain size, intermetallic phase thickness, volume fraction and type of reinforcement of energy dissipation and dislocation mechanisms have been

investigated by Jian et al [181]. It is seen that the fly ash content in aluminium matrix improved the overall temperature resistance of composite.

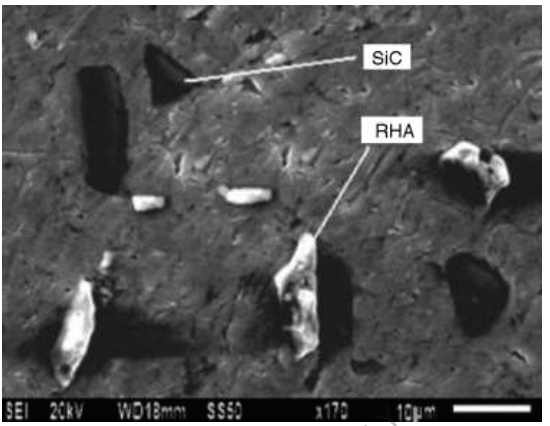

Fig 2.27: SEM image of hybrid composite [178]

2.7.4 Effect of Heat Treatment on the Damping Behaviour

Heat treating of Al-Mg-Si alloy has striking impact on the damping capacity. Hu et al [182] reported that the higher damping behaviour can be accounted due to the grain boundary sliding and dislocations that arise between the impurity atoms or vacancies. Further the same was demonstrated by Zhang et al [183] that heat treating TiC/AZ91 composites has improved the damping characteristics. Yu et al [184] witnessed that heat treating Cu-Al-Mn alloy specimens enhanced damping capacity, that reaches to the peak value at 60 $^{\circ}$C and starts to lessen with increasing ambient temperature as seen in Fig 2.28.

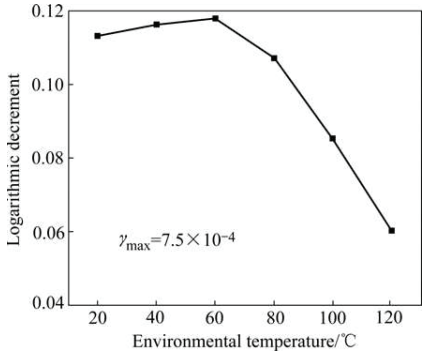

Fig 2.28: Influence of environmental temperature on logarithmic decrement of samples [184]

2.7.5 Effect of Metal Coatings on the Damping Behaviour

The damping behaviour of stainless steel substrates coated with NiCrAlY using arc ion plating technique was analyzed using dynamic mechanical analyzer by Guangyu [185]. It was concluded that fine network of Ni_3Al formed on the coated metal surface and adequate micro voids aided for better energy dissipation. In another study by Limarga [186], the energy dissipation of PWA 1484 single crystal super alloy substrate coated with nickel aluminide and yttria-stabilized zirconia (EB-YSZ) is reviewed. It was noted that the diffused aluminide bond-coating elevated the damping capacity for about 50% more than uncoated super alloy. This increased damping behaviour is accounted for the nucleation of γ-Ni_3Al phases at the sites of the metallic interface which is initially in β-NiAl phase when deposited. Similarly vapor deposited $Gd_2Zr_2O_7$ yielded higher damping capacities at much elevated temperature than the 7YSZ coating making it more preferable for compressor blade applications.

Damping characteristics of SnO_2 Bi_2O_3 coatings on pure aluminium substrates reinforced with alumina borate whiskers was reviewed by Liu et al [187-189] using a dynamic mechanical analyzer. And it was stated that the build-up of Bi–Sn eutectic at

matrix and filler interface resulted in enhanced energy dissipation due to energy dislocation damping and interfacial slip mechanisms occurring at lower temperatures. It was further stated that grain boundaries also exhibited viscous behaviour at elevated working temperatures and at low frequencies yielding higher damping peaks. The damping behaviour of the coated specimens showed up increase in energy dissipation due to coating constituents. The increased damping capacities at elevated temperatures and frequencies are due to the thermoelastic and interfacial slip damping which causes the softening of Bi sited at Al/Bi interface. The tensile strength and the damping properties are greatly enhanced upon increasing the coating contents. This feature is evident by observing reduced number of micro voids that occur on the substrates which exhibits better adhesion.

The damping properties of vapour deposited TiN coatings on 304 stainless steel have been greatly improved due to high density dislocations occurring at the metal matrix reinforcement and the martensitic transformation from 'γ' to 'α' was reported by Colorado [190]. Jinhai [191] reviewed energy dissipation behaviour of copper electroless deposited silicon carbide powders reinforced with pure magnesium particles. It was noted that interfacial damping enabled higher damping peaks at higher working temperature for Cu coated specimens in comparison to the uncoated specimens.

The damping characteristics of Rokide A (aluminium oxide) coatings on beam specimens are depicted in Fig 2.29 [192-193]. It was observed that maximum damping capacity of 0.066 at elevated temperatures is due to the interfacial damping occurring between the lamellar interfaces. The modulus of elasticity tends to be minimum at higher strain rates due to poor interfaces and is maximum at lower strain rates due to recovering interfaces.

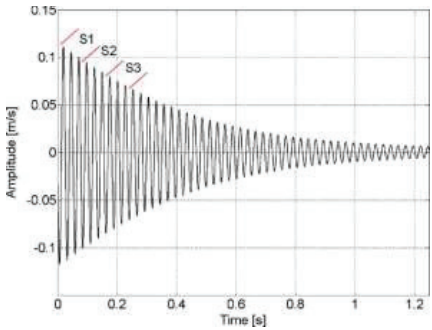

Fig 2.29: Typical decay curve from the Rokide® A coated specimen (22°C) [193]

The damping behaviour of Inconel beams coated with yttiria-stablized zirconia using two different deposition techniques was reviewed by Gregori [194], the zirconia coating deposited through APS yielded better energy dissipation because of the local movement occurring at interfaces and reduced elastic stiffness due to porosity which causes voids and splats.

Kantesh [195] examined that Al_2O_3-CNT nano composite coating has elevated damping capacity i.e. from 0.26 to 0.39 with an increase in the contents of coatings i.e. 8 wt % CNT. Conversely Qing et al [196] investigated that SiC coating on carbon reinforced silicon carbide composites has not displayed any important impact on the damping properties, reduced damping capacities are accounted for decreased porosity and microstructural changes arising in the materials.

Potekhin et al [197] identified that porosity of the coating is responsible for non-uniformity of the stress state which leads to low damping properties in the coatings. This damping behaviour was observed after applying coating without annealing and after 2 hr annealing at 1000°C as shown in Fig 2.30.

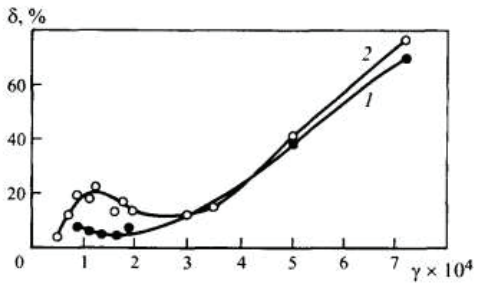

Fig 2.30: Amplitude dependence of the internal friction of the specimens 1)in the initial state 2) after 2-hr vacuum annealing at 1000°C). [197]

They also identified that two compatible damping mechanisms magneto mechanical and dislocation mechanisms can be combined in one specimen. In ferro-magnetic materials, magnetoelastic coupling is the main source for internal friction which leads to high damping capacity. On this basis to reduce voice and vibration damages high damping alloys have been developed such as high chromium ferritic steels which possess good mechanical properties and high corrosion resistance [198].

Amano et al [199] observed that Fe-Cr-Al alloys, magnetic properties and loss capability are responsible for reduction of vibrations and identified that even a small amount of aluminium will have significant effect on the damping capacity. And the damping value obtained was inversely related to the coercive force of the material. Karimi et al [200] observed that as received alloys exhibited low damping capacity than the annealed samples. They also understood that plasma sprayed coatings required more annealing process than cast alloys. An alloy containing Al compositions possessed high damping capacity than that of the alloys which contains Mo as composition and these coatings have low damping capacity than that of cast alloys. This feature can be observed from the Fig 2.31.

Patsias et al [201] investigated hard coatings on internal as well as external surfaces. The effective damping is noted to be linearly proportional to the thickness of the damping. But an oversize of the coating thickness will have an adverse effect on the strength of the entire coated structure [202].

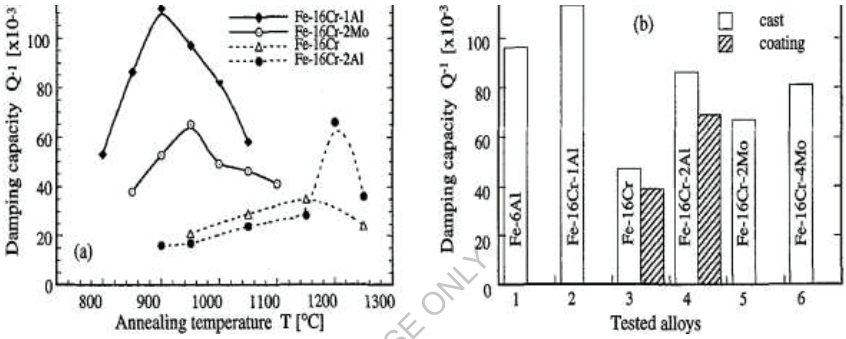

Fig 2.31: Effect of annealing on the damping capacity. a) Further annealing decreases hysteresis damping Q^{-1} solid line is cast alloy and dashed line is coating
b) Comparison of the maximum damping capacity Q^{-1} of various alloys [200]

Liming et al [203] tested the damping efficiency of the coated systems by varying the substrates and the coatings and perceived that there exists a thick coating layer that enables the coated material to get good properties as shown in Fig 2.32. The damping properties and dynamic mechanical characteristics of different types of coatings such as metal coatings, ZrO_2 ceramic nano coatings, quasi crystalline coatings and ferro magnetic coatings were compared by applying on the same substrate 1Cr 18Ni 9Ti stainless steel using plasma spraying technique and identified that the coated structures have high damping capacity than compared to the substrate and best dynamic mechanical properties were possessed by ZrO_2 ceramic nano coatings [204].

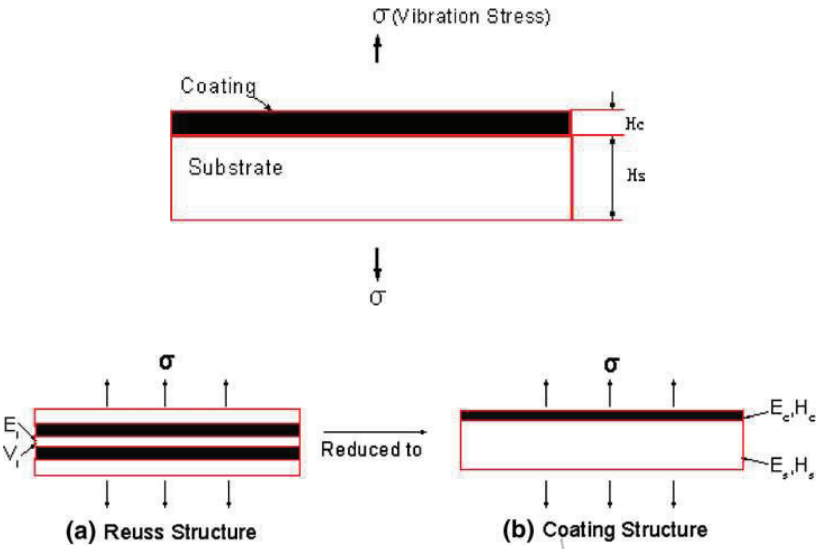

Fig 2.32: The sketch of a coating structure under vibration loaded. [203]

Blackwell et al [205] studied the damping features of mag spinel which was applied as a coating on both the sides of thin plates of titanium which resembled as turbine blades. Even at very low strains they have identified that mag spinel coated plates had tremendous improvement in the damping capacity. Shancan et al [206] fabricated a composite by MCrAlY as coating deposited on to the substrate by using two different techniques Air Plasma Spraying(APS) and Electron Beam Physical Vapor Deposition (EB-PVD) to observe the dissipation energy in both vertical and horizontal interface structures as seen in the Fig 2.33. They observed that damping capacity was high in vertical structures with high dissipation energy than that of horizontal structures.

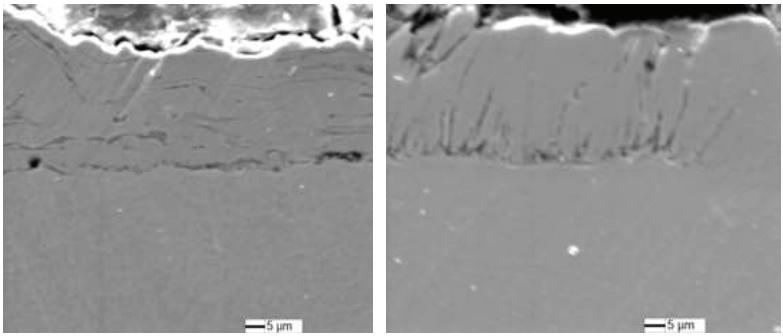

APS Coating **EB-PVD Coating**

Fig 2.33: SEM images of APS coating and EB-PVD coating's cross-section [206]

2.7.6 Effect of Wire EDM parameters on the Damping Behaviour

The effect of WEDM parameters like pulse-on time, pulse-off time, peak current and voltage on metal removal rate (MRR) and surface roughness of hybrid composites has been investigated [207-209]. Their findings reported that the MRR increases with increase in pulse on time and peak current while decreases with increase in pulse off time and voltage. Nihat Tosun et al. [210] investigated the effect and optimization of machining parameters on the cutting width and MRR in WEDM operations. Experiments were conducted to determine optimal parameters using Taguchi under varying pulse duration, open circuit voltage, wire speed and dielectric flushing pressure.

Works of Han et al [211] proved that the surface roughness can be improved by decreasing pulse on time, pulse off time and discharge current. From the earlier works, it was deduced that the damping capacity for wire cut EDM machined specimens exhibited low damping values when compared with milling machined specimens. This can be attributed to the formation of a white layer when the specimens are machined with the wire cut EDM process [212-213]. Also, it was reported that pulse-on time has a great influence on damping behaviour [214].

Prohaszka et al [215] discussed the effect of electrode material on machinability of wire EDM and discussed the improvements in WEDM. The effect of pulse on time, pulse off time, gap voltage, discharge current, wire tension and wire feed on cutting velocity and surface roughness was studied using Taguchi's orthogonal array by Bagherian Azhiri et al [216]. Results reported that pulse on time and current were found to have a significant effect on cutting velocity and surface roughness. Vishal Parashar et.al [217] also performed experiments using Taguchi orthogonal array on stainless steel by varying parameters like gap voltage, pulse on time, pulse off time, wire feed and dielectric flushing pressure.

2.8 Summary

A precise study is endeavoured to sum up the prevailing literature related to aluminium based MMCs and various coating characteristics, keen attempts have been made to grasp the minimum requirements of the ever blooming composite industry. This embraces different facets of the methods and features acquired. The conclusions drawn from this study are aluminium based metal matrix composites are mostly preferred over conventional alloys because of their excellent castability, low melting point, and wide-spread applications in engineering components. There exists a huge volume of information in the literature for different types of reinforcements and fabrication methods. It has varieties of methods for fabrication. Each having its own pros and cons. Many manufacturers and researchers enthusiastically preferred easy and low cost fabricating processes. Therefore, stir-casting technique has an important part in fabrication of the MMC's in commercial sectors today. Various strengthening mechanisms that strengthen the material core system are discussed.

High velocity oxy fuel (HVOF) coating is identified as an efficient coating that extends the material life by significantly increasing corrosion, wear resistance and

corrosion protection. Hence, the techniques, methodology and the influence of process parameters that are involved while coating and abrasive or sand blasting process are presented thoroughly. A detailed study is made on HVOF coating process on MMC's to understand the effect of the coating parameters on the fatigue strength of the base material and the development of residual stresses on the surface due to high velocity impact of the coatings.

To our best knowledge it is identified that there exists no literature regarding the damping behaviour of WC-Co coating on aluminium-rice husk ash particulate reinforced composites. Therefore, a deep learning is made to understand the research carried out from the past literature on the damping behaviour of metals, alloys, composites, heat treated composites and coated composites. As there is a high demand for low cost reinforcements, the cost effective reinforcement particles are primarily investigated in this study to incorporate into the matrix for the enhancement of damping characteristics. Also, significant research is carried out to know the effective Wire EDM parameters for optimal coating thickness while machining.

CHAPTER - III
MATERIALS AND METHODS

The present chapter chiefly describes about the various materials and methods used in current researcher work. By using stir casting technique A356.2/RHA composites with different weight percentage are fabricated. The basic mechanical properties like ultimate tensile strength, hardness and density of the composites were determined for the base alloy and A356.2/RHA composites. WC-Co coating is deposited on to the base alloy and MMCs using a high velocity oxygen fuel process. The samples for damping were machined using electronica wire electrical discharge machine. The mechanical damping is identified by Perkin Elmer dynamic mechanical analyser (DMA8000) for all the specimens. The microstructure characterization of the composites and the coated surface morphology is characterised using SEM and XRD.

3.1 Materials

3.1.1 Matrix material

Aluminium (A356.2) alloy is mainly considered for the present study by the researcher. It is third most abundantly available to next to oxygen and silicon. Aluminium is of smooth and soft texture and silver in colour. It is one of the most commonly used metals. It has low melting point and fabricated into low cost wrought and cast products such as foils, rolled plates, extruded tubes etc. When silicon carbide is embedded with aluminium, Al-SiC alloy has an excellent characteristic which has lot of engineering applications in our daily needs. A356.2 alloy among the available cast aluminium alloy has lot of applications in various sectors such as aircraft fuel pump components, automobile transmission cases, aircraft fittings, flywheel castings, engine control units, nuclear energy installations etc. A356.2 aluminium alloy comes under hypoeutectic class of alloy. This class of alloys consists of excellent features like fine

weldability, exceptional wear resistance which are influenced by microstructure characteristics and production methods used. Toughness and ductility enhanced by inclusion of fibrous reinforcement particles to Al-Si alloy. To further improve the mechanical properties, the alloy is heat treated. Due to which there is a change in microstructure morphology and so alters the characteristics.

The following are the main causes for choosing A356.2 alloy is due to

- Abundantly available.
- Have higher strengths, ductility and greater elongation.
- Refined mechanical properties due to the lower iron content.
- Excellent requirements for mechanical strength, hardness, fluidity, pressure tightness, machinability and fatigue strength.
- Heat treatment enhances the mechanical characteristics with maximum tensile strength and elongation.
- Good machinability
- Surface finishing operations like electroplating, coatings, vapour deposition, plasma coating and anodising can be easily done.
- Better weldability.
- Exceptional corrosion resistance.

The chemical composition of A356.2 alloy is shown in Table 3.1 which was done using Optical emission spectroscopy as shown in Fig 3.1

Table 3.1: Chemical composition of A356.2 Al Alloy

Si	Fe	Cu	Mn	Mg	Zn	Ni	Ti	Bal
6.5-7.5	0.15	0.03	0.10	0.4	0.07	0.05	0.1	Al

Fig 3.1: Optical emission spectroscopy (model: Spectromax)

3.1.2 Reinforcing material

One of the main agricultural products cultivated in India is paddy from which rice is obtained which also which accounts for the generous availability of rice husk.India is estimated to produce nearly 122 million tons of paddy per year out of which, 20-22 % rice husk is obtained from processing. Burning of this husk yields rice husk ash, it is estimated that 100 kilograms of rice yields about 40 kilograms of rice husk which in turn produces 5 kilograms of rice husk ash upon controlled burning. As disposal of rice husk is becoming endangerous threat to the environment, many techniques have been investigated for its disposal by many researchers. Out of which, instead of cement, rice husk ash is being used in all building codes around the globe which is to be as best disposal technique. During the production of rice hush ash several factors such as controlled burning, temperature and duration of burning time play a vital role. Since it is an agricultural by-product, it contains almost 75% of organic volatile matter. The rice husk is initially washed and cleaned with water thoroughly to eliminate all impurities and then it is dried. Then it is heated at 200°C for one hour to get rid of moisture. Then it is heated at 600°C for a period of 12 hours to eliminate even tiny traces of carbonaceous materials. The left over is the required rice husk ash which is

rich in silica and utilised as reinforcement fiber as shown in Fig 3.2.The chemical composition of RHA was shown in Table 3.2

Fig 3.2: Rice husk ash

Table 3.2: Chemical composition of RHA

Constituent	Silica	Graphite	Calcium Oxide	Magnesium Oxide	Potassium Oxide	Ferric Oxide
%	90.23	4.77	1.58	0.53	0.39	0.21

3.2 Fabrication Process

3.2.1 Stir casting

This is a liquid - state fabrication technique which includes addition of the diffused phase into the molten metal using mechanical stirrer. The stirrer which is typically made of high temperature resistance material is used for mixing the molten metal and reinforcing material. The stirrer is equipped with two main components impeller and a cylindrical rod. The ends of this stirrer are connected to a motor shaft and impeller. The stirrer is normally positioned vertically and is rotated at higher speeds with the help of the connected motor. Stir casting technique enables to fabricate composites up to 30% volume fraction of reinforced materials. For the consistent distribution of the alloy and reinforcements the various parameters such as stirring speeds, stirrer angle, relative density, wettability of the composites are to be considered

carefully and chosen. It is observed that stirring temperature, speed and time etc. has an important part in stir casting.

3.2.1.1 Selection of process parameters

The following process parameters are strictly followed in the present research in order to enhance the mechanical characteristics and minimize the casting defects of the test samples.

- **Stirring speed**: To overcome the surface tension between materials during fabrication of metal matrix materials stirring speed is a crucial parameter. It controls the flow pattern of the liquid metal and helps in diffusion of the reinforcement particles uniformly. Stirrer speed is maintained at 500-700 rpm to increase wettability and to avoid parallel flow of the molten metal in the present research. It is observed that when the stirrer speed is above 850 rpm there is splattering of the liquid metal.
- **Stirring temperature:** Stirring temperature is the main criteria which plays a crucial role in stir casting. The aluminium alloy melts around 660°C. This temperature affects the viscosity and particle distribution of the matrix system. The ideal operating temperature is maintained to 750-800 °C which retains the aluminium alloy in a semisolid state in the present work. It is even noticed that when temperatures are above 800 °C and below 750 °C have exhibited difficulties in incorporating the reinforcement particles into the core matrix system.
- **Pre-treatment of the reinforcement:** Rice husk ash is preheated to 700-750 °C for 30 minutes to remove moisture present in the reinforcement. Preheating eliminates the chances of accumulation and enables better wetting environments between matrix and reinforcement phases.

- **Addition of Magnesium:** Addition of magnesium promotes wettability. In the present work 1% weight Mg is added, however increasing Mg content to above 1 wt. % accounts for increased viscosity which leads to non-homogenous distribution between matrix and reinforcing phases.
- **Stirring time:** Stirring improves uniform distribution among the liquid metal creating a perfect interfacial bond. In achieving a homogenous distribution, material flow pattern behaviour must be in bound. In the present work, the optimal stirring time is maintained between 5 to 10 minutes.
- **Blade Angle:** To maintain uniform molten material flow pattern number of blades and blade angles of the stirrer has crucial part. When the stirrer blade angles are maintained at 45° and 60°, homogenous distribution of filler materials is produced. A four blade stirrer is kept at a distance of 20 mm from the base of crucible to enable effective vortex of materials.
- **Inert Gas:** Molten aluminium tends to build up an oxide layer with time, if left untreated. The further oxidation results in hard undesirable surface layer. In order to avoid this inert gas like argon is incorporated into the liquid metal.
- **Reinforcement particles size and feed rate**: During the fabrication of composites, reinforcement particles size and feed rate is necessary for consideration. During present work the mean reinforcement particle size considered is 25 μm on incorporation which displayed uniform diffusion between matrix and filler materials. When higher and lower particle sizes are considered for incorporation, clusters of particles was observed. It is found that the optimum particle incorporation rate for superior diffusion is between 10-25 gm/min.

3.2.1.2 Fabrication of composites

In the present research, A356.2 aluminium alloy and RHA particulates were used as the matrix and reinforcement phases. Composite specimens were fabricated by stir casting process. RHA particulates were injected into the melt of magnitude 2, 4, and 6 wt. % in an argon gas environment. Before the incorporation of the RHA particulates in the molten metal, pre-treatment was performed to make them free from carbonaceous material.

Initially A356.2 aluminium alloy with theoretical density 2760 kg/m^3 is heated to 750 °C in a graphite crucible till the entire metal reached to molten state. Degassing tablet is than added to the molten metal for reducing porosity. Before incorporating the reinforcing phase, the rice husk ash particles are heat treated about 700-750°C in a muffle furnace for removing the moisture content and impurities contained within it. Simultaneously 1wt % magnesium is added for enhancing the wettability between RHA and A356.2 alloy. It is observed that without the addition of magnesium particles RHA particles outcaste from mixing up with the aluminium alloy. A stainless stirrer is lowered into the liquid metal and is stirred at of 500-700 rpm speed. The stirrer speed is regulated with help of a regulator.

Pre-treatment of RHA enables equal distribution of the particles into the matrix system. RHA particles are preheated and added to the liquid metal constantly. The stirring action is performed 5 minutes post the incorporation of the reinforcing material. The resultant mixture is poured into a pre-heated mould of 600 °C temperature and cooled for 35 minutes. By this, 2, 4, 6 % by weight RHA reinforced composites are fabricated. The experimental setup is shown in Fig. 3.3.

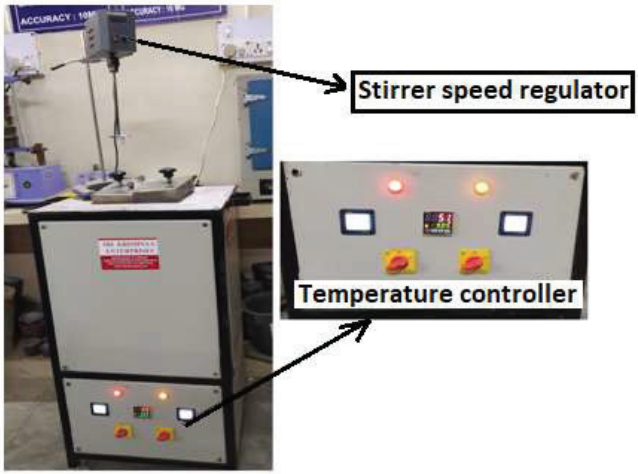

Figure 3.3: Stir casting experimental setup

3.3 Mechanical Properties of Base Alloy and Al/RHA Composites

The properties like density, hardness, porosity, tensile strength of A356.2 base alloy and Al/RHA composites have been investigated thoroughly.

3.3.1 Density measurements

The specimen's density is determined by employing Archimedes principle. This technique involves weighting the test specimen in any fluid of familiar density and weighting the sample in air. These measured values are used to determine density of the test material by the following expression

$$\rho_{mmc} = \frac{m}{m - m_1}\rho_w \tag{3.1}$$

Where, m represents the specimens mass in air, m_1 represents the test specimens mass in distilled water, ρ_w denotes the density of distilled water density.

3.3.2 Porosity measurements

In general porosity of a material is determined with the following expression

$$Porosity = \frac{\rho_{th} - \rho_m}{\rho_{th}} \tag{3.2}$$

Where, ρ_{th} and ρ_m denotes the theoretical and measured densities, ρ_{th} value is usually determined from the rule of mixtures

$$\rho_{th} = \rho_{Al} V_{Al} + \rho_{RHA} V_{RHA} \tag{3.3}$$

Where $\rho_{Al,}$ and ρ_{RHA} represents the concerned densities of base matrix alloy (A356.2) and reinforcing phases RHA. Similarly the volume fraction of the reinforcement is estimated from the following equation

$$V_{RHA} = \frac{\rho_{Al} - \rho_{mmc}}{\rho_{Al} - \rho_{RHA}} \tag{3.4}$$

3.3.3 Hardness measurements

Hardness of the material can be is the resistance of the material offered against localized deformations. The applied deformation can be due to indentation, bending, scratching. Hardness of the material directly influences strength, toughness, ductility, elastic stiffness and viscosity. Hardness of the base alloy and Al/RHA composites is determined using Brinell hardness tester following the ASTM E10 standards. A steel ball indenter is employed for the testing purpose; the samples are tested under a load of 500 Kg for a period of 30 sec. Brinell hardness of the test specimens is estimated using the following equation. Hardness value is calculated by taking an average of five readings.

$$BHN = \frac{2F}{\pi D\left(D - \sqrt{D^2 - d^2}\right)} \tag{3.5}$$

Where, F denotes the load applied in kg, D denotes the steel ball diameter in mm, d denotes indent size in mm.

3.3.4 Tensile test

The tensile property of a material system has a vital part in ascertaining the materials strength. Tensile testing employs by subjecting the test specimen to a controlled tension until failure occurs. These testing methods determine the efficiency of a material system which can perform under the action of various forces. In this research Al/RHA test composites of gauge length 60 mm and diameter 10 mm are prepared according to the ASTM E8 standards for testing using Instron tensile machine as depicted in Fig. 3.4. At an initial strain rate of 1.69×10^{-4} s^{-1} the test process is performed at room temperature.

Fig 3.4: Tensile test machine (INSTRON)

3.4 Sand/Grit Blasting Process

Before the specimens are coated they should be prepared for better adhesion. Using grit blasting equipment as shown in Fig 3.5, the specimens were blasted with

alumina grits followed by ultrasonic cleaning with acetone to obtain better adhesion between coating and substrate.

Fig 3.5: Grit blasting process

3.5 High Velocity Oxygen Fuel (HVOF) Coating

High velocity oxygen fuel (HVOF) coating comes under the method of thermal spray coating. Thermal spraying is an industrial coating method consisting of a source of heat and a powdered coating material, which is literally melted into small droplets and sprayed at high speed on the surfaces of the substrate. In HVOF coating technique, oxygen and variety of fuel gases like the propane, hydrogen, acetylene, liquid petroleum gas, ethylene, kerosene, methane etc. (any one of these gases) can be used with the oxygen and then it is fed in the torch to be applied as coatings. The combustion chamber ignites a combustible combination of petrol and oxygen under elevated pressure to produce a constant flame. At supersonic velocity, the combustion products exit the

nozzle with related "shock diamonds." Coating materials in the form of powder are axially or radially injected into the flame.

HVOF spraying allows comparatively dense coatings to be deposited which are suitable for engineering applications including wear-resistant. The resulting coatings are cost-effective, easy to obtain and give great safety. As a consequence, these coatings have discovered applications in different areas of industry. Although many coatings are deposited in a near-net shape, they still mostly require finishing. The finishing process can be troublesome for coatings that display such a degree of protection. It can be time-consuming and costly, representing up to 50% of production costs. In addition, incorrect finishing operations can lead to deterioration of the precision of the coating and the integrity of the surface. The schematic diagram of HVOF process is shown in Fig 3.6.

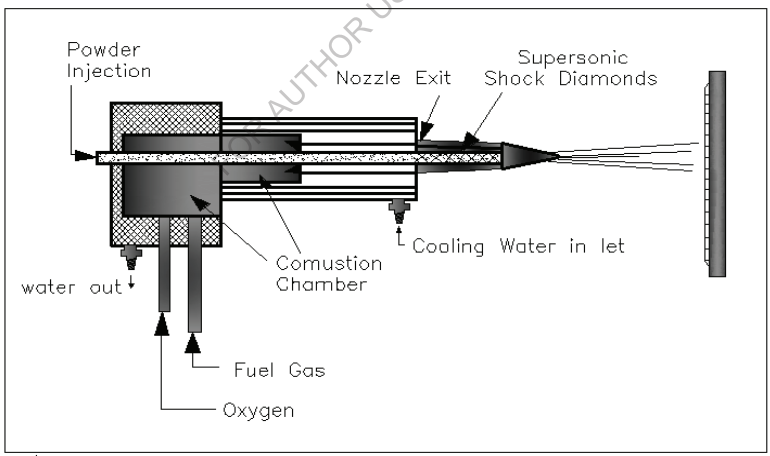

Fig 3.6: Schematic diagram of HVOF process

3.5.1 Materials used for HVOF coatings

The various types of materials are used for HVOF coating process are:

- Single-phase materials, such as metals, alloys, intermetallics, ceramics, and polymers
- Composite materials, such as cermet's (WC/Co, Cr_3C_2/NiCr, NiCrAlY/Al_2O_3, etc.), reinforced metals and reinforced polymers.
- Layered or graded materials, referred to as functionally gradient materials (FGMs).

3.5.2 Applications of HVOF coatings

HVOF coating process has many applications in several industrial areas like aviation, power generation, printing and paper, automotive, transportation, petro chemical, textiles, glass manufacturing, metal processing and general industry.

3.5.3 Problems encountered with HVOF coating process

- **Complex coating materials:** Materials that are utilised in this process are available in large numbers which vary in chemical compositions, application and microstructures which depends on many process variables hence leads to complex coating structures.
- **Powder sizes:** Coated materials are used in the form of powders. The size of these powders ranges from 5-60 μm.
- **Controlling of parameters:** During the coating process of small and tiny section parts the controlling of temperature or the work-piece is very threatening due to the generation of high velocity and energy output.
- **Coating of bores or internal surfaces:** In the HVOF coating process the spay distance is generally longer. So the coating on to the internal surfaces or on the bores is very difficult and almost restricted.
- **Health and safety issues:** While using HVOF coating process a specialized thermal spray booth must be used with suitable sound reduction and dust

extraction since the air flow in this process is turbulent and reverse and large amount of noise will be generated and there will also be reverse flow of dust. This also has burning hazard, if the operator is not cautious during the operation of the equipment may also lead to minor burns or loosing of skin on hands and arms.

- **Automated manipulation:** HVOF spaying guns is operated automatically hence well qualified, skilled and experienced operators are required to maintain consistency in the coated substrate and for safe operation. This also requires more investment.

3.6 WC-Co Coating

WC-Co coating is applied on the base alloy and Al/RHA composites using thermal spray coating method. Among different thermal spray coatings available, HVOF is the most popular and low cost technique which was used in the present work. These stock materials are heated by using different heating sources, by which molten or softened particles are accelerated before impacting on the substrate surface. The WC-Co powder used in the present study consists of spherical shaped particulates with petite pores on the powder particles with a mean size of 35 microns.

A mixture of gaseous or liquid fuel and oxygen are continuously ignited and combusted after being fed into combustion chamber as shown in Fig 3.7. The resultant hot gas at a pressure close to 1MPa spreads through a nozzle and travels and moves through straight area.At the exit of the barrel, the jet velocity will be greater than 1000m/s.Then a stock fed with powder gets injected in the gas stream and speeds up the powder upto 800m/s. Now the powder and hot gas stream moves towards the surface to get coated. In the stream the powder melts partly and gets deposited on the substrate. The resultant coating is now rich in bond strength but low in porosity. In the Table 3.3

and 3.4, the parameters related to the process which are used for coatings are presented. However, to check for optimum coating thickness the samples are coated for 150 μm and 250 μm thickness.

Table 3.3: Fuel gas parameters

Gas	Parameter	
	Pressure	Flow
LPG	6-8 bar	60-80 slpm
Oxygen	9-11 bar	200-300 slpm
Air	6-7 bar	450-600 slpm

Table 3.4: WC-Co powder feeding parameters

Powder feeder	Parameter
Powder feed rate	23-30 gms/min
Flow rate	12-20 slpm
Powder feed carrier pressure	30-50 psi

Fig 3.7: Experimental setup for HVOF coating process

3.7 Wire Electrical Discharge Machining

An important electro thermal production process, wire EDM machining (Electrical Discharge Machining) is a process in which the sample is machined with a thin metallic wire. It is then immersed in a tank containing dielectric fluid like deionised water. The wire held between upper and lower guides is constantly fed from a spool. The guides which are usually CNC-controlled move in the x–y plane. The water aids in removing the debris from the cutting zone. This also aids in understanding the rate of feeds for various materials thickness.

This method requires lesser cutting forces for removal of material. Thus, there are less residual stresses in the work-piece. The various applications of Wire EDM process are used in various sectors such as Aerospace, dies, fixtures, gauges and cams manufacturing etc. In the present study samples were machined with Electronica wire electrical discharge machine to obtain 40 mm x 10 mm x 2 mm dimensions to observe damping capacity. Fig 3.8 shows the experimental set up and specimen machining using Wire EDM.

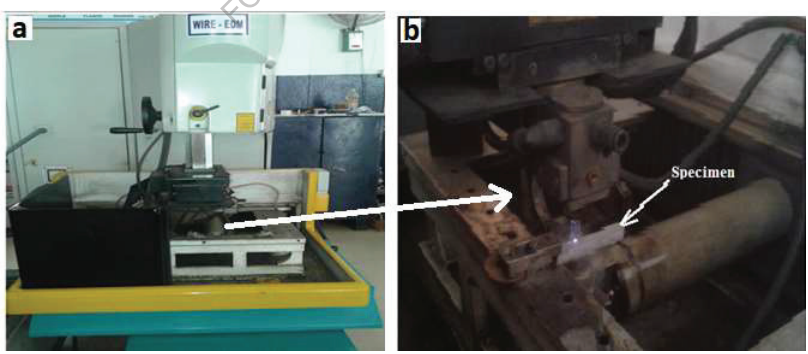

Fig 3.8: Experimental setup a) Wire EDM machine b) Detailed view

3.8 Damping

3.8.1 Dynamic mechanical analyser

Dynamic mechanical analyser is versatile equipment which is employed for determining the materials modulus, compliance and damping (tan delta). The dynamic mechanical analysis usually known as DMA is a non-destructive testing technique for determining the damping behaviour and the schematic diagram is shown in Fig 3.9. In this method the specimen is treated with forced oscillations for analysing the damping behaviour. The DMA analyses the raw signals of amplitude of deformation, force and phase angel for calculating storage and loss stiffness (E' and E''), the damping ratio tan is measured as ratio between storage and loss modulus. Storage and loss modulus are obtained by multiplying with materials stiffness. This analyser accommodates different fixtures for testing the samples. Materials bulk properties are characterised by varying the temperatures and frequencies. Phase shift is determined using Fourier analysis and phase lag method. Computer software usually depicts the analysis report. Besides, DMA can also determine the creep, elasticity, viscosity, glass transition temperature with respect to the varying strain rate, frequency and temperature.

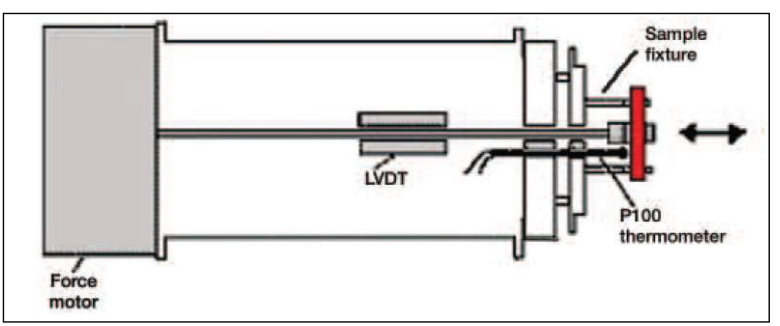

Fig 3.9: Schematic Diagram of DMA8000

3.8.2 Principle of DMA

Dynamic mechanical analyser is employed for determining the materials mechanical properties with respective to time, temperature and frequency which are subjected to an external sinusoidal oscillating force shown in Fig 3.10 a. When an external force i.e. stress is exerted it triggers a relative deformation i.e. strain whose amplitude and phase lag are calculated.

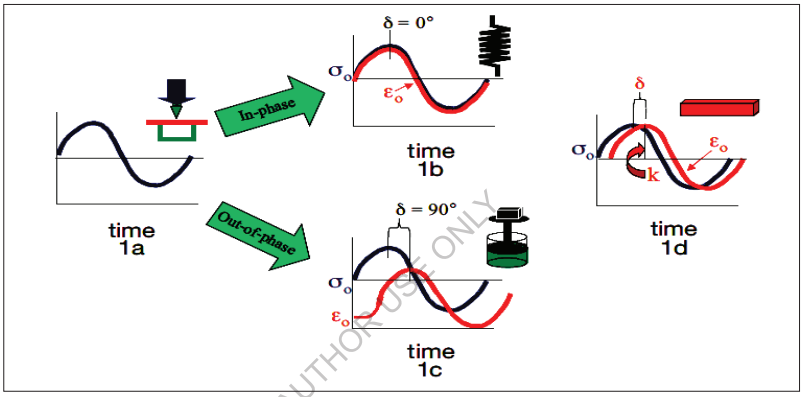

Fig 3.10: Representation of DMA principle

The materials damping capacity is an integral part of both storage modulus E' (real part) and loss modulus E'' (imaginary part). The dynamic elastic aspects depend on the nature and state of the material, their magnitude typically varies with the frequency, load applied, working temperatures and conditions. The various parameters like stress strain relaxations; amplitude of deformation, time and displacements are employed for determining the material characteristics.

Storage modulus (E') defines the amount of energy a material can store within, storage modulus determine the stiffness of a material under repeated loading. Loss

modulus (E'') determines the viscous response of a material, usually represents the amount vibrational enegery dissipated though heat. Tan delta determines the energy dissipation of material. Its value ranges from 0 to 90°. As the tan delta value reaches 90° the material becomes purely viscous in nature and when the tan delta is 0° the material tends to be purely elastic. Higher tan delta value denotes greater energy dissipation i.e. the materials is being more non-elastic, lower values of tan delta denotes the material being more elastic under the application of load. The damping capacity in terms of loss tangent (tan δ) or loss factor (η), is given as

$$\tan \delta = \eta = \frac{E''}{E'} \tag{3.6}$$

3.8.3 Damping Measurement

Damping measurement was done using Dynamic mechanical analyzer (DMA 8000) at three different frequencies like 0.1, 1, 10 Hz. Over a temperature range of room temperature to 150°C. The experimental setup is shown in Fig. 3.11. At constant strain of 10 N all the damping measurements were taken. In the dual cantilever mode the samples were arranged and as function of temperature the values of the tanδ and the storage modulus were observed.

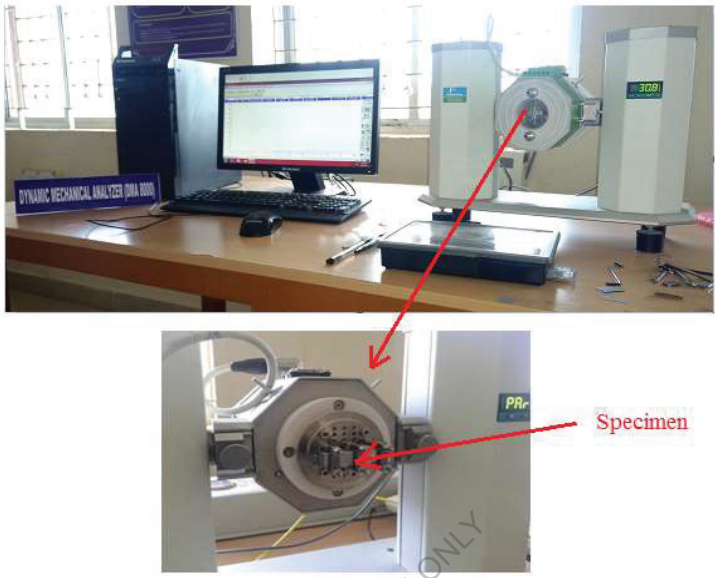

Fig 3.11: Dynamic mechanical analyser (DMA 8000)

3.9 Micro-structural Characterization

Prior to the micro-structural analysis of the test samples, these are cleaned thoroughly by using sandpapers of different grit sizes (P220, P400, P800 and P1200) accompanied by cloth buffing. The resultant test samples are etched for 15 seconds using Keller's reagent. After immersion, test specimens are cleaned using concentrated HNO_3 and distilled water. The micro-structural characterization of the base alloy, Al/RHA composites, WC-Co coated base alloy and WC-Co coated composites are performed by JSM-6610LV Scanning electron microscope (SEM) as shown in Fig. 3.12. FESEM is also employed for studying the WC-Co coated substrates characteristics.

Fig 3.12: JEOL JSM-6610LV scanning electron microscope (SEM)

3.10 X-Ray Diffraction (XRD):

PANalytical X-Pert Pro as shown in Fig. 3.13 is used to find the residual stresses on the surface of the WC-Co coated samples. The technique of X-ray diffraction is used to measure residual stress because it is a strong instrument for assessment of failure or studies of process development. This technique is frequently used to observe the magnitude and type of residual stress on machined surfaces that determines the value of the surface.

Since stresses cannot be measured directly, the strain in a set of lattice planes, in a certain direction is observed as a shift of the 2θ angle of the diffraction peak. The peak shift is recorded as a function of the sample tilt angle ψ in the strained sample at Φ angle and then the elasticity theory can be used to calculate residual stress.

Fig 3.13: PANalytical XPert PRO XRD

3.11 Summary

This chapter briefly explains about the various materials and methods adopted during the experimentation process. The base material used for the fabrication is aluminum alloy A356.2 and reinforcement material used is Rice husk ash (RHA). Stir casting technique is used to produce the composites by varying the RHA percentages as 2%, 4% and 6% by weight. After fabrication of composites WC-Co coating are applied on the base alloy and composites by using HVOF thermal spray process. After coatings are applied, the specimens will be cut by applying Wire EDM method for required dimensions for damping measurement using Dynamic mechanical analyzer DMA8000. The microstructural characterization will be done using SEM and XRD. Various mechanical properties to be studied are density, porosity, hardness and tensile strength.

CHAPTER-IV
OPTIMIZATION OF WIRE EDM PARAMETERS

Wire EDM (WEDM) technique is used to machine the substrates into required dimensions for the study of damping capacity. This process requires optimization of various parameters to have uniform work pieces. The present chapter briefly describes the need for optimization and the various parameters that are to be optimized to obtain the maximum damping efficiency.

4.1 Need for optimization of wire EDM parameters

In the present work, damping studies have been performed using dynamic mechanical analyzer (Perkin Elmer DMA 8000). For this, dimensions of 40-50 mm length, 8- 12 mm width and 0.5- 2 mm thick samples are required. The samples of ≤ 2 mm thick are accurately machined by using WEDM process which otherwise difficult using other conventional techniques. Hence WEDM is selected for machining the samples for damping measurements. WEDM machining involves several parameters which include Pulse on time (T_{ON}), pulse off time (T_{OFF}), peak current (IP), wire speed, wire tension, dielectric flow rate etc. From the past works it is clear that these parameters influence several properties including damping [218, 219]. Hence an optimal combination of these WEDM parameters is very much essential with an intention to increase the damping capacity. To find the optimal parameters the analysis was carried on A356.2 base alloy. The obtained optimal parameters were then used to machine all the samples includes base alloy, A356.2/RHA composites, WC-Co coated base alloy, WC-Co coated A356.2/RHA composites.

4.2 Process Parameters

There are various process parameters that regulate the WEDMprocess such as:

- **Pulse on Time (T_{ON}):** It refers to the application of voltage between the sample and the electrode that result in discharge. If this is high, the energy supplied too will be high and it generates more amount of heat energy. Thus the removal rate of material depends on the quantity of energy supplied to T_{ON}.
- **Pulse off Time (T_{OFF}):** When this is reduced cutting speed is incremented exponentially which leads to additional fruitful discharges per unit time. But a major drawback of this pulse off time is it overloads the wire and damages it without even permitting necessary time to cleanse the waste materials.
- **Peak Current (IP):** It refers to the process of escalation of current to a point of pre-set value during each T_{ON}. The duration of the attainment of the peak current depends on the surface area to be machined. For large machining areas, high peak current is required.
- **Wire feed rate:** With the increase in wire feed rate, usage of wire increases which leads to the increase in the cost of cutting. During the high cutting speeds if low feed rate is applied it will result in the breakage of the wire.
- **Wire Tension:** By a significant increase in wire tension within a considerable range, the cutting speed and accuracy increases rapidly. The wire vibration amplitude reduces with higher tension and it in turn reduces the width of cut. But, if the tension applied is higher than the wire strength, it causes breakage.
- **Spark gap voltage:** It refers to the gap on which a specific voltage has to be supplied. The co-relation between the gap voltage and electric discharge remains same. Thus the peak current is inversely related to gap voltage. This is termed as open current voltage.

4.3 Process Characteristics

There are various process characteristics which depend on the control of various process factors such as:

- **Surface Roughness:** In wire EDM machining this is highly influenced by various characteristics. The predominant parameter is $T_{ON.}$
- **Material Removal Rate (MRR):** The relation between MRR, T_{ON} and IP is that these are directly proportional to each other and MRR is inversely proportional to T_{OFF}.
- **Width of cut (Kerf):** It refers to the performance measure of cutting procedure. The material which is wasted in this is defined by the kerf. This depends on various properties.
- **Wire wear ratio:** The process of erosion of wire materials during the machining of the sample by sparks because of presence of wire electrodes is known as wire - wear ratio. This has to be minimised.

4.4 Optimization of Wire EDM Parameters

As mentioned in preceding section, WEDM is used for machining the sample for DMA which requires a thickness of 2.5 mm or less which would not have been possible by any other machining procedure. The specimens were in of 40 x 7 x 2 mm^3dimensions which were machined by WEDM. Taguchi'sL9 orthogonal arrays under different combinations are used for experimentation. The effect of the parameters is also evaluated using signal to noise (S/N) ratio analysis. Optimum parameters which give maximum damping capacity are obtained.

4.4.1 Parameters of wire EDM for optimization

From the literature it is observed that the most influencing parameters in WEDM are T_{ON}, T_{OFF} and IP and hence the optimal values of these parameters are measured

using Taguchi's technique and the other parameters like wire feed rate, wire tension and spark gap voltage values are kept at default machining settings of 10 m/min, 10 Kgf, 1500 mm/min respectively. In each step, one parameter is considered as constant and the other two are at varying as shown in Table 4.1. In the first set of experiments T_{ON} is varied from 105 to 111 µsec and the other parameters, T_{OFF} and IP kept constant at 60 and 210 units respectively. In the second set of experiments T_{OFF} is varied from 57 to 63 µsec, keeping constant values for T_{ON} and IP at 108 µsec and 210 A respectively. In the final set, IP is varied from 190 to 230 keeping constant values for T_{ON} and T_{OFF} at 108 µsec and 60 µsec respectively.

Table 4.1: Process parameters and their levels for WEDM

Level	T_{ON} (µsec)	T_{OFF}(µsec)	IP (A)
1	105	63	230
2	108	60	210
3	111	57	190

4.4.2 Damping measurements

Damping measurements were carried out using Perkin Elmer dynamic mechanical analyser. Experiments are conducted at constant strain amplitude with a load of 2N at room temperature with frequencies in the range of 1 to 100 Hz in dual cantilever mode. The tan δ and the storage modulus were measured and presented.

4.4.3 Design of experiment

This step involves finding the optimal parameters after the analysis of the influence of the given parameters on the damping capacity, as proposed by Taguchi. Orthogonal array chosen was L9 which has 9 combinations of machining conditions as shown in the Table 4.2. These three parameters T_{ON}, T_{OFF}, peak current are experimented and damping capacity as the result is obtained as depicted in Table 4.3

and 4.4. Goal of performing this is to obtain maximum damping capacity by optimizing the machining parameters.

Table 4.2: L9 orthogonal array

Experiment	P1	P2	P3
1	1	1	1
2	1	2	2
3	1	3	3
4	2	1	2
5	2	2	3
6	2	3	1
7	3	1	3
8	3	2	1
9	3	3	2

Table 4.3: Design of Experiments

Experiment	T_{ON} (µsec)	T_{OFF}(µsec)	IP (A)
1	105	63	230
2	105	60	210
3	105	57	190
4	108	63	210
5	108	60	190
6	108	57	230
7	111	63	190
8	111	60	230
9	111	57	210

Table 4.4: Experimental conditions and damping response

Experiment	T_{ON}	T_{OFF}	IP	Damping
1	105	63	230	0.005000
2	105	60	210	0.006200
3	105	57	190	0.007500
4	108	63	210	0.009170
5	108	60	190	0.011358
6	108	57	230	0.012863
7	111	63	190	0.019863
8	111	60	230	0.025859
9	111	57	210	0.030433

4.4.4 Optimum values of parameters

Based on the experiments it is found that the damping capacity is highly dependent upon T_{ON}. The damping capacity at various T_{ON} is depicted in Fig 4.1. From the plot it was noticed that the damping capacity increases with the increase in frequency. It was further noticed that the damping capacity is found to be high for higher T_{ON}. A maximum of 0.03 has been recorded when the T_{ON} is kept at 111 µsec at 100 Hz and a minimum value of 0.022 has been obtained when the T_{ON} is kept at 105 µsec. An increase of 13% was observed when the T_{ON} is changed from 105 to 108 µsec and an increase of 20% has been observed when the T_{ON} is changed from 108 to 111 µsec. T_{ON} is the amount of time current runs into the gap before it turns off. Larger the T_{ON}, faster the cut was. At 111 µsec of T_{ON} the cutting speed was found to be 5.2 mm/min. It was found that the cutting speed was reduced to 4.1 mm/min and 3 mm/min when the T_{ON} is 108 µsec and 105 µsec. When the wire moves through the material at high cutting speed, the surface surrounding the wire region can easily melt the material and solidify within a short span of time leading to a thin white layer forming on the surface. On the other hand, as the cutting speed decreases, it forms a thick white layer on the surface due to slow solidification caused by the high temperature in the wire. Hence, when the T_{ON} increases, cutting speed increases, which results in the decrease of the white layer thickness. As the thickness of white layer increases, the damping capacity decreases.

Fig 4.2 depicts the impact of T_{OFF} on damping capacity. From the plots it was noticed that with an increment in T_{OFF} there is a decrement in damping capacity. When the samples were cut at 57, 60, 63 µsec it is noticed that the damping values are found to be 0.02, 0.017 and 0.015 respectively, which shows a decreasing trend from 15% to 11.7%. However a similar trend was noticed with respect to frequency. As the T_{OFF}

increases, cutting speed decreases. It is found that when the T_{OFF} increases from 57 µsec to 60 µsec the cutting speed decreased by 0.4 mm/min. Similarly, increase in T_{OFF} from 60 µsec to 63 µsec, results in the decrease of cutting speed by 0.4 mm/min. As the cutting speed decreases, the thickness of white increases and hence lower damping capacities were reported at higher T_{OFF}.

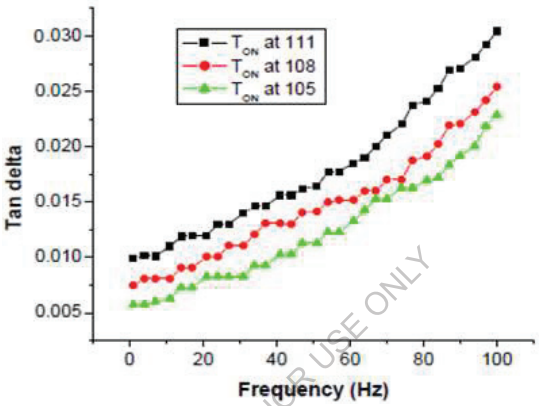

Fig 4.1: Tan δ *vs* Frequency curve for varying T_{ON}

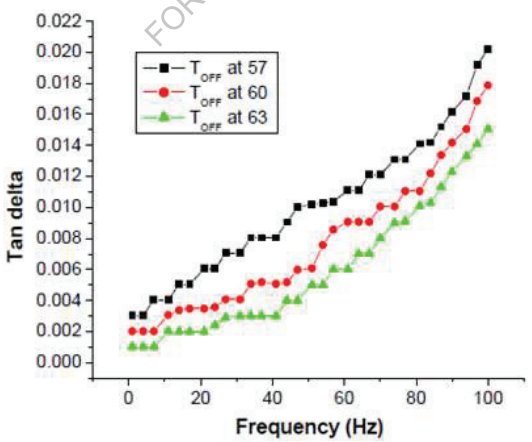

Fig 4.2: tan δ *vs* frequency curve for varying T_{OFF}

The damping capacity at various IP is depicted in Fig 4.3. Here T_{OFF} and T_{ON} are kept constant while IP changed from 230 to 190 A in phases of 20A. Damping capacity was found to increase with the increase in frequency. However, from the plots no significant variation was noticed with IP. At 100 Hz, a maximum damping capacity of 0.009 and a minimum of 0.0089 was recorded which indicates that the damping capacity is independent with peak current and hugely relies on T_{OFF} and T_{ON}. When the IP is changed from 190 A to 230 A, no significant decrease in the cutting speed has been observed. Also, a thick white layer was noticed at these conditions and hence low damping values were reported.

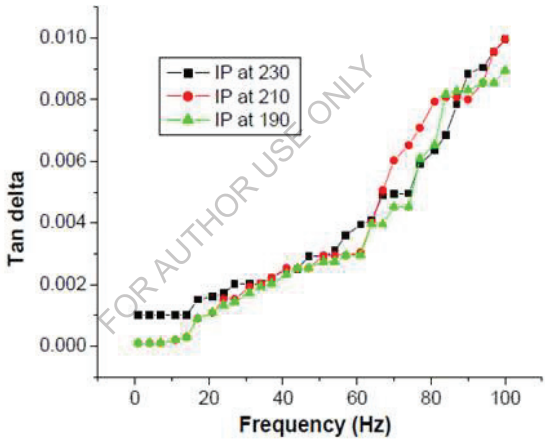

Fig 4.3: Tan δ vs frequency for varying IP

Experimental data are analysed using s/n ratio which depends on factors like maximum damping values are calculated theoretically and practically using the relation as follows

$$\eta = -10 \log (M.S.D) \quad (4.1)$$

M.S.D → the mean square deviation for the output characteristic

Using MINITAB 15 software, the study is done and the results are depicted in Fig 4.4 and 4.5 and values are depicted in Tables 4.5 and 4.6.

Table 4.5: Response table of means damping

Level	TON	TOFF	IP
1	0.006233	0.016932	0.012907
2	0.011130	0.014472	0.015268
3	0.025385	0.011344	0.014574
Delta	0.019152	0.005588	0.002361
Rank	1	2	3
Optimal Parameters	111	57	210

Table 4.6: Response table of S/N ratio

Level	TON	TOFF	IP
1	-44.22	-36.88	-38.48
2	-39.15	-38.26	-38.41
3	-32.04	-40.27	-38.53
Delta	12.18	3.39	0.11
Rank	1	2	3
Optimal Parameters	111	57	210

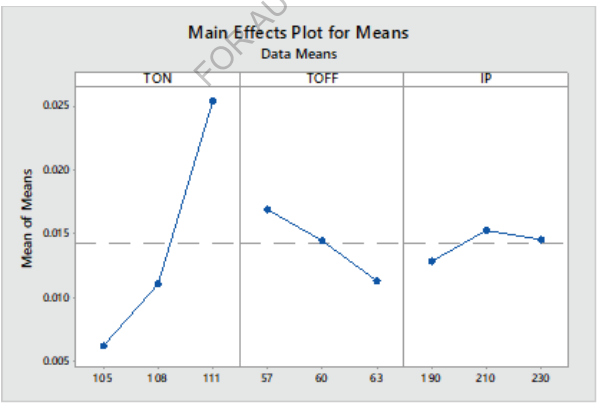

Fig 4.4: Main effects plot for means

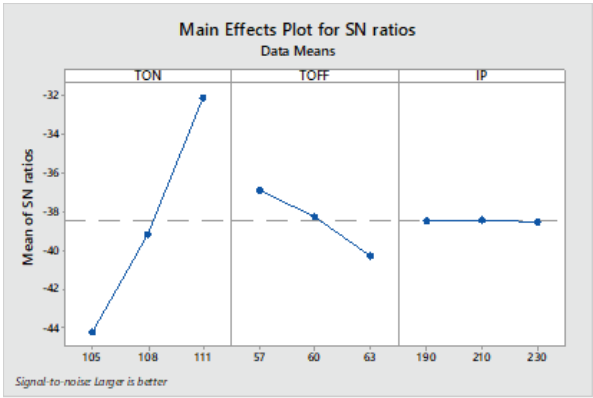

Fig 4.5: Main effects plot for S/N ratio

From the main effects of the plot of S/N ratio, the damping capacity is observed to be high at the following machining conditions:

T_{ON} = 111 µsec

T_{OFF} = 57 µsec

IP = 210 A

Using multiple regressions the relation among the factors is modelled as

Damping = - 0.283 + 0.00319 T_{ON} - 0.000931 T_{OFF} + 0.000042 I.P

Fig 4.6 shows that the development of white layer on the specimen when machined by using optimum parameter values i.e., T_{ON} 111, T_{OFF} 57 and IP at 210A. Fig 4.7 shows the formation of pores on the specimens when machined using optimum factors. This is noticed that on increasing the T_{ON} current and decreasing the T_{OFF} current the white layer width got decreased while on decreasing the T_{ON} current and incrementing the T_{OFF} current the white layer thickness got increased which in turn reduces the damping capacity. By using the Taguchi's experimental design the maximum damping capacity was observed is 0.03043 Hz when the specimen machined at T_{ON} = 111 µsec, T_{OFF} =57 µsec, Peak current IP = 210A.

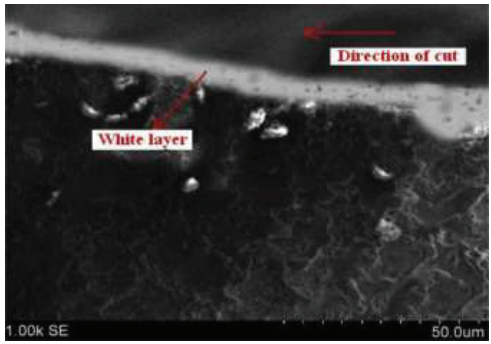

Fig 4.6: SEM image at optimal values for white layer

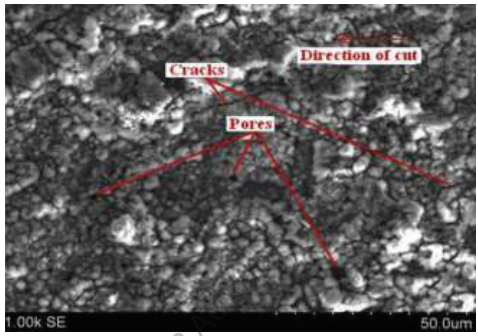

Fig 4.7: SEM image of the surface at optimal values

4.5 Summary

To machine the specimens to the required dimensions for the study of damping behaviour using Dynamic mechanical analyser DMA 8000, Wire EDM was used. It has various process parameters out of which T_{ON}, T_{OFF}, and IP are considered and were optimized to obtain the maximum damping efficiency. In the present study it is observed that with the increment in frequency the damping capacity also incremented. Damping capacity is incremented with an increase of T_{ON} and decrease with the elevation in T_{OFF} and independent of IP. Optimal values for maximum damping capacity has been obtained for A356.2 aluminium alloy when machined at T_{ON} = 111 µs, T_{OFF} = 57 µs IP= 210A.

CHAPTER-V

MICROSTRUCTURAL CHARACTERIZATION, MECHANICAL AND DAMPING BEHAVIOUR OF A356.2 AND Al/RHA COMPOSITES

The present chapter mainly describes about the various types of mechanisms, principles and propagation techniques related to the damping behaviour of a material system. The present researcher's main intention is to identify base alloy characterization and determining the dynamic mechanical behaviour of A356.2 alloy and Al/RHA composites with respective to varying frequencies such as 0.1, 1 and 10 Hz from room temperature to 150 °C. The dynamic mechanical behaviour of test specimens is evaluated by Perkin Elmer DMA (8000) and the surface morphology is characterised using SEM and FESEM.

5.1 Microstructural characterization of Al/RHA composites

As specified in previous chapter III (Materials and Methods), the fabrication of Al/RHA composites is done using stir casting technique by varying the RHA wt. % as 2%, 4% and 6%. The microstructural characterization of aluminium alloy and its composites is done using optical photographs and SEM. Figures. 5.1- 5.4 shows the optical images of the A356.2 alloy and the A356.2/x%RHA composites (where x=2, 4, and 6) respectively. It is clear from Fig. 5.1 that monolithic A356.2 alloy is made up of primary α phase. Figures. 5.2- 5.4 shows optical micrographs of composites containing 2%, 4% and 6% wt. RHA particulates. Presence of particulates in the microstructure of the A356.2 base alloy was noticed. From the micrographs it was observed that the clusters of particulates are found within the α-grains and close to eutectic structure. Also, identified refinement of size of grain took place with addition of reinforcement phase. Fig.5.5 a and b shows the SEM micrographs of rice husk ash sample. The mean size of the RHA sample is found to be 25μm.From the micrographs shown in Fig 5.6,

it is evident that particulates of rice husk ash are finely distributed into matrix core system i.e. in aluminium. It is even identified that there are no evident signs of unwanted agglomeration of the reinforcing phases. In addition the intermetallic interfaces between the matrix and reinforcement displayed superior bonding with no signs of chemical reactions. Considering the results from SEM characterisation, it evident that, RHA particulates are successfully incorporated into the aluminium core system without any adverse phase changes.

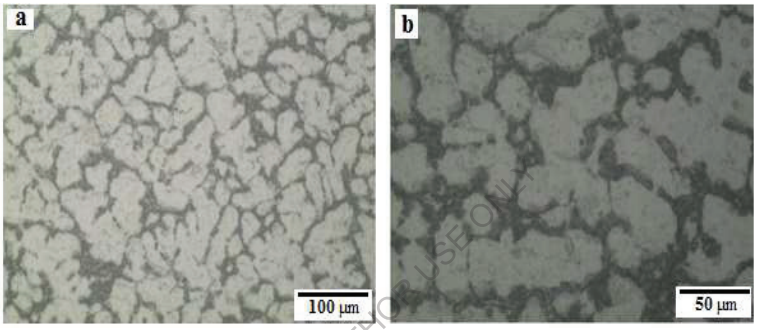

Fig 5.1: Microstructure of A356.2 unreinforced alloy

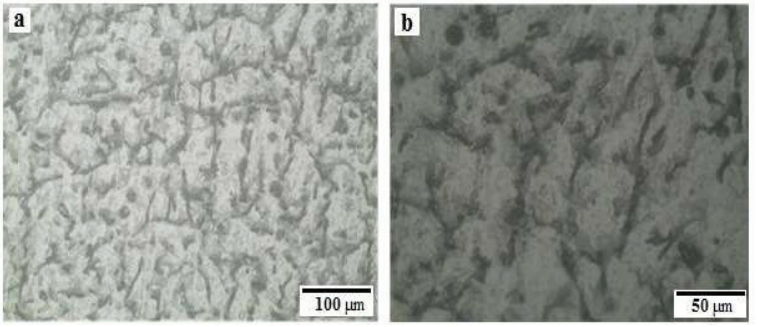

Fig 5.2: Microstructure of A356.2/2% RHA

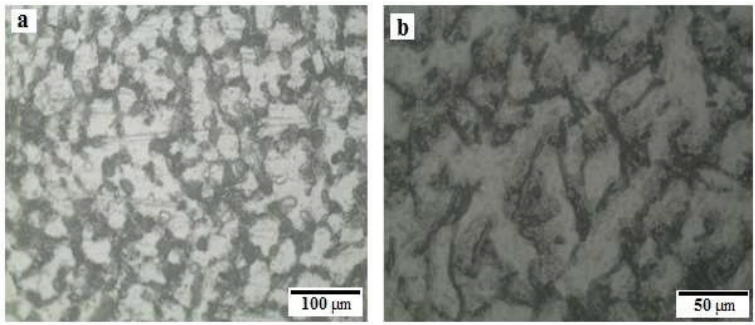

Fig 5.3: Microstructure of A356.2 /4% RHA

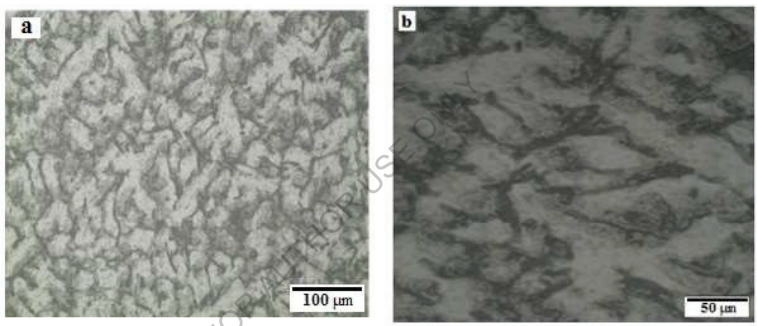

Fig 5.4: Microstructure of A356.2/6% RHA composite

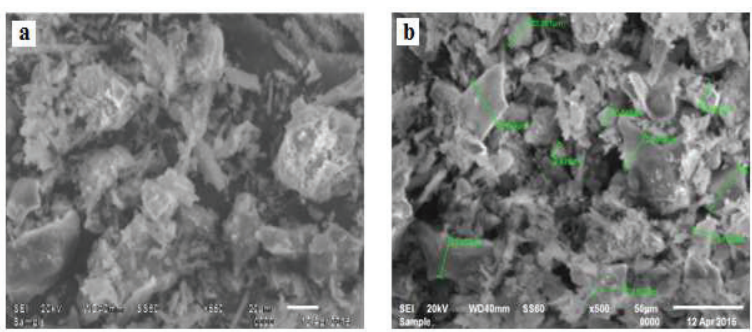

Fig 5.5: SEM image of RHA material

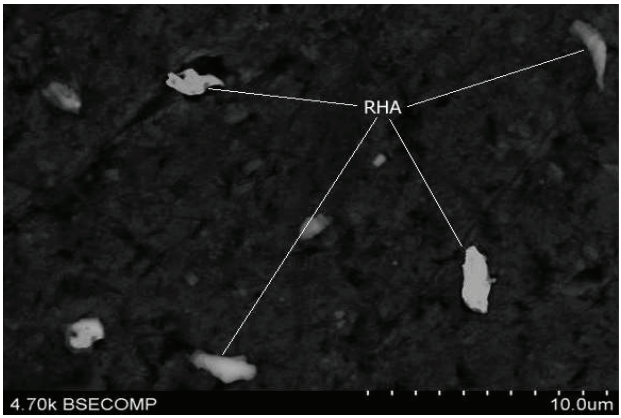

Fig 5.6: SEM image of Al/4% RHA

5.2 Mechanical Properties of Base Alloy and Al/RHA Composites

5.2.1 Density

Fig. 5.7 represents the measured densities of the base alloy and Al/RHA composites. It is noticeable from curve that an increase in RHA particles in metal matrix there is a decrease in material densities. This decrease in materials density can be related to the presence of lesser density of the reinforcing system in comparison to the aluminium.

5.2.2 Porosity

Fig. 5.7 represents the variation of porosity levels. It is observed that an increment in reinforcement particles results in a decrease of porosity. The decrease in porosity is due to the reasons such as preheating the reinforcement before incorporating into the liquid metal, elevated holding temperatures, working in an inert gas environment, preheating the mould to lower shrinkage, employing a steel mould for fabricating, rapid cooling rate to even diffusion of RHA particles in matrix material.

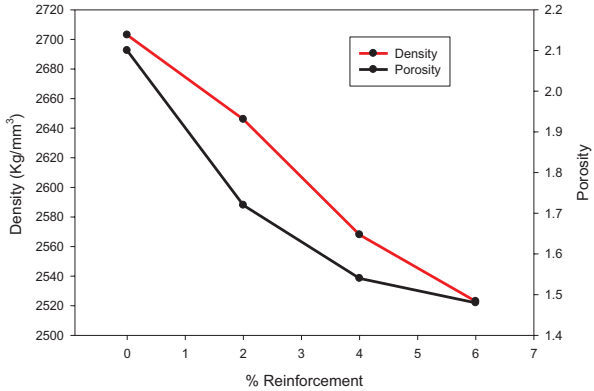

Fig 5.7: Variation of densities and porosity with weight % RHA

5.2.3 Hardness measurements

Hardness of a material has a greater effect in determining the materials mechanical behaviour. Fig. 5.8 represents the variation of hardness with RHA content. From the experiments it is evident that there is an increase in material hardness with an increase in RHA reinforcement particles. This hardness is due to incorporation of much harder particulates into the matrix core system. The presence of reinforcement phases offered higher resistance against the localised deformation caused due to indentation.

5.2.4 Tensile strength

This test outcome is depicted in Fig. 5.9. The graph shows that with addition of reinforcement particles of RHA there is increase in yield strength and tensile strength and decrease in % elongation.

5.3 Strengthening Mechanism

For determining the strengthening of MMCs various theories have been suggested. The composites strength doesn't solely relay on single method. Different methods are used for the defining the materials strength. In this work, it is observed that this is due to thermal mismatch of materials there is an increment in dislocation density.

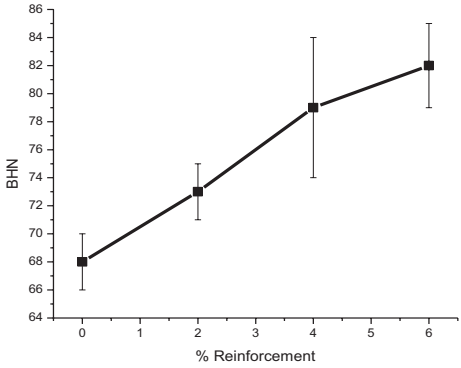

Fig 5.8: Variation of hardness with weight % RHA

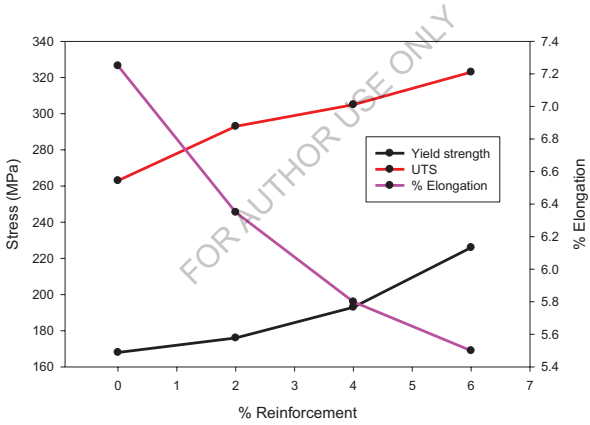

Fig 5.9: Properties variation with weight % RHA

5.4 Damping Measurement of Base Alloy and Al/RHA Composites

5.4.1 Specimen preparation

The samples of 40 x 7 x 1.2 mm^3 dimensions were cut by Electronica electro WEDM process as shown in Fig. 3.8 in Chapter-III. This is a thermally induced machining method which involves of machining of materials irrespective of their hardness. This Wire EDM working principle is shown in Fig 3.8in Chapter-III.

Unlike the conventional method, this method doesn't allow the electrode wire to come into contact with the specimen without creating any physical disturbances to it. This delivers cutting of complex shapes in the most precise and easy manner thereby minimizing the working hours required for machining. This machining technique eliminates the need for surface finishing as there will be no signs of leftover blurs. In the present study the base alloy and Al/RHA composites where machined at T_{ON} = 111, T_{OFF} = 57 and IP = 210A. Various factors taken are WFR (10 m/min), WT (10 Kgf) and SGV (1500 mm/min) are considered.

5.4.2 Damping measurements

Using Perkin Elmer DMA 8000 the damping measurements were done in dual cantilever mode at dynamic load of 10N at a constant strain by varying frequencies 0.1, 1 and 10 Hz and at temperatures range from room temperature to 150° C and rate of heating is 5 °C/min as shown in Fig's 3.11in Chapter-III to measure tanδ and storage modulus.

5.4.3 Damping behaviour of A356.2 alloy and Al/RHA composites

Fig. 5.10a-d displays the mechanical damping plot and modulus *vs* temperature at 0.1, 1, 10 Hz for unreinforced alloy, 2% RHA reinforced composite, 4% RHA reinforced composite and 6% RHA reinforced composites respectively. From the curves it is observed that, with the increment in temperature there is an increment in tanδ at all frequencies. Also there is decrement in storage modulus with an increment in temperature. However, an increment in frequency does not bring about any significant change in storage modulus. Hence storage modulus is not dependent on frequency whereas the damping depends on temperature and frequency. With the increment of RHA particles content modulus and damping increased. Addition of RHA particles plays a prominent role on damping capacity.

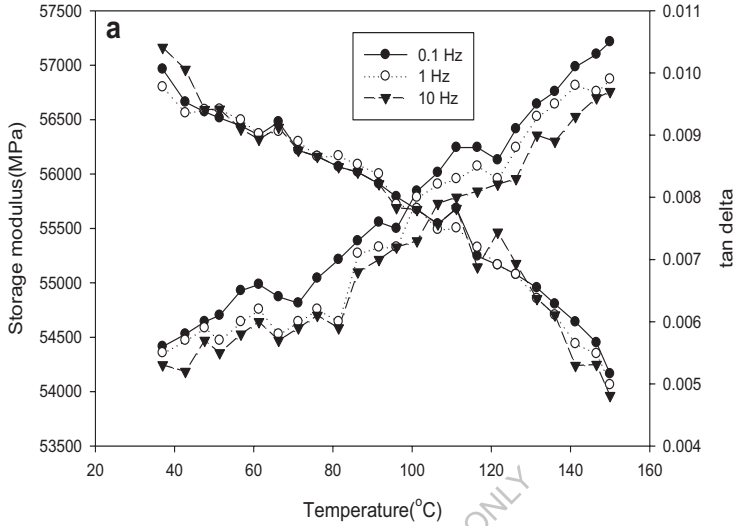

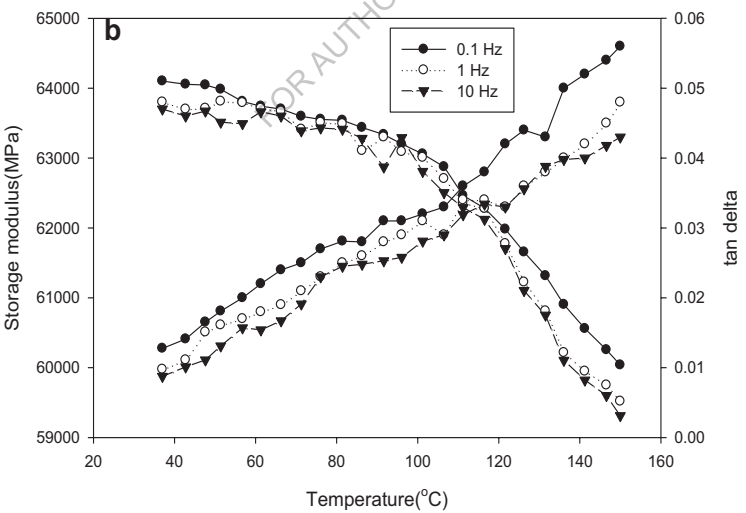

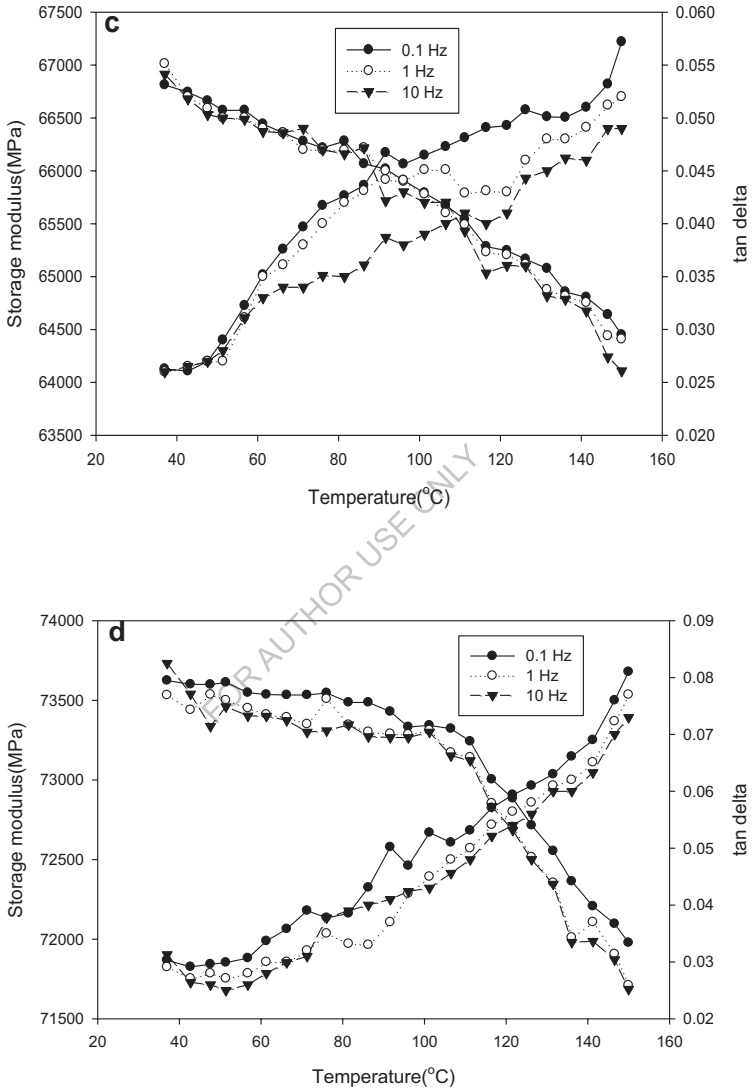

Fig 5.10: Damping behaviour of a) unreinforced alloy, b) 2% RHA reinforced composite, c) 4% RHA reinforced composite and d) 6% RHA reinforced composites

The increase in damping capacities with the addition of RHA particulates was due to following reasons:

5.4.3.1 Thermoelastic damping

According to Zener [220], the theory of thermoelastic damping is typically notable in materials undergoing varied deformations. Thermoelastic damping behaviour can be explained through an example such as when a beam is subjected to bending, the two ends of the beam experience compression and tension. The part of the beam undergoing tension gets hotter while the side of the beam undergoing compression is comparatively cool. Therefore a temperature gradient arises which results in the nonzero thermal conductive heat flow from across the beam. The following expression is for determining the thermoelastic damping:

$$Q^{-1} = \tan\delta = \frac{\Delta\omega\tau}{1+\omega^2\tau^2} \tag{5.1}$$

Where $\Delta = \frac{E\alpha^2 T}{C_V}$ and (5.2)

$$\tau = \frac{C_V h^2}{\pi^2 k} \tag{5.3}$$

Where, E denotes the young's modulus, C_v denotes the specific heat per unit volume, the coefficient of thermal expansion (CTE) is represented by α, ω denotes the angular frequency ($\omega = 2\pi f$), h indicates the beam thickness, T the absolute temperature and the thermal conductivity is represented by k. Following the data for A356.2 (α = 21.4x10^{-6}/ $^{\circ}$C, k = 151 J/sm$^{\circ}$C, C_v= 963 J/$^{\circ}$Cm^3) E= 72.4 GPa, h=1.5 mm) the tanδ value at 1 Hz is around 9.1x10^{-4}. From the previous literature [221] it is evident that thermoelastic damping is notable at frequencies higher than 100 Hz. In the present research the test samples are analysed up to 10 Hz, therefore the probability of having

thermoelastic damping are very shallow, indicating the existence of other damping mechanisms.

5.4.3.2 Generation of plastic zone

The incorporation of filler materials in particle reinforced materials origins higher internal stresses around the intermetallic interfaces due to thermal coefficient differences between the reinforcement and matrix systems. This variation in thermal coefficients leads to the formation of plastic zone around filler and matrix metallic interfaces. From the previous studies [222] the following equation is used to calculate the size C_s.

$$C_s = r_s\left[\frac{\Delta\alpha E\Delta T}{(1-\nu)\sigma_y}\right] \tag{5.4}$$

Where $\Delta\alpha$ indicates the difference between the CTE's of matrix and reinforcement systems, ΔT denotes the temperature difference, E and ν represents the matrix elastic modulus and Poisson's ratio respectively, σ_y indicates matrix the yield stress and r_s represent the radius of the particulate. Table 5.1 illustrates the concerned values.

Table 5.1: Plastic zone radius for composites

Specimen	CTE(α)	Plastic zone radius(μm)
Unreinforced alloy	21.4 x 10^{-6} /°C	--
Al/2%RHA composite	19.3 x 10^{-6} /°C	17.6
Al/4%RHA composite	17.6 x 10^{-6} /°C	31.9
Al/6%RHA composite	16.3 x 10^{-6} /°C	42.8

Carreno-Morelli in his research developed a model for understanding the damping because of plastic zone development by using following expression

$$\tan\delta = \frac{f_{ZP} G \int \sigma d\varepsilon}{\pi \sigma_o^2} \quad (5.5)$$

Where f_{zp} represents the plastic zone volume fraction, G indicates the shear modulus of the composite test sample, σ_o denotes the amplitude of alternating shear stress and ε represents the corresponding strain acting on the test specimen.

5.4.3.3 Dislocation damping

Density dislocations mainly occur because of the presence of filler particles which are hard in the core system and due to the difference in CTE between the matrix and reinforcing materials. In present research the CTE of the base alloy (A356.2) is 21.4×10^{-6}/ ˚C and RHA is 10.1×10^{-6}/ ˚C, therefore these variations in thermal expansions coefficients play a major part in dislocation damping. From the prior studies, the equation used for determining dislocation density (ρ) arising at intermetallic phases is

$$\rho = \frac{B \varepsilon V_{RHA}}{bd(1 - V_{RHA})} \quad (5.6)$$

Where B indicates the geometric constant that relays on the aspect ratio, ε represents the thermal mismatch strain, V_{RHA} denotes the volume fraction of the reinforcement, b represents the burgers vector, and the $d$is grain diameter of reinforcements.

The volume fraction (V_{RHA}) is represented by the equation

$$V_{RHA} = \frac{\rho_{Al} - \rho_{mmc}}{\rho_{Al} - \rho_{RHA}} \quad (5.7)$$

Where ρ_{Al} represents the density of A356.2, ρ_{mmc} indicates the density of composites and ρ_{RHA} represents the density of RHA. Equations 5.6 and 5.7 gives the dislocation density of various specimens computed considering values for the burgers

vector of 0.32 nm for Al [223]. Table 5.2 illustrates the theoretical results of unreinforced and Al/RHA composites.

Table 5.2: Dislocation density for composites

Specimen	Volume fraction	CTE(α)	Dislocation density (ρ) m^2
Unreinforced alloy	--	21.4 x 10^{-6} /°C	--
Al/2%RHA composite	0.028	19.3 x 10^{-6} /°C	8.8 x 10^{10}
Al/4%RHA composite	0.065	17.6 x 10^{-6} /°C	3.9 x 10^{11}
Al/6%RHA composite	0.086	16.3 x 10^{-6} /°C	7.3 x 10^{11}

Density dislocation damping mechanism is well illustrated through Granato-Lucke principle, when a dislocation arises typically due to impurities of atoms or due to the hard particulates a vibrating elastic wave (i.e. acts like vibrating string) is generated. Energy dissipation is much effective under lower amplitude cyclic loading; therefore at lower strain amplitude the damping capacity is independent of it. At higher strain rates and at high frequencies the damping capacity is elevated significantly due to the dislocations. This is predominantly depending on frequency and determined as follows:

$$Q^{-1} = \frac{a_0 B \rho L^4 \omega^2}{\pi^2 C b^2} \tag{5.8}$$

Where a_o represents the numerical factor of order 1, B indicates damping constant, ω refers to operating frequency, L represents convincing dislocation loop relaying on the pinning distance, C refers to the dislocation line tension (≈ 0.5 Gb^2), G represents shear modulus, b indicates the burgers vector and ρ represents the whole dislocation density.

Therefore the energy dissipation typically relays on the cyclic stress frequencies, dislocation densities, and material burgers vector b. Thus the elevated

dislocation densities are because of existence of hard RHA particulates in aluminium matrix system. It was also observed that, with an increment in RHA wt. % there is an increment in dislocation density. Therefore it can be concluded that, Al/RHA composites efficiently dissipates energy with an increment in RHA wt. %.

5.4.3.4 Interfacial damping

The intermetallic phase emerging between the materials has a major part in determining the composites characteristics. Two types of interfaces typically arise in metal matrix composites i.e. weak bonded and strongly bonded interface. Weak bonded interfaces displays interfacial slips occurring between metallic interfaces mostly due to sliding, whereas strong bonded interfaces displays phenomenal bonding resulting no sliding between the reinforcement and filler interfaces. In the present study the A356.2/RHA MMC may display feeble bonding interface between particulates due to presence of porosity. From the previous studies it is evident that interfacial damping is mostly due to the frictional losses occurring between the matrix and reinforcement systems under cyclic loading. Interfacial slips mainly occur at intermetallic phases between matrix and reinforcement when shear stress is adequate enough to overwhelm the frictional loads. Lederman's analysis is helpful in determining the interfacial slip damping in metal matrix composites, according to his principle the η_i based on interfacial slip is represented in the following expression

$$\eta_i = \frac{3\pi}{2} \frac{\mu \sigma_r \left(\varepsilon_o - \varepsilon_{crit}\right)}{\sigma_o^2 / E_c} V_{RHA} \tag{5.9}$$

where μ denotes the coefficient of friction arising between the metal matrix and reinforcement systems, σ_r represents the radial stress occurring between the materials interface, stress amplitude σ_o and corresponding strain amplitude ε_o, ε_{crit} represents the critical interface strain related to the critical interface shear stress, τ^{crit} where friction

energy dissipation initiates, E_c represents the elastic modulus of the composites, and V_{RHA} is the volume fraction of the reinforcement particulates. As regards of weakly bond interface the assumption is that ε_{crit} is much lesser than ε_o thus, equation 5.9 is written as

$$\eta_i = \frac{3\pi}{2}\frac{\mu\sigma_r}{\sigma_o}V_{RHA} \tag{5.10}$$

$$\eta_i = \frac{3\pi}{2}\mu k V_{RHA} \tag{5.11}$$

Where k is the coefficient of the radial stress concentration at the interface and equal to

$$k = \frac{\sigma_r}{\sigma_o} \tag{5.12}$$

Lederman's principle is applicable for specimens undergoing uniaxial stresses or residual stresses due to thermal mismatch under cyclic loading. When the test specimen undergoes bending due to damping, the test samples witnesses a non-uniform strain rate. During this at a certain part of the sample the stain level reaches a critical value to nucleate interfacial slip sighting between the matrix and filler particulate interfaces. The following expression is used to determine the interfacial slip

$$\eta_i = \frac{3\pi}{2}C\mu k V_{RHA} \tag{5.13}$$

For evaluating the impact of interface slip friction on the damping behaviour of the A356.2/RHA metal matrix composites, the magnitudes of the variables equation 5.13 are to be determined thoroughly. The constant (C) in equation 5.13 is considered as 0.5 by considering symmetry of the strain distribution of DMA test specimen. The stress concentration factor (k) is in the range of 1.1 to 1.3 at the metal matrix interfaces.

The friction coefficient (μ) of RHA acting on the A356.2 alloy surface ranges from 0.29 and 0.37, in the present case, mean of 0.33 is assumed. Final replacement of all data in equation 5.13 enables in determining the interfacial slip damping as 0.026 for the A356.2/4% RHA composite. This assessment is implemented for evaluating the resultant damping capacity of the A356.2/4%RHA at 1Hz. The dissimilarities in damping capacities arising between the A356.2/4%RHA MMC and A356.2 base alloy at 1Hz is roughly around 0.012, and this difference in damping capacities can be accounted for the intermetallic interactions occurring between the particulate/matrix systems. However equation 5.13 does not incorporate the effect of frequency on damping. Thus this is only an approximate.

5.4.3.5 Porosity

The various types of crystalline defects that are often noticed in composite materials are line defects such as dislocations, point defects i.e. vacancies and disorders, surface defects. In present study minor amount of porosity has been reported, it can be assumed that the existence of porosity with micro voids and micro cracks nucleating at intermetallic interfaces of matrix and reinforcement system has elevated the energy dissipation.

5.5 Summary

In this work A356.2/RHA metal matrix composites are made-up by employing conventional stir casting method. The fabricated A356.2/RHA composites were examined for material microstructural characterization using SEM. It is observed that RHA particles are successfully incorporated in matrix alloy system of A356.2. Density, porosity, hardness and tensile strength of the test specimens were thoroughly investigated. It is evident from results that porosity and density of metal matrix system decreased, as increasing weight percent of rice husk ash content. Similarly yield

strength and ultimate tensile strength showed elevated results upon increasing the rice husk content. This elevated strength can be accounted for the increase of dislocation density. The reinforcing particulates i.e. (RHA) have a crucial part in efficiently distributing loads between the material phases. The damping and modulus are increased with the addition of RHA particles.

CHAPTER- VI
CHARACTERIZATION AND DAMPING BEHAVIOR OF WC-Co COATED ALLOY AND Al/RHA COMPOSITES

The present work is chiefly entitled in the study of material characterization and dynamic mechanical behavior of WC-Co coated base A356.2 alloy and its coated Al/RHA composites with respective to the varying frequencies such as 0.1, 1 and 10 Hz and temperatures extending from room temperature to 150 °C. The damping behavior of test specimens is evaluated using DMA (8000) and the surface morphology is characterized using SEM and FESEM.

6.1 Surface Morphology

The SEM micrograph of the WC–Co powder is shown in Fig. 6.1. It was observed that the WC-Co powder consists of spherical shaped particulates with petite pores on the powder particles with an average size of 35 microns. Fig. 6.2a and b depicts the SEM images of the external area of WC–Co coated aluminium alloy. From the micrographs, the coating is found to be uniform with little evidence of pores.

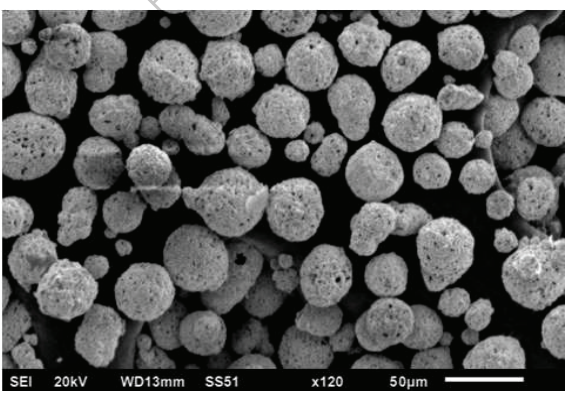

Fig 6.1: SEM micrograph of WC–Co powder

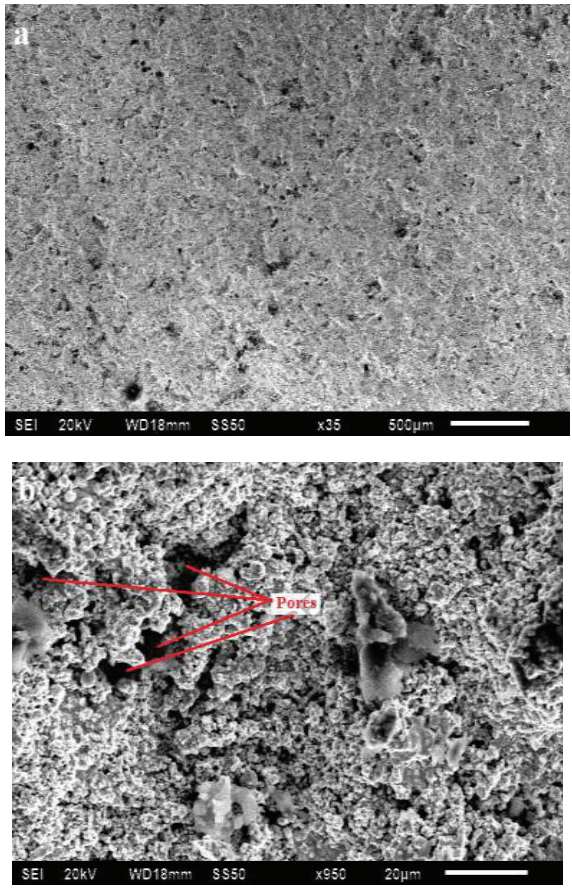

Fig 6.2: SEM micrograph of WC–Co coated aluminum alloy a) Low magnification b) High magnification

6.2 Bond Strength

A bond strength of 39.5 MPa was observed for an average coating thickness of 100 µm. During the pull off test, a slight delamination was observed which indicates good adhesion between coating and aluminum alloy.

6.3 Damping Behavior of a Coating Structure

In an ideally elastic material, strain lags behind stress by loss angle is denoted (δ) as 0 and σ/ε = *E*, where *E* is the elastic modulus. However, for an-elastic materials, δ is non- zero and the ratio is a complex quantity. The resultant is given as:

$$E^{*} = E^{'} + iE^{''} \tag{6.1}$$

$E^{'}$ and $E^{''}$ represents storage modulus and loss modulus.

The ratio of two modulus gives

$$\tan\delta = \frac{E^{''}}{E^{'}} \tag{6.2}$$

where tan δ is the loss tangent.

Fig.6.3demonstrates the schematic outline of the coated surface layer on the substrate.

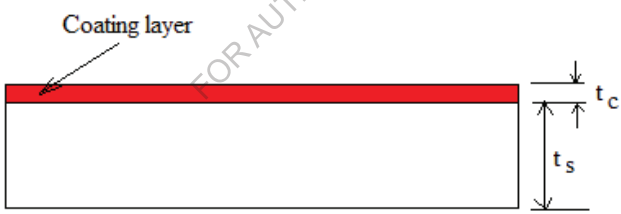

Fig 6.3: Schematic representation of the coating layer

Let the thickness and storage modulus of substrate and coating material be t_s , E_s, t_c , E_c respectively, then the damping behavior in terms of loss tangent (tan δ) of the coated material is given by the equation 3 for transverse loading [224].

$$\tan\delta \approx \frac{3E_c \tan\delta_c t_c}{E_s t_s} \tag{6.3}$$

According to the Reuss formula, the damping of a coating structure for the Fig. 6.3,

$$\frac{1}{E^*} = \frac{t_s}{E_s^*} + \frac{t_c}{E_c^*} \tag{6.4}$$

Substituting equation 6.1 into equation 6.4 and sorting out the imaginary and real part of E^*, the modulus and tan δ of the coating structure are acquired as [225]:

$$E = \frac{E_c/(1-t_c)}{\left((E_c/E_s)^2 + (t_c/(1-t_c))^2 + (E_c/E_s)(t_c/(1-t_c)) \dfrac{2(1+\tan\delta_s \tan\delta_c)}{\sqrt{(1+\tan^2\delta_s)(1+\tan^2\delta_c)}} \right)^{1/2}}$$

(6.5)

$$\tan\delta = \frac{(E_c/E_s)\tan\delta_s\sqrt{1+\tan^2\delta_c} + (t_c/(1-t_c))\tan\delta_c\sqrt{1+\tan^2\delta_s}}{(E_c/E_s)\sqrt{1+\tan^2\delta_c} + (t_c/(1-t_c))\sqrt{1+\tan^2\delta_s}}$$

(6.6)

From the equation 6.6 it is obvious that the loss tangent (damping) is a function of the ratio of modulus and the coating thickness.

6.4 Optimum Coating Thickness

The optimal coating thickness is obtained by equating the partial differential of $E\tan\delta$ *w.r.t* coating thickness to zero i.e. $\frac{\partial(E\tan\delta)}{\partial t_c} = 0$. The solution of the equation obtained from the MATLAB is the optimum thickness of the coating t_c. From Fig. 6.4 the optimum coating thickness is found to be 0.105 mm, and maximum $E\tan\delta$ is 0.935 GPa. Hence, a constant coating thickness of 100 microns was deposited on all the specimens as shown in Fig. 6.5 and the cross sectional SEM image of the coating is shown in Fig. 6.6.

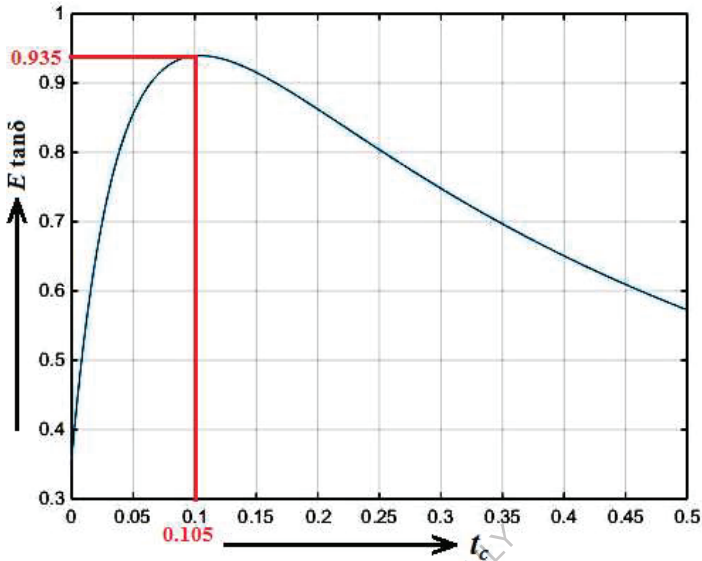

Fig 6.4: Optimum coating thickness (t_c)

Fig 6.5: WC-Co coated Al/2%RHA composites

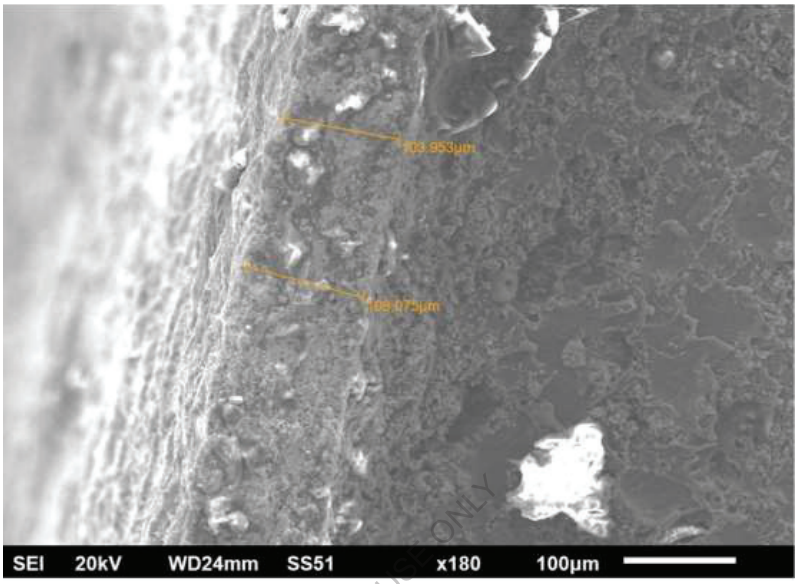

Fig 6.6: Cross sectional SEM image of WC-Co coated Al/2%RHA composites

6.5 Damping Behavior of WC-Co Coated A356.2 and its Composites

The damping behavior of WC-Co coated A356.2 and its composites are presented in Fig 6.7a-d. Fig 6.7a indicates the moduli and mechanical damping of A356.2 aluminium alloy coated with WC-Co. From the Fig 6.7, it is observed that the test specimens storage moduli tend to decrease with the deposition of WC-Co. It was further acclaimed that the storage modulus decreases with the rising temperature concerning all the frequencies studied herein. However, the damping was found to increase with the deposition of WC-Co coating. Also, it was perceived that the damping behaviour of the coated unreinforced alloy increments with the increasing temperature. Interestingly, the damping behavior was found to increase with the increase in frequency displaying a reverse trend with un-coated specimens.

The moduli and mechanical damping data for Al/x%RHA (x=2, 4, 6) composites, as documented by DMA, are illustrated in Fig 6.7b-d. The damping capacity of the coated Al/x%RHA (where x= 2, 4, 6) composites clearly shows an enviable increase of nearly 10 times greater than the damping capacity of A356.2 alloy at room temperature and nearly 7 times higher at 150 °C. Also, the damping behaviour was found to increase with the increase in frequency showing reverse trend as compared with un-coated Al/RHA composites. The modulus curve found to decline with the increase in temperature in all the cases. However, marginal increase of modulus was notable with the increased frequency.

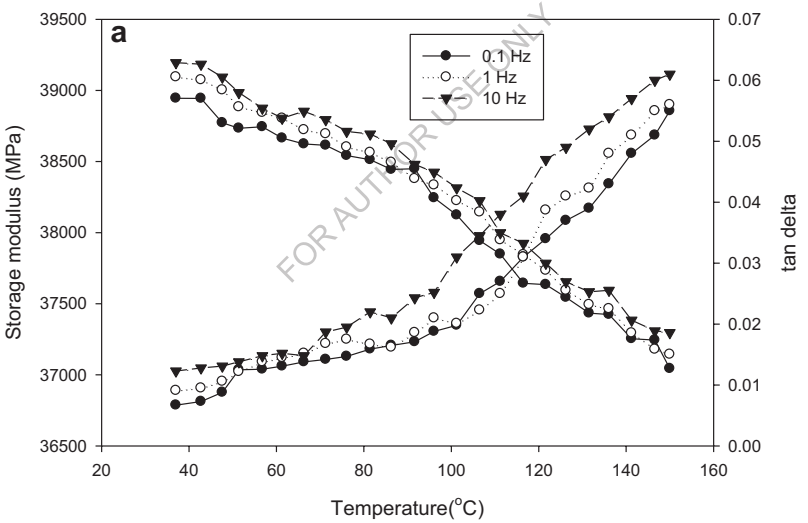

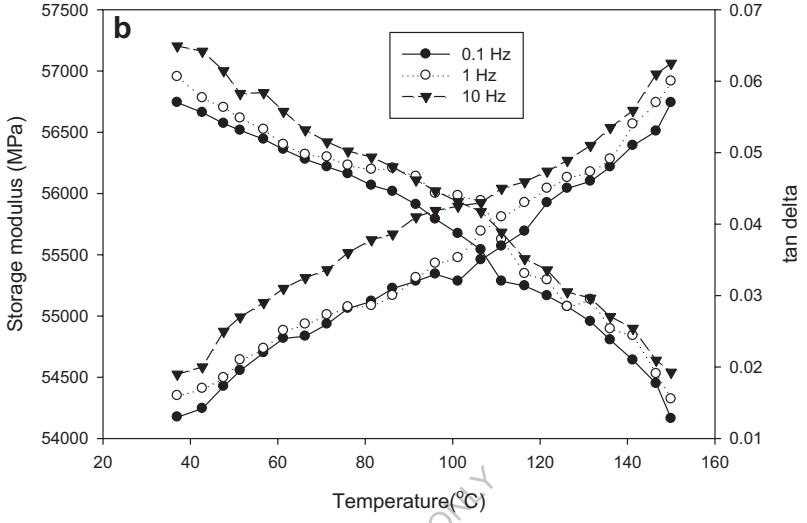

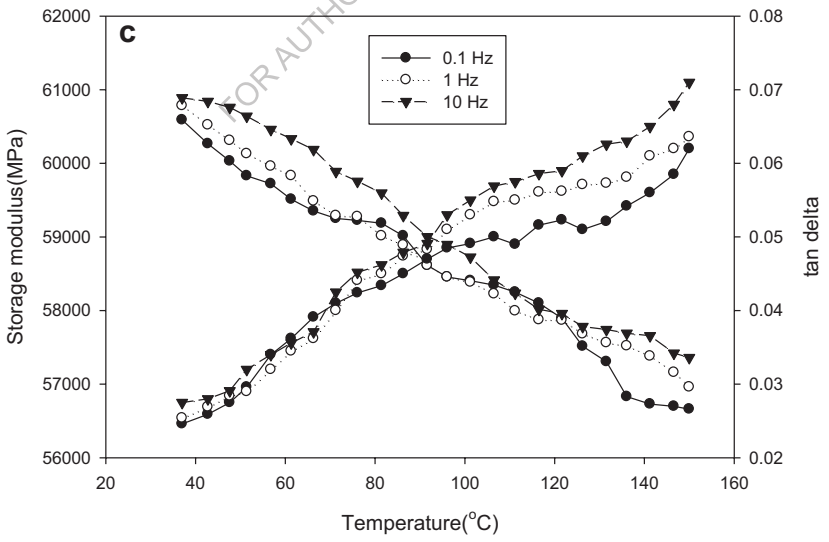

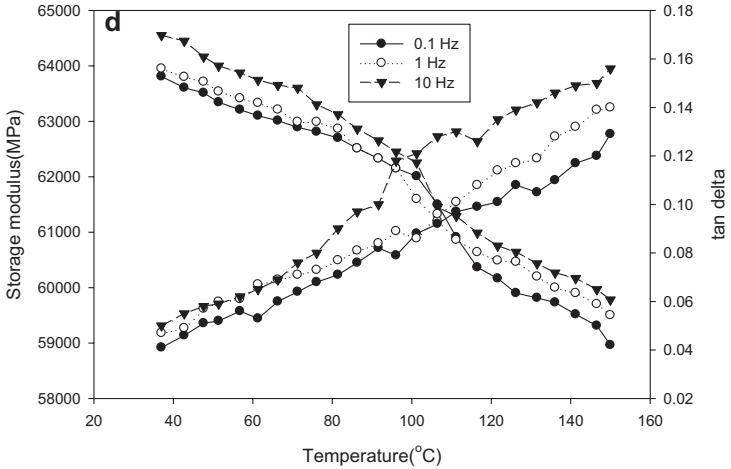

Fig.6.7: Damping behavior of WC-Co coated a) unreinforced alloy b) 2% RHA reinforced composite c) 4% RHA reinforced composite d) 6% RHA reinforced composite

Fig.6.8 shows the XRD pattern of the WC-Co coated sample. From the XRD pattern, it can be figured out that, peaks corresponding to WC and W_2C are clearly seen. The presence of W_2C in the coatings is due to the unsolicited de-carburization of WC. The presence of W_2C phase results in loss of hard phase, resulting in metal matrix embrittlement, which subsequently decreases the mechanical properties. This could be the possible reason for the decrease in the storage modulus for the WC-Co coated samples.

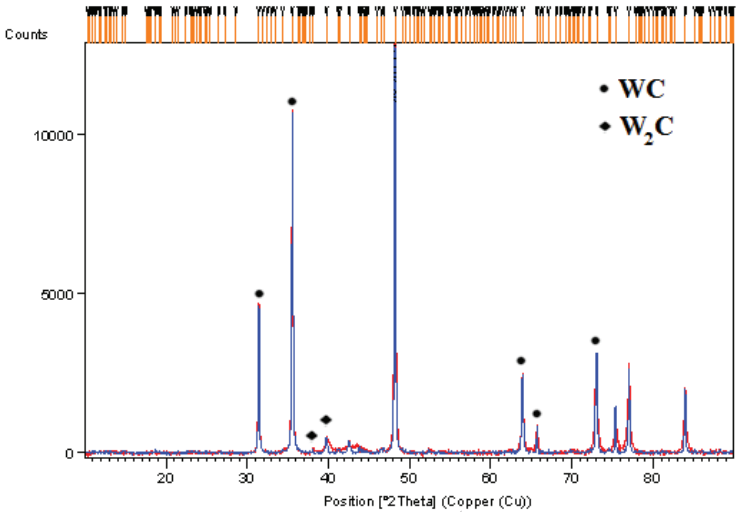

Fig. 6.8: XRD pattern for WC-Co coated A356.2 alloy

The presence of porosity on the coatings indicates the presence of voids which will enhance the damping capacity. Also, due to decarburization, free carbon may interact with oxygen to produce CO_2 gas that can be entombed in the coating to form porosity which in turn helps in enhancement of the mechanical damping. Also, the micro cracks initiates on the coating layer as a result of CTE difference in matrix and the coating material which in turn dissipates more energy through these micro cracks and this feature is illustrated in Fig. 6.9. It is noted that an increment in frequency results in high damping for the WC-Co coated alloy. As the frequency increases the coating fragmentation has been observed which is probably due to micro-cracks propagation which in turn helps in dissipation of more energy. This feature is presented in Fig. 6.10. However, no peeling of the coating has been observed.

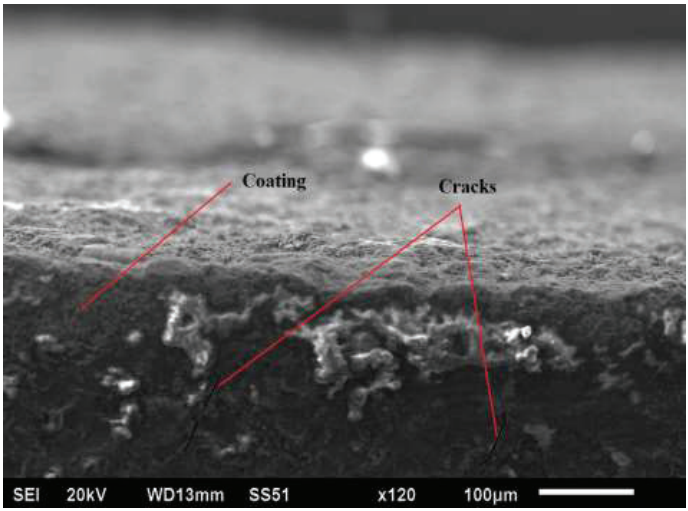

Fig.6.9: Cross sectional SEM image of the coating

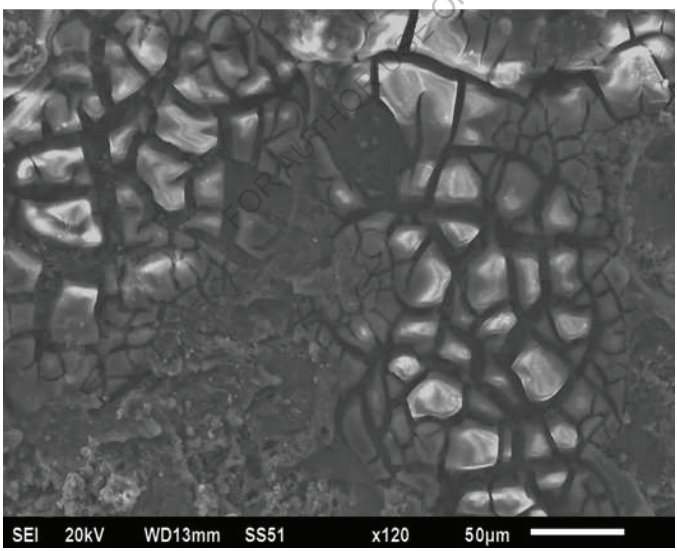

Fig. 6.10: SEM image on the surface of the coating at 10 Hz

The increase in damping capacity of the WC-Co coated Al/RHA matrix system can be explained in the following sub-headings:

6.5.1 Hardness

It was noticed that the hardness increases with the increase in RHA particles. As the base alloy is softer, the high velocity WC-Co coating easily shots into the soft base alloy thus creating a good mechanical bonding between the coating and the substrate. On the other hand, as the WC-Co coating on the composite cannot easily penetrate into the material due to the increase in hardness with the RHA reinforcement which thereby results in relatively low mechanical bonding at the interface. This feature is evident from cross sectional SEM micrographs which are shown in Fig. 6.11. This is more noteworthy as the reinforcement% increases. As the damping is the loss of energy due to cyclic load, the strong interface bonding between the WC-Co coating and base alloy would dissipate low energy when compared with WC-Co coated composites. The interfacial slip at the interface due to relatively low bonding between the WC-Co coating and alloy can be considered for high energy dissipation. Hence the hardness can be considered as one of the possible reasons for higher damping capacities of WC-Co coated Al/RHA composites. The results of the hardness of the matrix system are shown in Table 6.1.

Table 6.1: Hardness of the base alloy and its composites

Type	A356.2	Al/2%RHA composite	Al/4%RHA composite	Al/6%RHA composite
BHN	68	73	79	82

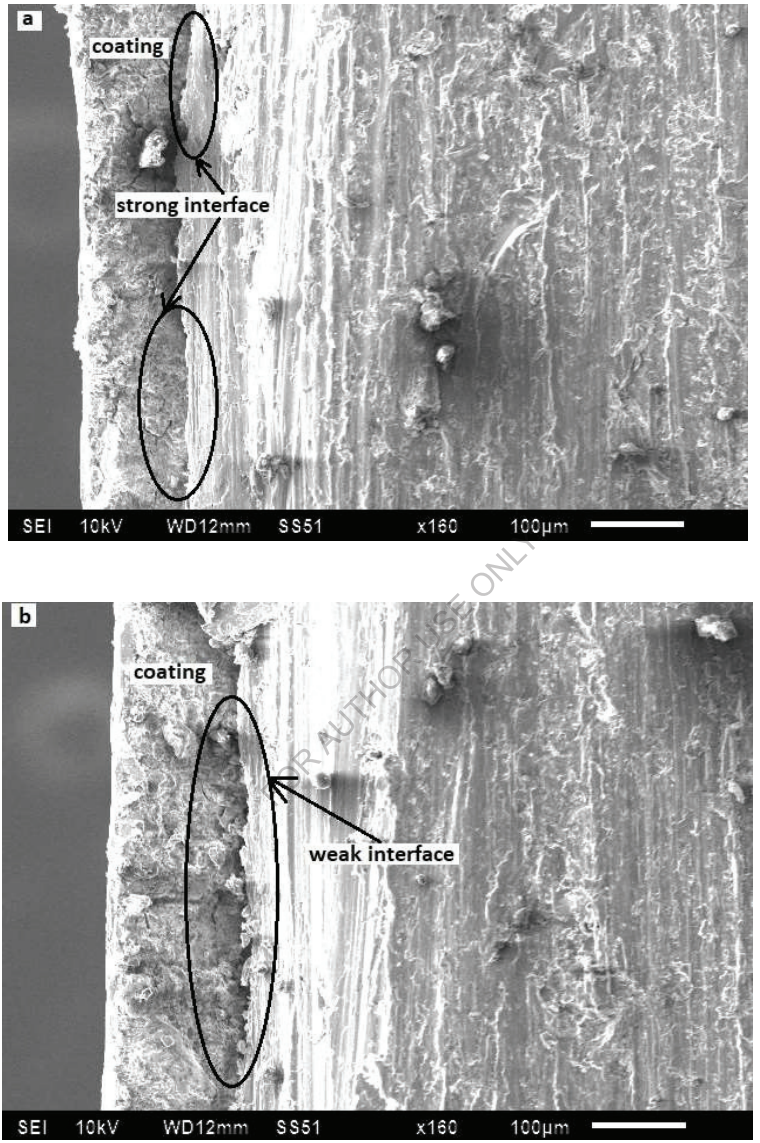

Fig 6.11: Cross sectional SEM micrograph of a) interface between coating and base alloy b) interface between coating and Al/6%RHA composite

6.5.2 Residual stresses

The development of residual stresses in the composites is a common phenomenon and study of such detrimental stresses is utmost importance in the present day scenario. Due to mismatch of matrix and the reinforcement, residual stress may initiate in the composites**.** Also, it is known that both the matrix and the reinforcement are thermally and mechanically isotropic. The high velocity impact of the WC-Co coatings on the material will also induces residual stresses. The resultant residual stresses on the WC-Co coated composites is the summation of residual stresses induced due to the thermal mismatch and due to deposition of WC-Co coatings if the measured stresses are few microns below the surface.

In the present work, a compressive residual stress of nearly 68.5 MPa and a tensile residual stress of 10.2 MPa was observed on the WC-Co coated base alloy and WC-Co coated 6% reinforced composite respectively. The d-spacing vs $\sin^2$ (Psi) plots was presented in Fig 6.12. The change in the nature of residual stresses for 6% reinforced RHA composite was probably due to decrease in the CTE with the increase in the RHA as studied in authors earlier works**.** This feature is appropriate with the studies of Oladijo et al. [219].Apart from this, the increased hardness for composite may also be a reason for tensile residual stresses in Al/6%RHA composite. The tensile residual stress initiates micro-cracks on the surface when a cyclic load is applied. As micro-cracks are the sources for energy dissipation, the damping capacity for WC-Co coated composites was found to increase with the increase in RHA content.

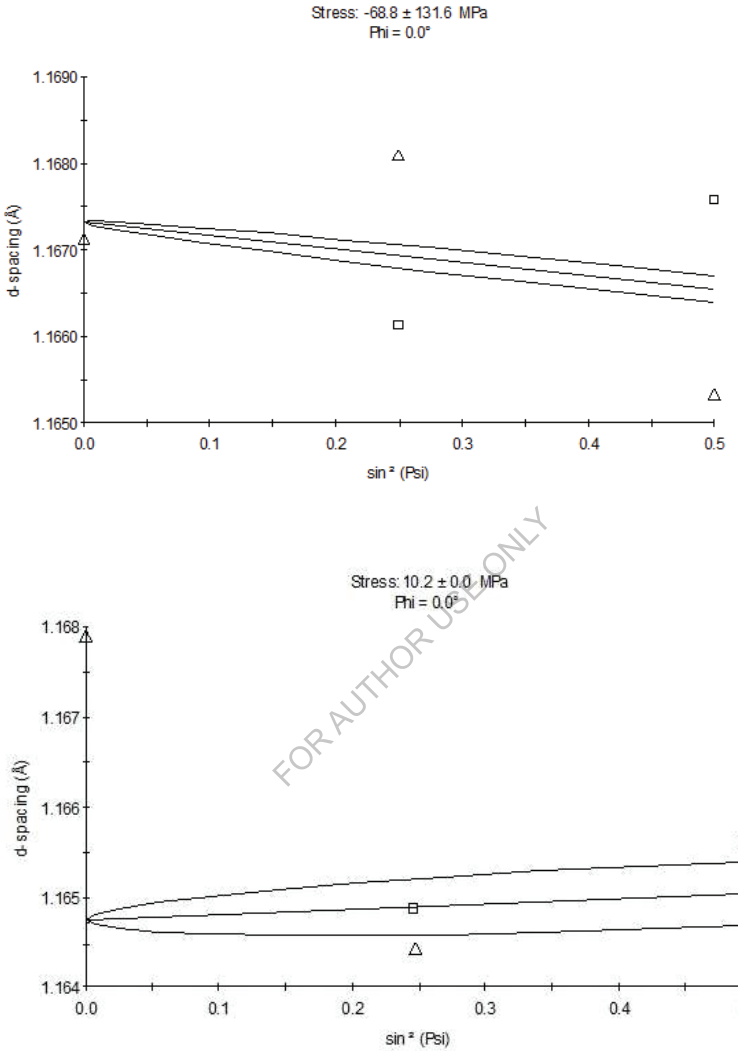

Fig 6.12: The d-spacing vs $\sin^2$(Psi) plot a) on the surface of the WC-Co coated base alloy b) on the surface of the WC-Co coated Al/6%RHA composite

6.5.3 Porosity

Porosity is a common phenomenon in coatings as well as in the composites. The presence of porosity indicates the presence of voids. These voids will act like a source for the energy dissipation. This is more significant because of enhanced RHA %. Therefore there is an increase in damping capacity along with an increase in RHA content for WC-Co coated Al/RHA composites.

The WC-Co considered in the study was about 37 μm and can be treated as coarse particles. In general, coarse particles will have more structural defects than fine particles and hence through these structural defects more heat energy will be dissipated. Also, due to decarburization, the free carbon interacting with the atmospheric oxygen to produce CO_2 gas that can be entombed in the coating to form porosity which in turn helps in enhancement of the damping behavior.

6.6 Summary

Inspection of the abovementioned results concludes that an optimum coating thickness of 100 microns was numerically obtained for maximum E tanδ and the same was deposited on all the specimens. High velocity oxygen fuel technique was successfully employed to deposit WC-Co coatings. WC-Co coated base alloy exhibit better damping capacity when compared to un-coated alloy. It is found that damping capacity of coated base alloy increases with the increase in temperature and frequency. With the incorporation of RHA particles in the matrix leads to the increment in the damping and modulus. WC-Co coated composites display more damping when compared to non-reinforced and WC-Co coated materials. The interface of coating and the RHA particles has a crucial part in increasing the damping of WC-Co coated composites. The hardness can be considered as one of the possible reasons for higher damping capacities of WC-Co coated Al/RHA

composites. As micro-cracks are the sources for energy dissipation, the damping capacity for WC-Co coated composites was observed an increase with RHA content increment. Hence the damping capacity increments with an increment in content of RHA for WC-Co coated Al/RHA composites. Due to decarburization, the free carbon interacting with the atmospheric oxygen to produce CO_2 gas that can be entombed in the coating to form porosity which in turn helps in enhancement of the damping behaviour. As the WC-Co coating enhances the damping these coatings can be used as a damping coating in automobile applications.

CHAPTER-VII
CONCLUSIONS

The main intention of this work is to fabricate A356.2 metal matrix composite consisting of RHA particles of 2, 4 and 6 wt. % through stir casting method. Thus, base alloy and the fabricated Al/RHA composites are coated with WC-Co using HVOF thermal spray process. The damping behavior of the WC-Co coated base material and its metal matrix materials were thoroughly investigated.

From the study the following conclusions are drawn.

- RHA an agro by-product was successfully incorporated as a filler material to produce aluminium based metal matrix composites. Micro-structural characterization of the fabricated composites indicated the presence of uniformly distributed rice husk ash particulates into aluminium A356.2 matrix core system.
- Mechanical properties such as density, porosity, hardness and tensile strength of the specimens were investigated and found that porosity and density (density decreased by 6.65% while hardness increased by 20.5%) of metal matrix system decreased with RHA content whereas yield strength and ultimate tensile strength (yield and ultimate tensile strength increased by 34% and 22.8%) exhibited elevated results with RHA content. This elevated strength can be accounted for the increase of dislocation density.
- The decrease in density can be attributed to the incorporation of lower density particles into the core matrix material. The increase in hardness can be ascribed to the addition of hard strengthened particulates. The enhanced yield and ultimate strength in the fabricated composites is probably due to the increment in the dislocation density with the percentage of reinforcement.

- An optimum coating thickness of 100 microns (numerically obtained from MATLAB for maximum E tanδ) was deposited on all the samples using high velocity oxygen fuel technique to deposit WC-Co coatings on A356.2 and A356.2/RHA composites.
- Fine, adherent and uniform WC-Co coating onto the metal substrate and tiny pores are evident from the micro-structural study.
- Taguchi technique is successfully used to optimize WEDM parameters while machining the samples (base alloy, Al/RHA composites, WC-Co coated A356.2 and WC-Co coated Al/RHA composites) in order to investigate damping capacity by employing dynamic mechanical analyzer. Hence, T_{ON} and T_{OFF} have been observed to have a crucial role in improving damping capacity. Also, optimal parameters for maximum damping capacity has been obtained for A356.2 aluminium alloy when machined at T_{ON} = 111 µsec, T_{OFF} = 57 µsec and I.P is 210A. Henceforth, the obtained optimal parameters were utilised while machining all the samples for damping measurement.
- Through the experimental investigation it is well noted that the damping capacities of Al/RHA composites is elevated with incrementing the RHA wt. % due to increased plastic zone, dislocation density and porosity The mechanical damping increases with the increase in the temperature for all the frequencies whereas storage modulus is found to decrease with the increase in the temperature and no considerable change was seen with frequency. This may be accounted for the decrease in material stiffness with temperature.
- From the investigations, it was also noticed that the mechanical damping is significantly improved by depositing WC-Co on the aluminium alloy. The

presence of porosity on the coatings and the interface between the coating and the substrate has a vital role in enhancing the mechanical damping.

- The storage modulus was found to decrease with deposition of WC-Co. The existence of W2C phase due to the de-carburization of WC results in the decrease of storage modulus. The storage modulus was found to increase with RHA weight % and this is due to the increased stiffness with reinforcement.
- The damping capacity of the WC-Co coated composites exhibited increased damping capacity with the increase in RHA content. Hardness of the composites, residual stresses on the surface of the coating and porosity plays an uncompromising role in the enhancement of the damping capacity.
- Hardness is considered as one of the possible reasons for higher damping capacities of WC-Co coated Al/RHA materials. WC-Co coating on the composite cannot easily penetrate into the material due to the increase in hardness with the RHA reinforcement and this may result in relatively low mechanical bonding at the interface. At the interface an interfacial slip exists which can be attributed for high energy dissipation.
- It is studied that high velocity impact of the WC-Co coatings on the samples induces residual stresses. A compressive residual stress of nearly 68.5 MPa and a tensile residual stress of 10.2 MPa was observed on the WC-Co coated base alloy and WC-Co coated 6% reinforced composite respectively. The tensile residual stress initiates micro-cracks on the surface when a cyclic load is applied. As micro-cracks are the sources for energy dissipation, the damping capacity for WC-Co coated composites was found to increase with the increase in RHA content.

- The presence of porosity indicates the presence of voids at the interface of particle and matrix which acts as a source for the damping behaviour. As the percentage of reinforcement increases this feature is more significant. Hence, the damping capacity increases with the increase in the content of RHA for WC-Co coated Al/RHA composites. As, WC-Co coated particles are found to be coarse with 37 μm grain size, they have more structural defects than fine particles and hence through these structural defects more heat energy will be dissipated.
- Also, due to decarburization, free carbon interacting with the atmospheric oxygen to produce CO_2 gas can be entombed in the coating to form porosity which in turn helps in enhancement of the damping behaviour.
- From the conclusions it is clear that the WC-Co coating enhances damping capacities and hence, these coatings can be used as a damping material in automobile and other industrial applications.

FUTURE STUDY

- The effect of heat treatment on the energy dissipation is to be studied.
- Damping behaviour of the composites can be investigated under cryogenic and harsh environments.
- Incorporation of multi layered coatings through thermal spray process can be reviewed.
- Fabrication of multi-layered RHA and other harder reinforcement material is to be identified and its damping behaviour can be investigated.
- The effect of WC-Co coatings on damping behavior can be modeled using FEA simulations.

- Numerical equations on damping behavior can be developed for WC-Co coatings and can be compared with other FEA techniques.

REFERENCES

[1]. N. Rahul Reddy, Composite materials-history, types, fabrication techniques, advantages and applications, International Journal of Mechanical and Production Engineering, 2017 ,5(9),pp 82-87.

[2]. Chawla Krishan Kumar, Composite materials, Science and Engineering, Springer, 2012.

[3]. T. W. Clyne and P. J. Withers, An introduction to metal matrix composites, Cambridge University Press, Cambridge, 1993.

[4]. Qing Liu, Fugong, Qiang Wang, Haimin Ding, Kaiyu Chu, Yuan Liu, Chong Li, The influence of particles size and its distribution on the degree of stress concentration in particulate reinforced metal matrix composites, Materials Science and Engineering: A2018, 731, pp 351-359.

[5]. Kyuhong Lee, Chang Young Son, Sang Bok Lee, Sang Kwan Lee, Sunghak Lee, Direct observation of micro fracture process in metallic-continuous-fibre-reinforced amorphous matrix composites fabricated by liquid pressing process, Materials Science and Engineering: A, 2010, . 527 (4), pp 941-946.

[6]. D.R. Moore, J.G. Williams, A. Pavan, Fracture mechanics testing methods for polymers, Adhesives and Composites, Elsevier, 2001.

[7]. Chung and D. L Deborah, Composite materials, Science and Applications, Springer, 2010.

[8]. M. Nagaraj Chelliah, Rishi Raj, Harpreet Singh, M.K. Surappa, Processing, microstructural eution and strength properties of in-situ magnesium matrix composites containing nano-sized polymer derived SiC NO particles, Materials Science and Engineering: A, 2017, .685, pp 429-438.

[9]. A. Hahnel, E.Pippel, A. Feldhoff, R. Schneider, J. Woltersdorf, Reaction layers in MMCs and CMCs: structure, composition and mechanical properties, Materials Science and Engineering,1997,.237(2), pp 173-179.

[10]. Isaac Dinaharan and Esther TitilayoAkinlabi, Low cost metal matrix composites based on aluminium, magnesium and copper reinforced with fly ash prepared using friction stir processing, Composites Communications, 2018, .9, pp 22-26.

[11]. Bhaskar Chandra Kandpal, Jatinder Kumar, Hari Singh, Manufacturing and technological challenges in Stir casting of metal matrix composites– A Review, materials today proceedings, 2018, .5(1), pp 5-10.

[12]. https://www.researchgate.net/figure/Classification-of-composite-materials-a-Based-on-matrix-materials-and-b-based-on_fig1_280921582.

[13]. M. Zadra and L. Girardini, High-performance, low-cost titanium metal matrix composites, Materials Science and Engineering: A, 2014, .608, pp 155-163.

[14]. Peng Dong, Zhe Wang, Wenxian Wang, Shaoping Chen, Jun Zhou, Interfacial characteristics and fracture behavior of spark-plasma-sintered TiNi fibre-reinforced 2024Al matrix composites, Materials Science and Engineering: A, 2017,.691 , pp 141-149.

[15]. X. Liu, Y. Liu, D. Huang, Q. Han, X. Wang, Tailoring *in-situ* TiB_2 particulates in aluminium matrix composites, Materials Science and Engineering: A, 2017,.705, pp 55-61.

[16]. Kyeong Ho, BaikPatrick, S. Grant, Microstructural evaluation of monolithic and continuous fibre reinforced Al-12wt. %Si produced by low pressure plasma spraying, Materials Science and Engineering: A, 1999, .265 (1), pp 77-86.

[17]. A. Muthuchamy, G.D JanakiRam, V. SubramanyaSarma, Spark plasma consolidation of continuous fibre reinforced titanium matrix composites, Materials Science and Engineering: A, 2017, .703, pp 461-469.

[18]. E. Jonathan Spowart and B. Daniel The influence of reinforcement morphology on the tensile response of 6061/SiC/25p discontinuously-reinforced aluminium, Materials Science and Engineering: A, 2003, .357 (1), pp 111-123.

[19]. Henry Cay, Huiru Xu, Qizhen Li, Mechanical behavior of porous magnesium/alumina composites with high strength and low density, Materials Science and Engineering: A, 2013 .574, pp 137-142.

[20]. M. Zadra and L. Girardini, High-performance, low-cost titanium metal matrix composites, Materials Science and Engineering: A 2014, .608, pp 155-163.

[21]. P. Prabhakara Rao, J. Pranay Kumar, R. Rahul, Production of copper metal Matrix composite through powder metallurgy route, International Journal of Engineering Technology Science and Research,2017,. 4(12), pp 855-864.

[22]. M. LohithakshaMaiyar, RamanujamRadhakrishnan, Jerald Jayaraj, Optimization of machining parameters for end milling of inconel 718 super alloy using taguchi based grey relational analysis, Procedia Engineering,2013,.64, pp 1276 – 1282.

[23]. M. Haghshenas, Metal–Matrix Composites, Materials Science and Materials Engineering Elsevier, 2016.

[24]. Jiang Wenming, Fan Zitian, Liu Dejun, Microstructure, tensile properties and fractography of A356 alloy under as-cast and T6 obtained with expendable pattern shell casting process, Transactions of Nonferrous Metals Society of China, 2012, 22, pp 7−13.

[25]. Dora Siva Prasad and A. Rama Krishna, Tribological properties of A356.2/RHA composites, Journal of Materials Science and Technology, 2012, 28, 4, pp 367-372.

[26]. S. Satya Shiv kumar, L.wang, C. Keller, Impact Properties of A356-T6 Alloys, Journal of Materials Engineering and Performance, 1994, 3-1, pp 83-91.

[27]. H. Moller, Application of shortened heat treatment cycles on A356 automotive brake callipers with respective globular and dendritic microstructures, Transactions of Nonferrous Metals Society of China, 2010, 20, pp 1780−1785.

[28]. LI B, Microstructure evolution and modification mechanism of the ytterbium modified Al-7.5%Si-0.45%Mg alloys, Journal of Alloys and Compounds, 2011, 7, pp 3387−3392.

[29]. M. Penchal Reddy, F. Ubaid, R.A Shakoor, GururajParande, VyasarajManakari, A.M.A Mohamed, Manoj Gupta, Effect of reinforcement concentration on the properties of hot extruded Al-Al_2O_3 composites synthesized through microwave sintering process, Materials Science and Engineering: A,2017,696, pp 60-69.

[30]. K. Shirvanimoghaddam, H. Khayyam, H. Abdizadeh, M. Karbalaei Akbari, A.H Pakseresht, E. Ghasali, M. Naebe, Boron carbide reinforced aluminium matrix composite: Physical, mechanical characterization and mathematical modelling, Materials Science and Engineering: A, 2016,658, pp 35-149.

[31]. Mansour, RahseparHamed, Jarahimoghadam, The influence of multipass friction stir processing on the corrosion behavior and mechanical properties of zircon-reinforced Al metal matrix composites, Materials Science and Engineering: A, 2016, 671, pp 214-220.

[32]. Qing Liu, Fugong, Qiang Wang, Haimin Ding, Kaiyu Chu, Yuan Liu, Chong Li, The influence of particles size and its distribution on the degree of stress

concentration in particulate reinforced metal matrix composites, Materials Science and Engineering: A, 2018,731, pp 351-359.

[33]. Xichen Tao, Yongqin Chang, YuanhangGuo, Wuming Li, Mingyang Li, Microstructure and mechanical properties of friction stir welded oxide dispersion strengthened AA6063 aluminium matrix composites enhanced by post-weld heat treatment, Materials Science and Engineering: A, 2018, 725, pp 19-27.

[34]. A. P. S. V. R. Subrahmanyam, J. Madhukiran, G. Naresh, S. Madhusudhan, Fabrication and characterization of Al 356.2, rice husk ash and fly ash reinforced hybrid metal matrix composite, International Journal of Advanced Science and Technology, 2016, 94, pp 49-56.

[35]. K.K Alanemea and T.M Adewalea, Influence of rice husk ash – silicon carbide weight ratios on the mechanical behaviour of Al-Mg-Si Alloy matrix hybrid composites, Tribology in Industry, 2013, 35(2), pp 163-172.

[36]. D Siddharth and JinuguBabu Rao, Synthesis & characterization of RHA (rice husk ash) particulates reinforced A7075 composites, International Journal of Advances in Mechanical and Civil Engineering, 2017, 4(3), pp 2394-2827.

[37]. A. P. S. V. R. Subrahmanyam, G. Narsaraju, B. Srinivasa Rao, Effect of Rice Husk ash and Fly ash reinforcements on microstructure and mechanical properties of aluminium alloy (AlSi10Mg) matrix composites, International Journal of Advanced Science and Technology, 2015, 76, pp 1-8.

[38]. D. Lingaraju, G. Venkata Sreekanth, Rice husk ash reinforced in aluminium metal matrix nanocomposite: A Review, Journal of Basic and Applied Engineering Research, 1, No: 3; October, 2014 ,pp 35-40

[39]. M. Rajkumar Reddy, T. Prasad, P. Ravikanth Raju, Study on wear properties of rice husk ash and fly ash reinforcement in aluminium (Al 6061) metal matrix composites, International Journal of Current Engineering and Scientific Research, 2018, 5(4), pp 116-122.

[40]. Srikant Tiwari, M.K Pradhan, Effect of rice husk ash on properties of aluminium alloys: A review, materials today proceedings, 2017, 4 (2), pp 486-495.

[41]. KamilBochenek, WitoldWęglewski, JerzyMorgiel, MichałBasista, Influence of rhenium addition on microstructure, mechanical properties and oxidation resistance of NiAlobtained by powder metallurgy, Materials Science and Engineering: A, 2018, 735, pp 121-130.

[42]. PengDong, ZheWang, Wenxian Wang, Shaoping Chen, Jun Zhou, Interfacial characteristics and fracture behavior of spark-plasma-sintered TiNi fibre-reinforced 2024Al matrix composites, Materials Science and Engineering: A, 2017, 691, pp 141-149.

[43]. http://www.pm-review.com/introduction-to-powder-metallurgy/the-powder-metallurgy-process/

[44]. Yao Wei, Wu Aiping, Zou Guisheng, Ren Jialie, Formation process of the bonding joint in Ti/Al diffusion bonding, Materials Science and Engineering: A, 2008, 480(2), pp 456-463.

[45]. Guoping Liu, Qudong Wang, Teng Liu, Bing Ye, Haiyan Jiang, Wenjiang Ding, Effect of T6 heat treatment on microstructure and mechanical property of 6101/A356 bimetal fabricated by squeeze casting, Materials Science and Engineering: A, 2017, 696(1), pp 208-215.

[46]. http://www.substech.com/dokuwiki/doku.php?id=liquid_state_fabrication_of_metal_matrix_composites

[47]. Amit Pal, Abhishek Verma, SansarSwaroopSaxena, Bhaskar Chandra Kandpal, Stir Casting of Metal Matrix Composites – A Review, International Journal of Computer & Mathematical Sciences, 2015, 4, pp 1-3.

[48]. Y. Pazhouhanfar and B. Eghbali, Micro structural characterization and mechanical properties of TiB_2 reinforced Al6061 matrix composites produced using stir casting process, Materials Science and Engineering: A, 2018, 710, pp172-180.

[49]. K. Amouri, A. Momeni, Sh. Kazemi, M. Kazazi, Microstructure and mechanical properties of Al-nano/micro SiC composites produced by stir casting technique, Materials Science and Engineering: A, 2016, 674, pp 569-578.

[50]. A. Dehghan, Hamedan and M. Shahmiri, Production of A356–1 wt% SiC nanocomposite by the modified stir casting method, Materials Science and Engineering: A, 2012, 556, pp 921-926.

[51]. https://www.researchgate.net/figure/Schematic-diagram-of-Stir-casting-technique-for-the-fabrication-MMCs_fig20_276152382

[52]. G.Li. Surface Engineering, Mechanical Industry Publishing House, Beijing, 1998.

[53]. J.Deng, T.Lee, Surf.Eng, 2000, 16(5), pp 411-414.

[54]. A.Raykowski, M.Hader, wear, 2001, 249, pp 127-132.

[55]. B.Djurovie,E.Jean, Wear , 1999, 224, pp 22-37.

[56]. Deng Jianxin, Liu Lili, Ding Mingwei, Erosion wear behaviour of Sic/(W,Ti)C laminated ceramic nozzles in dry sand blasting process, Materials Science and Engineering A, 2007, 444 , pp 120-129.

[57]. www.wise.greek.org/what-is -sand blasting.htm (date accessed: 30/3/2018).

[58]. E.T.Akinlabi, E.Ogunmuyiwa, S.A.Akinlabi, Characterizing the effects of sand blasting on formed steel samples, world academy of science, Engg& technology, Int.J. of Mechanical and Mechatronic Engineering, , 2013, 7, No: 11.

[59]. T.Kosmac, C.Oblak, P.Jevnikar, N.Funderk, L.Marion, The effect of surface grinding and sand blasting on flexural strength and reliability y-TZP Zirconia ceramic, Dental Material Academy of Dental Materials, Eleseiver Science ltd, 1999, 15, pp 426-433.

[60]. G.E.DIETER: Mechanical Metallurgy, Mc Graw Hill, 1986, pp 409.

[61]. F.V.Lawrence and P.K.Mazumdar, Low cycle fatigue strength and Elastoplastic behavior of materials (ed. K.T.Rie and E.Heibach), Stuttgart, 1979, pp 469-475.

[62]. X.Li, J.Ye, H.Zhang, T.Fung, J.Chen, X.Hu, Sand blasting induced stress release and enhanced adhesion strength of diamond films deposited on austenite stainless steel, Applied Surface Science, 2017, 412 , pp 366-373.

[63]. http://en.wikipedia.org/wiki/abrasive-blasting (June 2017).

[64]. Bouazaouih L, Li A, Analysis of steel/ concrete interfacial shear stress by means of pull out test. Int J. AdhesAdhes 2008, 28, pp 101-108.

[65]. Golaz B, Michard V, Lavanchy S, Manson J.A.E, Durability of titanium sdhesive joints for marine applications, Int J. AdhesAdhes 2013, 45, pp 150-157.

[66]. Jiang X P, Wang X Y, Li J X, Li D Y, Man C S, Shepard M J, Zhai T, Enhancement of fatigue and corrosion properties of pure Titanium by sandblasting, Materials Science and Engineering A , 2006, 429 , pp 30-35.

[67]. Critchlow G W, Brewis D M, Review of surface pretreatments for aluminium alloys, Int J. Adhes 1996, 16, pp 255-275.

[68]. Njuhovic E, Brau M, Wolff-Fabris F, Starzynski K, Altstadt V, Identification of interface failure mechanism of metallized glass fibre reinforced composites using acoustic emission analysis, Composites B, 2014, 66 , pp 443-452.

[69]. Bresson G, Junnel J, Shanahan M E R, Serin P, Strength of adhesive bonding joints under mixed axial and shear loading, Int.J.AdheXiasAdhes , 2012, 35, pp 27-35.

[70]. Anna Rudawska, Izabela Danczak, Miroslav Muller, Petr Valasek, The effect of sandblasting on surface properties for adhesion, International Journal of Adhesion & Adhesives, 2016, 70 , pp 176-190.

[71]. ShaoningGeng, Junsheng Sun, LingyuGuo, Effect of sandblasting and subsequent acid pickling and passivation on the microstructure and corrosion behavior of 316 L stainless steel, Materials and Design, 2015, 88, pp 1-7.

[72]. Hong-Yuan Wang, Rui-Fu Zhu, Yu-Peng Lu, Gui-Yong Xiao, Kun He, Y.F.Yuan, Xiao-Ni Ma, Ying Li, Effect of sandblasting intensity on microstructures and properties of pure titanium micro-arc oxidation coatings in an optimized composite technique, Applied Surface Science, 2014, 292, pp 204-212.

[73]. Xiaoming Tang, Kai Huang, Jian Dai, Zhaoying Wu, Liang Cai, Lili Yang, Jie Wei, Hailang Sun, Influences of surface treatments with abrasive paper and sandlasting on surface morphology, hydrophilicity, mineralization and osteoblasts behaviors of n-CS/PK composite, Scientific Reports, 2017, 7, 568, pp 1-22.

[74]. B. Bacchelli, G. Giavaresi, M.Franchi, D.Martini, V.D.Pasquale, A.Trire, M.Fini, R.Giardino, A.Ruggeri, Science Direct, Acta Biomaterialia, 2009, 5, pp 2246-2257.

[75]. F.J.Gil, J.A.Planell, A.Padros, C. Aparicio, The effect of shot blasting and heat treatment on the fatigue behavior of titanium for dental implant applications, ImplantbDent, 2002, 11 (1), pp 28-32.

[76]. Md.Hafizuddin, MdBasir, B.Abdullah, S.Khadijah Alias, MdHafizuddinJumandin, MdHussian Ismail, Analysis on microstructure hardness and surface roughness of shot blasted paste boronozed 316 Austenitic Stainless Steel, JurnalTeknologi, 2015, 76(3), pp 75-79.

[77]. S.Ji, K.Roberts, Z.Fan, Effect of shot peening on the fatigue performance of ductile iron castings, Materials Science and Technology, 2002, 18, pp193-197.

[78]. Y.He, K.Li, L.S.Cho, C.S.Lee, I.G.Park, J.Song, C.W.Yang,J.H. Lee,K.Shin, Microstructural characterization of SS304 upon various Shot Peening Treatments, Applied Microscopy, 2015, 45(3), pp 155-169.

[79]. S.J.Laine, K.M.Knowles, P.J.Doorbar, R.D.Cutts, D.Rugg, Microstructural characterization of metallic shot peened and laser shock peened Ti-6Al-4V, ActaMaterialia, 2017, 123, pp 350-361.

[80]. R.C.Tucker,Jr., Thermal Spray Coatings, Surf.Eng, ASM Handbook, ASM International, 1994,5, pp 1-10.

[81]. T.S.SIDDU, S.Prakash, R.D.Agarwal, State of the Art of HVOF Coating Investigations – A Review, Marine Technology Society Journal, 2005, 39(2), pp 53-64.

[82]. T.Y.Cho, J.H. youn, S.K.Hew, H.G.Chun, Shi – Hong Zhang, Surface Modifications by HWOF coating of HWOF Coating of Micron sized WC- Metal powder and Laser heating of the coating, Material science Forum, 2011, 686, pp 654-660.

[83]. J.R.Davis, Handbook of Thermal Spray Technology, ASM International, USA, 2004, pp 1-10.

[84]. S.y.Park, C.G. Park, j.Kor, Mat & Meter, 2004, 42, pp 582.

[85]. B.D.Sharteel, R.Kestlen, K.O.Legg., W.Assink, A,.Nardi, J.Schell, Validation of HVOF WC/Co, and Tribology T800 Thermal Spray Coatings as a replacement for Hard Chrome plating on C-2/E-2/P-3 and C-130 Propeller Hub System Components, Naval Research Laboratory, Washington, DC, USA, 2003.

[86]. T.Y.Cho, J.H.Yoon, K.S.Kim,K.O.Song, Y.K,Joo,W.Fang, S,H. Zhang, S.J.Youn, H.G.CHUN, S.Y.HWANG, Surface and Coating Technology, 2008, 202, pp 5556.

[87]. T.Y.Cho, J.H.Yoon, K.S.Kim,K.O.Song, Y.K,Joo,W.Fang, S,H. Zhang, S.J.Youn, H.G.CHUN, S.Y.HWANG, Journal of Advanced Material Research, 2007, 26-28, pp 1325.

[88]. SaleemHasmi, P.Sahoo, J.PauloDarvin et.al, Comprehensive Materials Finishing, 1st Edition, Science Direct, 2017.

[89]. K.V. Rao, Properties and Characterization of Coatings made using Jet kote, Thermal spray technique, Proceedings of 11th International Thermal Spray Conference, Montreal, Canada, 1986, pp 873-882.

[90]. V.V Sobole, J.M. Guilemany AND J Nutling, HVOF Spraying, B0655, Maney, I0M3, 2004, pp 5.

[91]. Zhao, L.ugschaiinder, E.Fisher.A and Reimann.A, 2001, Thermal Spraying of High Nitrogen duplex austenitic – Ferritic Steel, Surface Coat Technology, 141, pp 208-215.

[92]. Zhao, L.Ugschaiinder, High Velocity Oxy.- Fuel Spraying of NiCoCrAlY and an intermetallic NiAl – TaCr alloy, Surface Coat Technology, 2002, 149, pp 230-235.

[93]. Zaho, W.M.Wang, Y.Han, T.Wu, K.Y.andXue.J, Electrochemical evaluation of Corrosion Resistance of NiCrBSi coatings deposited by HVOF, Surface Coat Technology, 2004, 183, pp 118-125.

[94]. C.M.Nygards, K.W.White, K.Ravi Chandar, Strength of HVOF coating – Substrate interfaces, Thin Solid Films, 1998, 332, pp 185-188.

[95]. A.K.Maiti, N.Mukopadhyaya and R.Raman, , Improving the Wear behaviour of WC-Co-Cr based HVOF Coating B Surface Grinding, Journal of Materials Engineering and Performance, 2009, 18(8), pp 1060-1066.

[96]. J.A.Picas, A.Forn, G.Matthaws, HVOF coatings as an alternative to hard chrome, for pistons and valves, Wear, 2006, 261, pp 477-484.

[97]. B.S.Mann, B.Prakash, High Temperature Friction and Wear Characteristics of various coating materials for steam valve spindle applications, Wear, 2000, 240, pp223-230.

[98]. P.Vuoristo, K, Neimi, T.Mangyla, L.M.Berge, M.Nebelung, Thermal spray science and Technology, AS M International Materials Park, OH, USA, 1995, pp 309.

[99]. AW PK, Tan BH, Study of Microstructure, Phase and Micro hardness, Distribution of HVOF Spray multi-model structured and conventional WC-17Co coatings, Journal of material processing Technology, 2006, 174, pp 305-311.

[100]. J.H.Chen ,P.N.Chen ,P.H. Hera,Y. Chang and W.Wu, Mater. Trans, 2009, 50, pp 689-694.

[101]. L.Zhao, M.Maurer, F.Fischer, R.Dicks, E.Lugscheider, Influence of spray properties on the particle in-flight properties and the properties of HVOF coatings of WC-Co-Cr, Wear, 2004, 257, pp 41-46.

[102]. H.J.C Voorwald, R.C Souza, W.L Pigatin, M.O.H Cioffi, Evaluation of WC-17Co and WC-10Co- 4Cr thermal spray coatings by HVOF on the fatigue and corrosion strength of AISI 4340 steel, Journal of surface coat Technology, 2005, 190, pp 155-164.

[103]. M.A.S Torres, H.J.C Voorwald, An evaluation of the shot peening residual stresses and stress relaxation on the fatigue life of AISI 4340 steel, International journal of Fatigue , 2002, 24, pp 877-886.

[104]. Hui Gon Chun, Yun KonJoo, Jae Hong Yoon, Tong Yui Cho, Wei Fang and Shi-Hong Zhang, Wear and corrosion resistance of Inconel 718, HVOF coating of WC- metal powder and laser Heat – treated coating, Applied Mechanics and Materials, 2013, 419, pp381-387.

[105]. Q.Wang, S.Zhang, Y.Cheng, J.Xiang, X.Zhao, G.Yang., 2013, Wear and Corrosion performance of WC-10Co-4Cr Coatings deposited by different HVOF and HVAF spraying processes, Surface and Coating Technologies, 2013, 218, pp 127-136.

[106]. K. Van ackev, D.Vanhoyweghen, R.Persoons and J.Vangriderbeek, Influence of Tungsten Carbide particle size and distribution on the wear resistance of laser clad WC/Ni coatings, Wear, 2005, 258, pp 194-202.

[107]. T.Ogawa, K.Tokoji, T.Ejimat, Y.Kobayashi, Y.Harada, Proceedings of the 15th International Thermal spray Conference, 1998, 25-29, Nice, France, pp 635.

[108]. R.Ahmed, Wear, 2002, 253(3-4), pp 473.

[109]. K.Padilla, A.Valasquez, A.J.A Berrios, E.S.Pushi Cabrea, Journal of surface coat Technology, 2002, 150(2), pp151.

[110]. M.P.Nadcimento, R.C. Souza, W.L.Pigaton, H.J.C. Voorwald, International journal of Fatigue, 2001, 23(7), pp 607.

[111]. R.Ahmed, M.Hadfield, Journal of Thermal Spray Technology, 2002, 11(3), pp 333.

[112]. E.S.PushiCarbera, E.S.Berrios, J.A.Da-Salva, J.Nunes, Journal of surface coat Technology, 2003, 172(2-3), pp 128.

[113]. H.Y.Al-Fadhli, J.Stokes, M.S.J.Hashmi, B.S.Yilbas, HVOF coating of welded surfaces: Fatigue and Corrosion Behaviour of stainless steel coated with Inconel -625 alloy, Surface and Coatings Technology, 2006, 200, pp4904-4908.

[114]. H.J.C Voorwald, L.F.S. Vieira, M.O.H. Cioffi, Evaluation of WC-10Ni thermal spraying coating by HVOF on the fatigue and corrosion AISI 4340 steel, Procedia Engineering, 2010, 2, pp 331-340.

[115]. K.Murugan, A.Raghupathy, V.Balasubramanian, K.Sridhar, Developing Empirical Relationship to product Harness in WC-10Co-4Cr HVOF sprayed coatings, International conference on Advances in Manufacturing and Materials Engineering, AMME, 2014, Procedia Materials Science, 2014, 5, pp 918-927.

[116]. O.C.Brandt, Journal of Thermal spray Technology, 1995, 4(2), pp147.

[117]. K.Korpiola, Journal of Thermal spray Technology, 1997, 6(4), pp469.

[118]. J.Stokes and L.Looney, Residual stress in HVOF thermally sprayed thick deposit, Surface and Coating Technology, 2004, 117-117, pp 18-23.

[119]. Y.Y.Santana, La Barbera – Sora, J.G.Staia, M.H.Lesage, J.Puchi – Cabrera, E.S.Chicot, D.Bemporad, Measurement of residual stress in thermal spray

coatings by the incremental hole drilling method, Surface and coatings Technology, 2006, 201(5), pp 2092-2098.

[120]. R.G.Azar, J. Mostaghismi, S.Chandra, Modeling development of residual stresses in thermal spray coatings, Computational Materials Science, 2006, 35, pp 13-26.

[121]. MC.Grann, R.T.F Greving, D.J.Rybicki, J.R.Bodger, B.E.Somerville, Effect of residual stress in HVOF tungsten Carbide coatings on the fatigue life in bending of thermal spray coated aluminium, Journal of Thermal spray Technology, 1998, 7(4), pp 546-552.

[122]. L.Zhao, M.Maurer, F.Fischer, R.Dicks, E.Lugscheinder, Influence of spray parameters on the particle –in flight properties and the properties of HVOF coating of WC-Co-Cr, Wear, 2004, 257, pp 41-46.

[123]. Z.Y.Taha-al, M.S.Hashmi, B.S.Yilbas, Effect of WC on the residual stress in the laser treated HVOF coating, Journal of Materials Processing Technology, 2009, 209, pp 3172-3181.

[124]. WEI Sha-sha, WU Chun-du, Study on TiAlN coated cemented carbide tool, Journal of Yanshan University, 2005, 29(6), pp485-488.

[125]. Xiao Jiming, Liyan, Bai Lizing, Research on cutting performance of graded CrAlTiN Coatings of High Speed Steel tools, Journal of Mechanical Science and Technology, 2005, 24(11) , pp 1347-1349.

[126]. CaiZhi Hai, Zhang Ping, ZhooJunjan, Dujun, Green Manufacturing Technologies of CrAlTiN Composite coatings as an alternative to chromium electro plating for piston rings, 2010, ICRM 2010-Green manufacturing, Ningbo, China.

[127]. N.A.Ahmad, Z.Kamdi, Z.Mohamad, A.S.Omar, N.AbdulLalif, A.L.MohdJobi, Characterization of WC-10Ni HVOF Coating for carbon steel blade, International conference on Applied Science (ICA 2016), Materials Science and Engineering, 2017, 165, pp 12022.

[128]. Q.Guo, J.Wang ,B.Sun, M.Nishio et al, Thermal spray Technology, 2002, 11, pp 261.

[129]. M.Manjunatha., R.S.Kuilarni, M.Krishna, Investigation of HVOF Thermal sprayed Cr_3C_2 –NiCr Cermet Carbide coatings on Erosive performance of AISI 316 Molybdenum steel, International Conference on Advances in Manufacturing and Materials Engineering, AMME 2014, Procedia Materials Science , 2014, 5, pp 622-629.

[130]. H.Hamatani, Y.Iciyamma, J.Kobayashi, Mechanical and Thermal properties of HVOF sprayed Ni based alloys with carbide, Journal of science and technology of advanced materials, 2002, 3, pp 319-326.

[131]. P.L.Tan, Tailoring of transition metal silicide as protective thin films on austenitic stainless steel, 2011, PhD thesis, Chalmers University of Technology, Gothenburg, Sweden.

[132]. D.Connetable, O.Thomas, First –principles study of Nickel- silicide ordered phases, Journal of Alloys and Compounds, 2011, 509, pp 2639-2644.

[133]. L.Pawlowski, The science and Engineering of Thermal Spray Coatings, 2nd Edition, John Wiley & Sons, 2008, New York.

[134]. J.R.Davis, Handbook of Thermal Spray Technology, ASM International, 2004, Ohio.

[135]. M.M.Verdian, K.Raeissi, M.Salehi, Fabrication and corrosion resistance of HVOF –sprayed Ni_2 Si intermetallic compound, Applied Surface Science, 2013, 273, pp 426-431.

[136]. V.H Carneiro, H. Puga, J. Meireles, Heat treatment as a route to tailor the yield-damping properties in A356 alloys, Materials Science and Engineering: A, 2018, 729, pp1-8.

[137]. A. Puskar, Internal Friction of Materials, Cambridge International Science Publishing, Cambridge , 2001.

[138]. D. Siva Prasad and A. Rama Krishna, Effect of T6 heat treatment on damping characteristics of Al/RHA composites, Bull Material Science, 2012, 35, pp 989-995.

[139]. B.J Lazan, Damping of Materials and Members in Structural Mechanics, Pergamon Press, Oxford, 1968.

[140]. Tie Tian, Zhaocheng Yuan, Wei Tan, Lin Mi, Effect of the dynamic eution of dislocations under cyclic shear stress on damping capacity of AZ61 magnesium alloy, Materials Science and Engineering: A, 2018,710(5), pp 343-348.

[141]. X.S Hu, K. Wu, M.Y Zheng, W.M Gan, X.J Wang, Low frequency damping capacities and mechanical properties of Mg–Si alloys, Materials Science and Engineering: A, 2007, 452, pp 374-379.

[142]. Dezhao Qin, Jingfeng Wang, Yongliang Chen, Ruopeng Lu, Fusheng Pan, Effect of long period stacking ordered structure on the damping capacities of Mg–Ni–Y alloys, Materials Science and Engineering: A, 2015, 624, pp 9-13.

[143]. ZhenyuZhong, Wenbo Liu, Ning Li, Jiazhen Yan, JinwuXie, Dong Li, Ying Liu, Xiuchen Zhao, Sanqiang Shi, Mn segregation dependence of damping capacity

of as-cast M2052 alloy, Materials Science and Engineering: A, 2016, 660, pp 97-101.

[144]. S.C Sharma, M Krishna, A Shashi shankar, S. Paul Vizhian, Damping behaviour of aluminium/short glass fibre composites, Materials Science and Engineering: A, 2004, 364(2), pp 109-116.

[145]. J.N Wei, H.F Cheng, Y.F Zhang, F.S Hanz, C. Zhouj, P. Shui, Effects of macroscopic graphite particulates on the damping behavior of commercially pure aluminium, Materials Science and Engineering: A, 2002, 325(2), pp 444-453.

[146]. C.S Kang, K. Maeda, K.J Wang, K. Wakashima, Dynamic Young's modulus and internal friction in particulate SiC/Al composites, Acta Materialia, 1998, 46, pp 1209-1220.

[147]. N. Srikanth, D. Saravanaranganathan, M. Gupta, Effect of presence of SiC and operating frequency on the damping behaviour of pure magnesium, Material Science Technology, 2004, 20, pp 1389-1396.

[148]. M.N Ludwigson, R.S Lakes, C.C Swan, Damping and stiffness of particulate SiC-InSnomposite, Journal of Composite Materials, 2002, 36, pp2245-2254.

[149]. J.H Gu, X.N Zhang, M.Y Gu, Mechanical properties and damping capacity of (SiCp+Al_2O_3 centre dot SiO_2f)/Mg hybrid metal matrix composite, Journal of Alloys and Compounds, 2004, 385, pp 104-108.

[150]. C.S Kang, K. Maeda, K.J Wang, K. Wakashima, Dynamic Young's modulus and internal friction in particulate SiC/Al composites. Acta Materialia. 1998, 46, pp 1209-1220.

[151]. N. Srikanth, M. Gupta, Determination of energy dissipation in Mg/SiC formulations using a new method of suspended beam coupled with circle fit approach, Scripta Materialia, , 2006, 45, pp 1031-1037

[152]. J. Zhang and R.J Perez, Lavernia, E.J. Effect of SiC and graphite particulates on the damping behavior of metal-matrix composites. Acta Metall. Mater. 1994, 42, pp 395-409.

[153]. J.H Gu, X.N Zhang, MingyuanGu, Min Gu, Xike Wang, Internal friction peak and damping mechanism in high damping 6061Al/SiCp/Gr hybrid metal matrix composite Journal of Alloys and Compounds, 2004, 372, pp 304-308.

[154]. H.S Chu, K.S Liu, J.W Yeh, Damping behavior of in situ Al-(graphite, Al4C3) composites produced by reciprocating extrusion, Journal of Materials Research, 2001, 16, pp 1372-1380.

[155]. E. Carreno Morelli, S.E Urreta, R. Schaller, Mechanical spectroscopy of thermal stress relaxation at metal-ceramic interfaces in aluminium-based composites, ActaMaterialia, 2000, 48, pp 4725-4733.

[156]. S. Elomari, R. Boukhili, M.D Skibo, J. Masounave, Dynamic-mechanical analysis of prestrainedAl_2O_3/Al metal-matrix composite, Journal of Materials Science, 1995, 30, pp 3037-3044.

[157]. H. Zhang, M. Gu, Internal friction behavior in SiC particulate reinforced aluminium metal matrix composite in thermal cycling, Journal of Alloys and Compounds, 2006, 426, pp 247-252.

[158]. R. J Perez, J. Zhang, M. N Gungor, E. J Lavernia, Damping behavior of 6061Al/Gr metal matrix composites, Metallurgical Transactions A, 1993, 24(3), pp 701–712

[159]. A. Wolfenden and V.K Kinra, Mechanics and Mechanisms of Material Damping, American Society for Testing and Materials: Philadelphia, 1997, pp 313-330.

[160]. E.J Lavernia, R.J Perez, J. Zhang. Damping behavior of discontinuously reinforced Al-alloy metal-matrix composites. Metallurgical and Materials Transactions, 1995, 26, pp 2803-2818.

[161]. Ranjit Bauri and M. K. Surappa, Damping behavior of Al-Li-SiC_p composites processed by stir casting technique, Metallurgical and Materials Transactions A, 2005, 36(3), pp 667–673

[162]. J.N Wei, D.Y Wang, W.J Xie, J.L Luo, F.S. Han, Effects of macroscopic graphite particulates on the damping behaviour of Zn-Al eutectoid alloy. Phys. Lett. A 2007, 366, pp 134-136.

[163]. Zhonghua Ma, Fusheng Han, Jianning Wei, Junchang Gao, Effects of macroscopic bulk defects on the damping behaviours of materials, Science in China Series A: Mathematics, 2001, 44 (5), pp 655-661.

[164]. P.K Rohatgi, N. Murali, H.R. Shetty, R. Chandrashekhar, Improved damping capacity and machinability of graphite particle-aluminium alloy composites, Materials Science and Engineering, 1976, 26(1), pp 115-122.

[165]. N. Srikanth, D. Saravanaranganathan, M. Gupta, Effect of presence of SiC and operating frequency on the damping behaviour of pure magnesium. Material Science Technology, 2004, 20, pp 1389-1396.

[166]. Dong In Jang, JinKyu Lee , Dae Up Kim , Shae K Kim, Influence of CaO on damping capacity and mechanical properties of Mg alloy, Transactions of Nonferrous Metals Society of China, 2009, 19, pp 76−79.

[167]. RanjitBauri and M.K Surappa, Damping behaviour of al-li-SiCp composites processed by stir casting technique, Metallurgical and Materials Transactions A, 2005, 36, pp 667-673.

[168]. C.F Deng, D.Z Wang, X.Z Zhang, Y.X Ma, Study the damping behavior of composites, Materials Letters, 2007, 61, pp 3319-3229.

[169]. David Dunand and Andreas Mortensen, Thermal mismatch dislocations produced by large particles in a strain-hardening matrix, Materials Science and Engineering A, 1991, 135, pp 179-184.

[170]. M. Taya and R. Arsenault, Metal matrix composites—thermo mechanical behavior, Pergamon Publishers, 1989, pp 1-274.

[171]. J.E Bishop and V.K Kinra, Analysis of elastothermodynamic damping particle-reinforced metal-matrix composites, Metallurgical and Materials Transactions A, 1995, 26, pp 2773–83.

[172]. Srikanth, Narasimalu, Manoj, Gupta, FEM based damping studies of metastable Al/Ti composites, Journal of Alloys and Compounds, 2005, 394 (2), pp 226-234.

[173]. R. Thirumalai and R. Gibson, Characterisation of dynamic extensional modulus and damping of reinforcing fibre for advancedcomposites at elevated temperatures, American Society of Mechanical Engineers, 1993, 12, pp 37–44.

[174]. X. Liu,S.Takamori, Y.Osawa, F. Yin, The damping capacity for the unannealed and annealed cast irons with and without the addition of aluminium, Journal of Materials Science, 2005, 40, pp 1668-1773.

[175]. K. Sudarshan and M.K. Surappa, Synthesis of fly ash particle reinforced A356 Al composites and their characterization, Materials Science and Engineering: A, 2008, 480, pp 117-124.

[176]. DenniAsraAwizar, NorinsanKamil Othman, AzmanJalar, Abdul RazakDaud, I. Abdul Rahman, N. H Al hardan, Nano silicate extraction from rice husk ash as green corrosion inhibitor, International Journal of Electrochemical Science,2013, 8, pp 1759 – 1769.

[177]. Ali Nazari, Ali Bagheri, ShadiRiahi, Properties of geo polymer with seeded fly ash and rice husk bark ash Materials Science and Engineering: A, 2011, 528(24), pp 7395-7401.

[178]. Dora Siva Prasad and Chintada Shoba, Experimental evaluation onto the damping behavior of Al/SiC/RHA hybrid composites, Journal of Materials Research and Technology, 2016, 5(2), pp 123-130.

[179]. G.H Wu, Z.Y Dou, L.T Jiang, J.H Cao, Damping properties of aluminium matrix–fly ash composites, Materials Letters, 2006, 60(24), pp 2945-2948.

[180]. M. Yadollahpour, S. Ziaei-Rad, F. Karimzadeh, J. Eskandari-Jam, A numerical study on the damping capacity of metal matrix nanocomposites, Simulation Modelling Practice and Theory, 2011,19, pp 337–349.

[181]. Jian Gu, Gaohui Wu, Qiang Zhang, Preparation and damping properties of fly ash filled epoxy composites, Materials Science and Engineering. A, 2007, 452, pp 614–618.

[182]. X.S Hu, K. Wu, M.Y Zheng, W.M Gan, and X.J Wang, The effect of Si content on low frequency damping capacities and mechanical properties of as-cast Mg–Si alloys, Materials Science and Engineering, 2007, 452, pp 363-374.

[183]. Zhang Xiadong, Wu Renzie, Li Xiaocui, Damping behavior of metal matrix composites with interface layer, science in china, 2001, 44(6), pp 640-646.

[184]. Yuqin Jiao, Yuhua Wen, Ning Li, Jiaqiang He, JinTeng, Effect of environmental temperature on damping capacity of Cu-Al-Mn alloy, Transactions of Nonferrous Metals Society of China, 2009, 19(3), pp 616-619.

[185]. Guangyu Du, Damping Properties of Arc Ion Plating NiCrAlY Coating with Vacuum Annealing, MDPI Coatings, 2018, 8, pp 1-20.

[186]. M. Andi Limarga, High-temperature vibration damping of thermal barrier coating materials, Surface & Coatings Technology, 2007, 202, pp 693–697.

[187]. G. Liua, Damping behaviour of SnO_2 Bi_2O_3-coatedAl18B4O33 whisker-reinforced pure Al composite under gone thermal cycling during internal friction measurement, Materials Science and Engineering, 2015, 624, pp 118–123.

[188]. G. Liu, Effects of the sintering temperature of whisker with $SnO_2 \cdot Bi_2O_3$ coatings on the damping behavior in Al18B4O33w/Al composite, Materials Science and Engineering, 2011, 530, pp 9–14.

[189]. G. Liu, Damping behavior of Bi_2O_3-coated Al18B4O33 whisker-reinforced pure Al Composite, Materials Science and Engineering, 2010, 527, pp 5136–5142.

[190]. H.A. Colorado, Damping behavior of physical vapor-deposited TiN coatings on AISI 304 stainless steel and adhesion determinations, Materials Science and Engineering, 2006, 442, pp 514–518.

[191]. JinhaiGu, Damping behaviors of magnesium matrix composites reinforced with Cu-coated and uncoated SiC particulates, Composites Science and Technology, 2005, 65, pp 1736–1742.

[192]. S. Patsias, Ceramic coatings: Effect of deposition method on damping and modulus of elasticity for yttria-stabilized zirconia, Materials Science and Engineering, 2006, 442, pp 504–508.

[193]. S. Patsias, Hard damping coatings: An experimental procedure for extraction of damping characteristics and modulus of elasticity, Materials Science and Engineering, 2004, .370, pp 412–416.

[194]. Giuliano Gregori, Vibration damping of super alloys and thermal barrier coatings at high-temperatures, Materials Science and Engineering, 2007, 466, pp 256–264.

[195]. Kantesh, Damping behaviour of carbon nanotube reinforced aluminium oxide coatings by nano mechanical dynamic modulus mapping, Journal of Applied Physics, 2008, 104, pp 63511-63517.

[196]. Qing Zhang, Laifei Cheng, Wei Wang, Litong Zhang, Yongdong Xu, Effect of SiC coating and heat treatment on damping behaviour of C/SiC composites, Materials Science and Engineering,2008, 473, pp 254–258

[197]. B.A.Potekhin, S.G.Lukashenko and S.P.Kochugon, Effect of plasma coatings on the damping properties of structural steels, Metal Science and Heat Treatment, 2000, 42, pp 407-410.

[198]. G.W.Smith and J.R.Birchak, Journal of applied physics, 1969, 40(13), pp 5174-5178.

[199]. K.Amano, m.Sahashi, H.Toroko and M.Nakagawa, Proc. 6thIntConf on Internal friction and ultrasonic attenuation in solids, July 4-7, 1977, pp 763-768,Tokyo edited by R.R.Hasiguti and N.Mikoshika.

[200]. A.Karimi, P.Giauque, J.Martin, G.Barbezat, A.Salito, High damping capacity coatings for surface vibration control, Journal de Physique IV colloque, 1996, 06(C8), pp C8-779 to C8-782.

[201]. S.Patsias, C.Santon, M.Shipton, Hard damping coatings: An experimental procedure for extraction of damping characteristics and modulus of elasticity, Material Science and Engineering A, 2014, 370, pp 412-416.

[202]. R.S.Lakes, High damping composite materials: Effect of structural hierarchy, Journal of composite materials, 2002, 36(03), pp 287-297.

[203]. Liming Yu, Yue Ma, Chungen Zhou, Huibin Xu, Damping efficiency of the coating structure, International journal of solids and structures, 2005, 42, pp 3045-3058.

[204]. Liming Yu, Yue Ma, Chungen Zhou, Huibin Xu, Damping capacity and dynamic mechanical characteristics of the plasma-sprayed coatings, Materials Science and Engineering A, 2005, 407 , pp 174-179.

[205]. Christopher Blackwell, Anthony Palazotto, Tommy J George and Charles J Cross, The evaluation of the damping characteristics of a hard coating on titanium, Shock and Vibration, IOS press, 2007, pp 37-51.

[206]. Shancan Fu, Yue Ma, Shengkai Gong, Effect of microstructure of interface between MCrAlY coating and substrate on damping property, 2011 Chinese material conference , Procedia Engineering, 2012, 27, pp 1024-1032.

[207]. Wei Sun and Rong Liu, Damping optimization of hard coating thin plate by the modified modal strain energy method, Coating, 2017, 7(2), pp 1-15.

[208]. S.Ramesh, N.Natarajan, V. Krishnaraj, Indian journal of Engineering and Materials sciences. 2014, 21, pp 409-417.

[209]. H. Singh and R. Garg, Journal of Achievements in Materials and Manufacturing Engineering, 2009. 32, pp 70-74.

[210]. N. Tosun, C. Cogun, G. Tosun, Journal of Materials Processing Technology. 2004, 152, pp 316-322.

[211]. F. Han, J. Jiang, D. Yu, the International Journal of Advanced Manufacturing Technology 2007, 34, pp 538-546.

[212]. D. SivaPrasad, Ch.Shoba and B.S. Prasad, Journal of Materials Science & Engineering A, 2014, 591, pp 78–81.

[213]. D. SivaPrasad and Ch.Shoba , Materials Science & Engineering A 2014, 599 , pp 25–27.

[214]. D. Siva Prasad, Ch. Shoba, K. Rahul Varma, Abdul Khurshid Journal of Alloys and Compounds 2015 , pp 646 , 257–263.

[215]. J.Prohaszka, A.G. Mamalis and N.M.Vaxevanidis, Journal of Materials Processing Technology, 1997, 69, pp 233-237.

[216]. R. BagherianAzhiri, R. Teimouri, M. GhasemiBaboly, Z. Leseman, International Journal of Advanced Manufacturing Technology, 2014, 71, pp 279 - 295.

[217]. Vishal Parashar, A.Rehman, J.L.Bhagoria, Y.M.PuriInternational Journal of Engineering Science and Technology, 2010, 2, pp 1021-1028

[218]. R.E. Williams, K.P. Rajurkar, Study of wire electrical discharge machining surface characteristics, J. Mater. Process. Technol, 1991, 28, pp 486-493.

[219]. T. Sone, K. Masui, Application of ion nitriding to wire-electrical-discharge machined blanking dies, Mater. Sci. Eng, 1991, 140, pp 486-493.

[220]. C. Zener, Internal friction in solids II: General theory of thermoelastic internal friction, Physical Review, 1937, 53, pp. 90-99.

[221]. Joseph E. Bishop and VikramK.Kinra, Elastothermodynamic damping in laminated composites, International Journal of Solids and Structures, 1997, 34(9), pp 1075-1092.

[222]. D.C.Dunand and A.Mortensen, Dislocation emission at fibers—I. Theory of longitudinal punching by thermal stresses, Acta Metallurgica et Materialia, 1991, 39(7), pp 1405-1416.

[223]. Taya M and Arsenault R J, Metal matrix composites—thermomechanical behaviour (New York: Pergamon Publishers), 1989.

[224]. R. S. Lakes, High Damping Composite Materials: Effect of Structural Hierarchy, Journal of Composite Materials, 2002, 36(3), pp 287-297.

[225]. M. Shen and H. Herman. Development of a free layer damper using hard coatings, Proceedings of 7th National Turbine Engine High Cycle Fatigue Conference, 2002.

LIST OF PUBLICATIONS

The work reported in the thesis is partially covered in the following publications:

1. Dora Siva Prasad, **Palukuri Tulasi Radha**, Chintada Shoba, Pujari Srinivasa Rao, Dynamic Mechanical Behaviour of WC-Co coated A356.2 Aluminium Alloy, Journal of Alloy and Compounds, 767 (2018) 988–993, 2018. (https://doi.org/10.1016/j.jallcom.2018.07.203) **(Indexed in SCIE, Scopus etc)**

2. Dora Siva Prasad, **Palukuri Tulasi Radha**, Chintada Shoba, Abdul Kurshid, M.Kaustubh, Optimizing of Wire EDM Parameters for Damping Capacity of Aluminium Alloy, Materials Today Proceedings 5 (2018), 16832-16839, SCICON 2016, **(Indexed in SCIE, Scopus etc)**

3. Dora Siva Prasad, **Palukuri Tulasi Radha**, Chintada Shoba, Srinivasa Rao Pujari, Energy dissipation in WC-Co coated A356/RHA composites, Journal of Engineering Science and Technology, an International Journal, **Elsevier (Indexed in SCIE, Scopus etc)**

Appendix-I

To check for optimal coating thickness the samples were also coated with higher coating thickness of 250 µm and the damping measurements were made using dynamic mechanical analyzer. Fig. 1a and b shows the damping behavior of WC-Co coated specimens at 100 and 250 µm respectively. A slight decrease in damping and increase in modulus was observed with the increased coating thickness. However, *E* tanδ was found to be maximum for the specimens coated with 100 µm. Hence, it was considered as the optimal condition and discussion in the present work is confined to specimens coated with 100 µm.

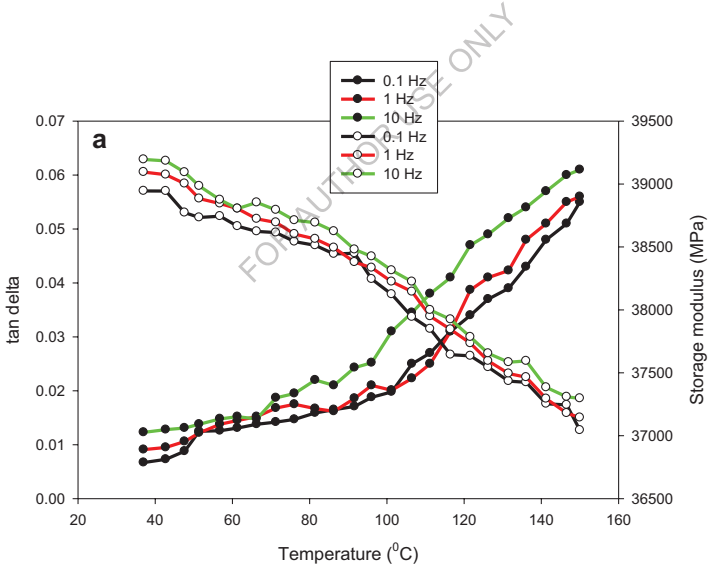

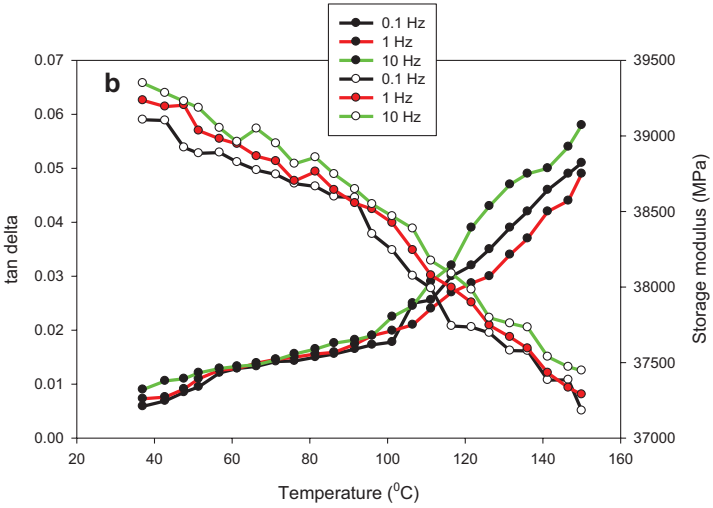

Fig 1: Damping behavior of WC-Co coated base alloy a) 100 µm b) 250 µm